FEASIBILITY STUDY FOR FIELD-SCALE USE OF UREOLYSIS-INDUCED CALCITE PRECIPITATION (UICP) FOR ROADBED IMPROVEMENT.

by

Hudson Thomas Dorian

A thesis submitted in partial fulfillment of the

requirements for the degree of

Master of Science

in

Civil Engineering

MONTANA STATE UNIVERSITY

Bozeman, MT

July 2023

ACKNOWLEDGEMENTS

The research presented here would not have been possible without the funding and guidance of the United States Airforce Research Laboratory in Dayton, Ohio.

This research would also not have been possible but for the expertise and leadership of Adrienne Phillips, Mohammad Khosravi, and Al Cunningham. Sincere thanks are also owed to the fellow student researchers that dedicated their time to this project's completion: Pinar Gunyol, Olayinka Durojaye, Ben Pak, Ethan Dudley, and Jenna Lauf.

TABLE OF CONTENTS

1. INTRODUCTION 1

Context 1
Research Objectives 4
Scope 5
Thesis Outline and Summaries 5

2. PAPER 1 - DIRECTIONALITY OF MICROBIALLY-INDUCED CALCITE PRECIPITATION, AND IMPLICATIONS ON APPLICATIONS FOR ROAD STRUCTURES 8

Contribution of Authors and Co-Authors 8
Manuscript Information 9
Abstract 10
Introduction 10
Materials and Methods 13
Soil Choice 13
Soil Medium Preparation 14
Chemical Process 15
Treatment Design 17
Evaluation and Testing 18
Compressive Strength 18
Calcium Carbonate Content 18
Results 19
Conclusion 22
Acknowledgements 23
References 23

3. PAPER 2 - UREOLYSIS-INDUCED CALCITE PRECIPITATION (UICP): INJECTION STRATEGIES AND THE EFFECT ON STRENGTH AND FAILURE MECHANISM 26

Contribution of Authors and Co-Authors 26
Manuscript Information 28
Abstract 29
Introduction 29
Materials and Methods 33
Microbial Growth 33
Media 34
Batch Studies 35
Optical Density 35
Jung Assay 36

TABLE OF CONTENTS (CONT.)

pH Testing....36
Cost Analysis....36
Soil Column Testing....37
Injection Strategy....38
Effluent Fluid Sampling....39
Unconfined Compressive Strength....39
$CaCO_3$ Determination....40
Results....40
Cost Analysis of Recipes....41
Effect of Recipe on Bacterial Propagation....42
Effect of Injection Method on Specimen Strength....45
Effect of Recipe on Specimen Strength....48
Conclusions....50
References....52

4. PAPER 3 - EFFECT OF UREOLYSIS-INDUCED CALCITE PRECIPITATION (UICP) TREATMENT ON THE CBR VALUE OF SAND SPECIMENS, AND IMPLICATIONS FOR FIELD-SCALE PAVED STRUCTURE APPLICATIONS....57

Contribution of Authors and Co-Authors....57
Manuscript Information....59
Abstract....60
Introduction....61
Materials and Methods....65
Microbial Growth....65
Media....65
Soil Specimens....66
15-centimeter-diameter Specimens....66
30-centimeter-by-30-centimeter Specimen....68
Soil for Treatment and Soil Preparation....69
UICP Treatment....71
CBR Strength....75
Jung Assay....76
Calcium Digests and Assay....76
Results....78
Injection Strategy and Treatment Characteristics....79
Treatment Solution and Treatment Characteristics....82
Lessons from the 15-centimeter Specimens....83
Results of the 30-centimeter-by-30-centimeter Tests....84
Regression of Calcium Carbonate Content and CBR Value....87

TABLE OF CONTENTS (CONT.)

Conclusions....89
References....91

5. CONCLUSION....95

Suggested Areas of Research....97

CUMULATIVE REFERENCES....98

APPENDICES....109

Appendix A - Supplementary Material for Paper 2....111
Appendix B - Supplementary Material for Paper 3....114
Reactor Construction....115

LIST OF TABLES

Table Page

2-1. Soil parameters for selected materials. 14

2-2. Ingredient concentrations in solutions used for the MICP treatment process. 16

3-1. Alternative recipes for bacterial growth solutions. See Table A1 in the appendix for detailed description of ingredient type. 34

3-2. Alternative recipes for calcium solution. See Table A1 in the appendix for detailed description of individual ingredients. 35

3-3. Comparative cost of bacterial growth solution recipes in dollars per liter; YEH, YEM, and YEL are high-carbon, medium-carbon, and low-carbon variations of the same recipe. 42

3-4. Comparative cost of calcium solution recipes. Recipes are inherently the same as their non-calcium counterparts, but include 49 g/L of Calcium Chloride. 42

3-5. Peak UCS strength (kPa) for treated soil columns; letter indicates treatment method, and number is the specimen number for that method. 46

3-6. Peak UCS strength (kPa) for treated soil columns using yeast-extract-based solutions (YEH-, YEL+). 50

4-1. Solution recipes with associated per-liter costs. 66

4-2. 15-centimeter specimens with associated treatment conditions. 73

LIST OF FIGURES

Figure Page

2-1. General overview of treatment method:
a) the specimens mounted to the frame, attached
to the syringes and directed into waste containers;
b) image of the reactor; c) detailed section of the reactor. 15

2-2. a) Combined UCS testing results
and b) failure type by specimen. 20

2-3. Acid digest data. Data was collected from each of the three
layers (top, middle, bottom) for each of the specimens, and
used to create respective averages and spreads for each treatment method. 21

3-1. Testing setup for reactors, detailing treatment
methods and process, and showing reactor section. 38

3-2. Batch study optical density analysis over 24 hours;
averaged across 3 specimens per recipe, with 3 samples per specimen. 43

3-3. Batch study urea concentration over 24 hours,
determined by Jung Assay; averaged across 3
specimens per recipe, 3 samples per specimen. 44

3-4. Batch study pH level over 24 hours; measured every
other hour and at 24 hours; averaged across 3 specimens per recipe. 45

3-5. Comparative UCS stress versus strain between treatment
methods using standard recipes (CMM- and CMM+). 46

3-6. Calcium carbonate ($CaCO_3$) content by column segment,
organized by statistical results of 2 samples per method;
determined by percent mass through calcium digests of 1-gram samples. 48

3-7. UCS stress versus strain for YEH-/YEL+ treated specimens.....49

3-8. Calcium carbonate content by segment for YEH-/YEL+
treated specimens, determined by percent mass through calcium digests. 49

LIST OF FIGURES (CONT.)

Figure Page

4-1. Reactor design for 15-centimeter-scale specimens, showing the two injection methods used: top-down (left), with solutions injected onto the soil surface, and probe-injected (PI), with solutions injected into the soil medium past the surface through a probe. 67

4-2. Reactor design for 30-centimeter-by-30-centimeter specimen, assembled from four side walls, secured onto a base using threaded rods and wingnuts. Injection is done through a set of four probes, extending through the asphalt surface and crushed rock layer into the sand medium. 69

4-3. Demonstration of pluviation process and device used in the soil compaction process for the 30-centimeter-by-30-centimeter specimen. 71

4-4. 15-centimeter-scale reactor treatment setup, displaying the alternative injection methods. 72

4-5. 30-centimeter-by-30-centimeter-scale reactor treatment setup. 74

4-6. Division of 30-centimeter-by-30-centimeter specimen for CBR testing and calcium digest sampling. 76

4-7. Calcium digest sampling pattern for 15-centimeter specimens. 78

4-8. CBR testing results for 15-centimeter-diameter specimens, compared against 3 control specimens, showing a) stress-strain response during testing and b) the resulting CBR value taken at 2.5 mm. 80

4-9. Calcium carbonate distribution over depth for 15-centimeter specimens, evaluated at three discrete layers. These specimens received 19 pulses each, using the same media recipes. The sample PI P19 was inverted for CBR testing, requiring a flat surface, so the ‘bottom’ during treatment became the CBR testing surface. 81

4-10. Calcium carbonate distribution over depth for 15-centimeter-diameter specimen, treated with 14 pulses using the top-down method, using the YE-based media. 83

4-11. 30-centimeter-by-30-centimeter CBR strength by section over depth. 85

LIST OF FIGURES (CONT.)

Figure Page

4-12. 30-centimeter-by-30-centimeter calcium carbonate content by section over depth. 85

4-13. Calcium Content and CBR value linear regression with 95% confidence interval. 88

ABSTRACT

A series of tests were conducted to evaluate the feasibility of using ureolysis-induced calcium carbonate precipitation (UICP) to improve the strength of the soil layers used to in the construction of roads. This process involved three series of tests conducted on soil specimens of gradually increasing volume.

The first series regarded the relative effect of treatment direction, comparing top-down treatment to bottom-upwards and alternating treatment methods on 50-by-100-millimeter soil columns. This was evaluated through unconfined compressive strength (UCS) and the calcium carbonate distribution over the length of the soil, finding that all methods generated a reliable increase in the strength of the soil specimen. This phase of research also included a batch study, evaluating the growth of the ureolytic bacteria *Sporosarcina pasteurii* in a solution composed of commercially available ingredients, showing that the bacteria could be cultured at a far lower cost (as low as 20 cents per liter) than with lab-grade ingredients ($2.66 per liter).

The next series of tests compared the effect of applying treatment solutions to the soil surface directly and using a probe to inject solutions beneath the surface. This was done with 15-centimeter, cylindrical specimens, evaluated through the California bearing ratio (CBR) test. It was determined that the treatment process had the capacity to increase the CBR value substantially (from ~11% up to 188%), and it was suggested that each treatment mechanism resulted in a predictable distribution of calcium carbonate. There was also success in using alternative, commercially-sourced ingredients to facilitate the treatment and improve the CBR value.

The last tests centered on the treatment of a 30-centimeter-by-30-centimeter mock road section, combining the treatment mechanisms used at the 15-centimeter-scale to facilitate an increase in the CBR of a soil layer under pavement. Through UICP, the CBR value of this layer was successfully increased.

CHAPTER ONE

INTRODUCTION

Context

Any paved structure is inherently designed to be better at carrying load than the local, native ground, or 'subgrade,' which may contain organics, swelling clays, or generally weak constituent soils. However, that the road still needs to be founded upon this native ground. The design process for any paved structure, thus, desires to reduce the load 'felt' by the subgrade. The 'sub-base' is typically a natural (non-manufactured), free-draining, coarse soil, layered on top of the subgrade. The 'base,' a manufactured (e.g., sieved material or crushed rock), coarse, stronger material is then layered over the subbase. The paved surface is laid on top of the base material. Ideally, this combination of paved surface and 'substructure' disperses the load applied to the road surface to an amount appropriate for the subgrade. The necessary thickness of each of these additional layers is typically a function of the anticipated traffic load and volume, and the strengths of the individual materials, as exemplified by AASHTO's structural number (SN) parameter (AASHTO, 1993). The product is a road with a predictable design life, fulfilling the anticipated service with regular upkeep until the end of the life is reached, at which point the road needs to be replaced. This provides the opportunity to pursue funding and plan the reconstruction process. Therein, the proper design of a road is crucial to maintaining a balanced budget, as in 2020, $116.3 billion of state and local government expenditures in the United States went towards the maintenance, repair, and upkeep of existing roadways (USCB, 2020).

However, as there must be an assumed design load and volume for any design, a challenge to this process is presented by growth. As society continues to develop at a rapidly increasing pace, these assumed values may no longer be suitable. As a result, the road may become overburdened, its design life shortened and requiring a replacement sooner, therefore undercutting prior plans. Even before replacement can occur, the road may provide worse service under these conditions. The preferrable option, then, would be to improve the strength of the road's substructure to meet these new demands. The modern civil engineer, however, lacks a convenient method to accomplish this.

Beyond compaction, there are accepted methods of increasing the strength of the base and sub-base. Design manuals provided by the United States Army Corp of Engineers and the National Academy of Sciences (2009) outline a number of accepted methods of improving the strength of these soils. However, all of these methods are based around an admixture, such as lime, bitumen, or Portland cement, and must be mixed with the soil before laying to achieve an effective improvement to strength. As a method to improve the strength of a soil while in-situ, high-mobility polyurethane grout has potential, able to be injected into target soils and improve their mechanical behavior (Sabri et al., 2021). However, this method is currently "costly" relative to other options of soil improvement and involves the use of mildly toxic ingredients (Saleh et al., 2019), and was found to cause a reduction in permeability of the targeted material (Buzzi et al., 2010), complicating its suitability for roads.

Herein is the appeal of ureolysis-induced calcium carbonate (calcite) precipitation (UICP). This process uses the enzyme 'urease,' commonly resourced from certain strains of bacteria, which converts urea into carbonate, reacting with calcium to precipitate calcium carbonate crystals, as summarized in Equations 1-1 and 1-2. When conducted within a soil, this reaction results in

calcium carbonate ‘bridges’ forming between the soil particles, shown to be an effective means of soil solidification (Gowthaman et al., 2019[1]; DeJong et al. 2022), erosion mitigation (Sun et al., 2022; Salifu et al., 2016), and strength improvement (DeJong et al., 2006). This process was also found to consume fewer resources than traditional methods of soil improvement (Rahman et al., 2020), and has been successfully adapted to use recycled or waste materials to facilitate the reaction (Yang et al., 2022; Fouladi et al., 2023). Thus, UICP also has the potential to be a more sustainable method of soil improvement. UICP has since become a popular subject of research in regard to its potential use in engineering applications. Such research efforts have investigated methods of reducing the relative cost of treatment (Yang et al., 2022; Achal et al., 2009), optimizing the treatment process to achieve higher increases to strength (Terzis and Laloui, 2019; Hoang et al., 2020, Li et al., 2017), and adapting the treatment process to field conditions (Kirkland et al., 2020; Kirkland et al., 2021; van Paassen, 2011).

$$CO(NH_2)_2 + 2H_2O + Urease \rightarrow 2NH_4^+ + CO_3^{2-}$$ Equation 1-1.

$$Ca^{2+} + CO_3^{2-} \rightarrow CaCO_3$$ Equation 1-2.

The treatment process usually applied to soils involves the introduction of two solutions through separate ‘injections’ into the soil, one supplying urease, the other calcium (typically calcium chloride) and urea, such as in the processes used by Whiffin (2004) and DeJong (2006). This aspect of the treatment process is promising in the treatment of road substructures, as these solutions could theoretically be introduced through the paved surface, generating the precipitate in the target soil layer below. However, little research has been done regarding the feasibility of this specific application. In essence, it is not certain whether the treatment process can be easily applied to the base or subbase, what the most effective mechanism for delivery of these solutions is, and whether the strength of the material can be effectively improved relative to the effort and cost

needed. Previous large-scale studies have had success with surficial treatment methods (Naeimi et al., 2023; Cheng et al. 2021). The envisioned treatment process would likely use a similar, modified approach, using access points ported through the pavement to treat the desired soil layer directly, administering the solutions from the top, downwards. However, it is unknown if this is the most effective approach. Aggregated in a state-of-the-art review by Rahman et al. (2020), a number of unconfined compressive strength (UCS) tests of various soil treated through UICP provided a range of peak strengths, ranging from 0.03 to 19.6 Megapascals. It seems that the effect of UICP on the soil's strength properties is a function of the characteristics of the treatment procedure used, such as the saturation of the specimen during treatment (Cheng et al., 2013), the time interval between injections (Danjo and Kawasaki, 2016), the strain of ureolytic bacteria used (Dick et al., 2006; Jain and Das, 2023) and the conditions used to grow them (Shrikawa et al., 2011; Rahamninezhad et al., 2022), among other variations. In such a context, the central decisions for the proposed treatment process for roads need to be investigated further, prior to any plans of field-scale use.

Research Objectives

This research was conducted to investigate an effective approach to the treatment of road substructures, targeting the compressive strength of a sandy soil. Decidedly, the main points to be addressed were 1) the direction and mechanism of treatment and the feasibility of top-down field treatment, 2) the cost-reducing measures, namely the replacement of lab-grade chemicals for commercial alternatives, 3) the scale of treatment, regarding the most effective means of treating larger volumes of soil. The goal was to evaluate the effect, if any were present, of each of these

decisions on the resulting characteristics of the treated soil compared to alternative approaches. Findings would be useful in forming a realistic, field-scale treatment plan.

Scope

The goal of this research is primarily to investigate the feasibility of the envisioned field-scale application. In essence, this was to determine whether this application is practical, and if so, what further research would be necessary to form an educated basis for creating a treatment plan. The efforts pursued here were all conducted in a laboratory environment, progressively scaling treatment to larger volumes of soil and towards soil profiles more closely resembling a layer of a road substructure. All portions of this research regarded the treatment of one soil type, that being sand, Sakrete® medium silica sand used as a target soil medium. Live cells of *Sporosarcina pasteurii* were used as the source of urease in the treatment process.

Thesis Outline and Summaries

The main body of this thesis is composed from three separate manuscripts. Chapter two is a conference paper published to GeoCongress 2023. Chapters three and four are two journal papers under review by the funding agency at the time of submission for this thesis, to be submitted for publication in the Journal of Geotechnical and Geoenvironmental Engineering in the near future. As such, each chapter has its own designated introduction, explanation of materials and methods, results, and conclusions.

Chapter two investigates the comparative effect of changing injection direction on the resulting distribution of calcium carbonate and unconfined compressive strength (UCS) of the treated soil specimen. This was done by comparing 50-millimeter-diameter, 100-millimeter-tall

soil specimens, each treated using a different injection direction: top-to-bottom, bottom-to-top, and alternating (where injection direction was switched on a regular basis).

Chapter three explores in more detail the results of the 50-millimeter-by-100-millimeter specimens, in addition to an evaluation of a set of alternative treatment solutions, made using commercially available ingredients to reduce the cost of treatment. These alternative recipes were investigated though a comparative cost analysis and a batch study, monitoring bacterial growth and ureolysis over a 24-hour period. A preliminary set of soil specimens were also treated using a set of the alternative recipes, evaluated in calcium carbonate distribution and UCS strength.

Chapter four investigates the relationship between UICP and the California bearing ratio (CBR) value of a target soil, a strength parameter commonly used in road and runway construction. This research was conducted in two stages. The first stage consisted of a series of 15-centimeter-diameter specimens, used to evaluate the impact of injection mechanism and recipe type on the resulting increase in the CBR value and the distribution of calcium carbonate. For the mechanism, a top-down treatment administered directly onto the soil surface was compared to a ‘probe-based’ injection method. For the recipe type, a set of the alternative recipes were used to treat the soil. The second stage centered on a 30-centimeter-by-30-centimeter specimen, used to experiment with the treatment process regarding road application, featuring a profile similar to a road section. The injection mechanism used was a combination of the two investigated in the first stage, and the treatment was conducted using the commercially-sourced treatment solutions. This larger specimen allowed for multiple CBR tests to be conducted over the surface and through the depth, each CBR test being associated with the average calcium carbonate content in its vicinity. This permitted the development of a preliminary regression between the CBR value and the calcium carbonate content.

Chapter five is an overall conclusion on the cumulative findings from these experiments, discussing their implications for the original research question and recommending further research.

CHAPTER TWO

PAPER 1 - DIRECTIONALITY OF MICROBIALLY-INDUCED CALCITE PRECIPITATION, AND IMPLICATIONS ON APPLICATIONS FOR ROAD STRUCTURES

Contribution of Authors and Co-authors

Manuscript in Chapter Two

Author: Hudson Dorian

Contributions: Held primary research position during experiments, conducting treatment of the soil specimens, strength evaluations, and acid digests. Conducted data analysis. Provided first draft of manuscript.

Co-Author: Pinar Gunyol

Contributions: Provided guidance in establishing treatment process and acid digest evaluation.

Co-Author: Jenna Lauf

Contributions: Provided assistance in treatment of specimens, conducting UCS testing, and conducting data analysis.

Co-Author: Mohammad Khosravi

Contributions: Provided research guidance and revisions to manuscript.

Co-Author: Adrienne Phillips

Contributions: Provided research guidance and revisions to manuscript.

Co-Author: Alfred Cunningham

Contributions: Provided research guidance.

Manuscript Information

Hudson Dorian, Pinar Gunyol, Jenna Lauf, Mohammad Khosravi, Adrienne Phillips, Al Cunningham

GeoCongress 2023: State of the Art and Practice in Geotechnical Engineering

Status of Manuscript:
_____ Prepared for submission to a peer-reviewed journal.
_____ Officially submitted to a peer-reviewed journal.
_____ Accepted by a peer-reviewed journal.
__X__ Published in a peer-reviewed journal.

American Society of Civil Engineers
https://doi.org/10.1061/9780784484661.037.

Abstract

The objective of this study is to conduct a laboratory-based assessment of Microbially-induced Calcium Carbonate Precipitation (MICP) as a viable approach to improving substructures beneath existing asphalt and concrete roadways. This was evaluated through Unconfined Compressive Strength (UCS) testing, which can be correlated with the resilient modulus for subsurface samples to assess the degree of strength improvement achievable by the treatment. The calcium carbonate ($CaCO_3$) distribution is a critical component of this study. Three different injection methods were adopted to investigate the effect of injection method on 1) the treatment efficiency of soil specimens, and 2) UCS and failure mechanism of bio-cemented sand, using Sakrete^{TM} medium commercial sand. The efficiency of the different injection strategies was tested using an acid digestion method, used to determine the $CaCO_3$ content at different locations of the treated samples. Results concluded that samples injected in a top-to-bottom direction had better efficacy in terms of strength and uniformity over the alternatives.

Introduction

Roads and runways are largely geotechnical structures. One of the primary components of road design is the mixture of the particular surfacing material (Portland-cement or asphaltic concrete), but the integrity of any roadway also relies on the subsurface design. For many locations, the native, near-surface earth (*subgrade*) is typically weak in compression and low-permeability. As a result, these materials may be susceptible to plastic deformation, and are not ideal for road construction. For this reason, a stronger substructure is needed for a road or runway, typically composed of a *base* and *subbase* layer, to protect the native soil.

For any ideal roadway, there is a specific method of substructure design. Stronger soils are layered and compacted over the subgrade, onto which the pavement surface is laid. Under the pavement surface is the *base* material: a manufactured, coarse-grained, free-draining soil which is the next-strongest besides the pavement surface. Under the base is the *subbase*, which is weaker and cheaper than the base material while still relatively free draining and coarse-grained. Under the subbase there is the *compacted subgrade*, which is the native material at its maximum reachable density, overlying the unimproved, in-situ *subgrade*.

In the design of any paved structure, including runways and roads, design measures often prescribe the necessary thicknesses of subsurface layers, depending on material strength, vehicle weight, and anticipated number of passes. Such an example are the charts provided in the Army's *Technical Manual for Theater of Operations: Roads, Airfields, and Heliports*, Chapter 4, correlating certain combinations of *California bearing ratio* (ASTM D1883) and layer thickness, and vehicle gross weight, to number of allowable passes. With this system, weaker materials typically require thicker lifts (U.S. Dept. of the Army, 2016, p. 4-50-4-51).

However, depending on location and budget and what materials are available, the quantities those materials may be obtained, and how well they can be compacted, certain deficiencies in the construction process may arise in the execution or design of the substructure. As such, there may be a need to retroactively improve these existing structures, especially if local infrastructural needs change, for example, if the paved structures may need to carry heavier loads or sustain more passes without an accelerated loss of integrity and shortened design life. Without completely excavating these existing structures, the specific material itself and the layer thicknesses cannot be changed, so the target for improvement could be the strength of these subsurface materials. If the subbase strength could be improved *in situ*, without excavation and reconstruction of the entire road or

runaway, the theoretical amount of work necessary to improve a roadway's performance could be reduced.

One method that could be implemented to improve subbase soil strength and integrity is *microbially-induced calcite precipitation* (*MICP*) This process is a urease-catalyzed precipitation of calcium carbonate, producing crystalline structures. The process may be capable of generating calcium crystalline structures between soil particles which can unify coarse-grained soils into more solid structures. This material has previously been used for the purposes of soil stabilization (Phillips et al. 2013b), with proven potential to increase soil strength as well, acting as a kind of 'bio-cement' for a soil medium. If applied to the base or subbase material for a road or runway structure, ideal for treatment due to its smaller particle size and free drainage, there is a potential to extend the design life of a paved structure or increase its loading capacity.

In a 2021 literature review from *Geosciences* (Arab et al. 2021), collecting over 100 research papers, several studies (Yasuhara et al. 2012, Beser et al. 2018) had used the unconfined compressive strength test (*UCS*) as a direct evaluation of improved soil strength after varying the solutions and concentrations used for treatment. In the literature, one question not addressed is the effect of injection treatment direction on the resulting UCS results and failure mechanism, or if there is any observable difference. If injection through a top-down approach provides usable strength improvements, then road subbase treatment would be more feasible as opposed to the more common bottom-up treatment method (Yasuhara et al. 2012), which is often performed in the laboratory but may not be feasible in field application. Additionally, UCS results can be correlated to the resilient modulus, shown by AASHTO to be relevant to roadway design (AASHTO 1993, p. II-12). Similar to the CBR value, this is a soil property based on stress-strain behavior, although specifically based on the cyclical loading behavior to which roads are typically

subjected and focusing on the recoverable, elastic portion of strain. Also like CBR values, results can be estimated based on correlations to other tests, although the resilient modulus can be more reliably associated with UCS results.

In this study, three injection strategies were utilized to treat coarse sandy soils with MICP (top-to-bottom, bottom-to-top, and alternating). Solutions were introduced with a constant flow rate directly into the soil into two-inch by four-inch (5.1 by 10.2-centimeter) samples of a uniform soil medium at 35% relative density. The resulting specimens were evaluated for strength through UCS tests. Peak stress before failure and the type of failure observed were recorded. After this, samples were dissected and analyzed for calcium carbonate content across the length of the sample through a calcium digest using acid. The UCS evaluations were also used to estimate respective resilience modulus values which were then used to estimate a CBR value. The CBR test (ASTM D1883) is frequently used as a measure of strength in roadbuilding materials and often used in runway construction practice. As this is a component of ongoing research, future plans include direct CBR testing of the improved material.

Materials and Methods

Soil Choice

The soil medium was coarse-grained, Sakrete® Commercial Medium Silica Sand, which was available commercially (Home Depot). The material was evaluated for grain size distribution (ASTM D422), specific gravity (ASTM D854), and minimum (ASTM D4254) and maximum density (ASTM D4253) and void ratio conditions (Table 2-1).

This material was appealing as a potential candidate in replicating an actual road base or subbase that could benefit from strength improvement. Sand is accepted as a usable material for road construction, but its uniformity can make ideal compaction difficult.

Table 2-1. – Soil parameters for selected materials.

Parameter	**Sakrete® Silica Sand**
Specific Gravity – G_S	2.66
Median Particle Size – D_{50}	0.67 mm
Uniformity Coefficient – C_U	1.69
Coefficient of Curvature – C_C	0.91
Minimum Void Ratio – e_{min}	0.53
Maximum Void Ratio – e_{max}	0.97

Soil Medium Preparation

The reactors were constructed with two-inch-diameter by four-inch-tall plastic concrete molds. This provided the desired sample size, with a snap-on top cap that was easily sealed using silicone sealant. The molds were provided with barbed fittings for 6-millimeter PVC tubing, affixed to the top cap and bottom with a flat hex bolt and rubber-backed gasket washers on either side (Figure 2-1c). To these fittings, tubes were attached to inject fluid *influent* (in-flowing solutions) and drain *effluent* (out-flowing waste).

The reactors were filled with the sand medium, compacted to a relative density of 35% using the modified wet tamping method (Ladd, 1978) in five lifts. A mesh filter was laid on the bottom and top of the soil medium to prevent losses during the injection process. In order to

account for the space occupied by the flat hex bolt at the bottom, the soil medium was underlain with a thin layer of Ottawa sand; this could be easily separated from the soil medium, resulting in a flat-surfaced cylindrical sample after testing. Figure 2-1 provides more detail on the interior of the reactor. The resulting soil medium had a porosity (*n*) of 0.49 and a pore volume of approximately 60 milliliters, so solutions were injected in 90-milliliter pulses (1.5 times the pore volume).

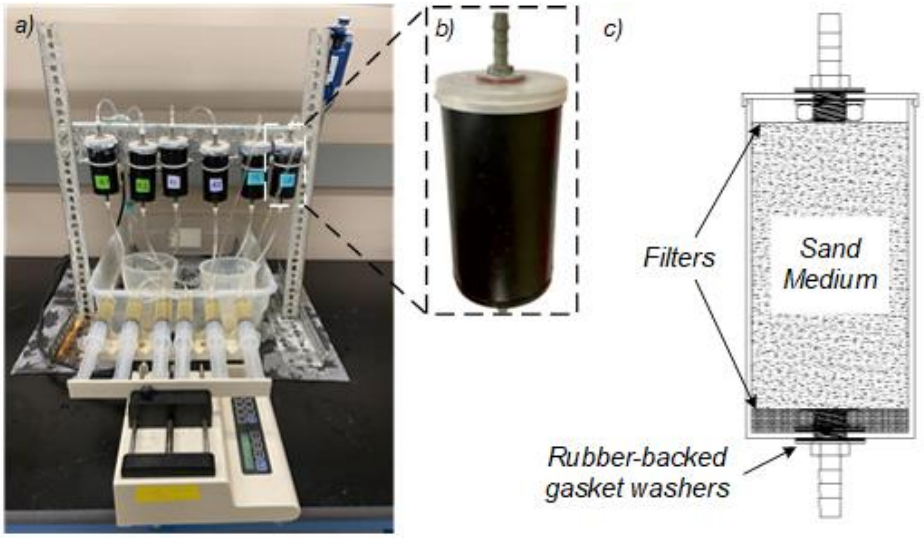

Figure 2-1. – General overview of treatment method: a) the specimens mounted to the frame, attached to the syringes and directed into waste containers; b) image of the reactor; c) detailed section of the reactor.

Chemical Process

The treatment process involved the injection of *Sporosarcina pasteurii* as the urease enzyme source and urea-calcium containing solutions which has been shown to result in the precipitation of calcium carbonate ($CaCO_3$) (Gunyol et al. 2022, Phillips et al. 2013a). This precipitation forms as bridging crystalline structures, adhering to the surrounding medium. There has been a significant amount of documentation of this process in similar experiments (Whiffin 2004, Phillips 2013, Montoya 2012).

For the treatment used in this experiment, there were two main solutions used. The calcium solution, *CMM+*, was used as a source of urea and calcium for the reaction (Table 2-2). A microbial solution of *S. pasteurii* was the source of urease was grown in CMM- (Gunyol et al. 2022). To prepare the solutions, the ingredients were mixed in an Erlenmeyer flask with a stir bar, and the pH was adjusted between 6.0 to 6.3, using four-molar hydrochloric acid (HCl) or sodium hydroxide (NaOH) as necessary. These solutions were vacuum filtered into autoclaved bottles.

Table 2-2. – Ingredient concentrations in solutions used for the MICP treatment process.

Ingredients	**CMM -**	**CMM +**
Difco Nutrient Broth	3 g/L	3 g/L
Fisher Scientific Ammonium Chloride	10 g/L	10 g/L
Fisher Scientific Urea	20 g/L	20 g/L
Fisher Scientific Calcium Chloride (Dihydrate)	N/A	48 g/L

For the bacterial solution, a one-milliliter frozen *S. pasteurii* stock was thawed and added into 150 milliliters of a sterile solution containing brain-heart infusion broth (37 g/L) and urea (20 g/L). After propagating for at least 16 hours, this was transferred at a one-percent ratio into a flask of CMM- and allowed to propagate for at least another 16 hours. This bacterial solution was used both for treatment and for starting the next bacterial solution.

A 10 g/L solution of ammonium chloride solution was used between injections of bacterial and calcium solutions. Enough was used to fill half of the tubing volume to mitigate precipitation in the tubing.

Treatment Design

Fluids were injected using a syringe pump into the sand-filled columns at a rate of four ml/min from either the bottom to top (*B*), top to bottom (*T*), or alternating in direction (*A*). The amount of fluid injected was determined by the *pore volume* of the soil specimen, defined as the volumetric space in a soil medium that is not occupied by solids, the influent volume taken as 1.5 times the pore volume. The flow rate and fluid injection volume were established by previous research (Gunyol et al. 2022). The three methods were conducted in replicates, two *specimens* per method, mounted to a metal frame using zip-ties. Before the injection process, the specimens were disinfected and saturated fully. The disinfection procedure was done by injecting a 10% bleach injection, followed by a 70% ethanol injection. This was rinsed from the reactor fully with deionized (*DI*) water. The bacterial solution was introduced and allowed to reside for a 16-hour period in the medium. After this period, and following a rinse of the tubing as described, the CMM+ was introduced at the same rate and allowed to react without flow for four hours. After the batch period, a new bacterial solution was introduced, and the pattern repeated until 14 full injections had been completed.

The effluent was sampled during the subsequent injection, as the previous fluid was pushed out by the new fluid. The sample was collected when half of the pore volume plus the volume of the tubing had been injected into the reactor, corresponding to when the fluid in the approximate center of the soil medium reached the sample port. A DI water injection was used to collect the effluent sample of the final injection. These samples were used to monitor the urea consumption during the batch period.

Evaluation and Testing

Compressive Strength

Strength of the treated soil specimens was evaluated through unconfined compressive strength (*UCS*) test (ASTM D2166). The test provided a means to compare the treated specimens against each-other. The cylindrical specimens, once dried, were extracted and had their surfaces filed to eliminate peaks or high points; these could cause unrepresentatively high stress on a very small area and lead to fractures. The specimens were individually placed on the load frame, held upright using a slotted surcharge weight. The piston was driven at a rate to cause a one percent increase in strain per minute, defined as one percent of the specimen's height. The amount of deformation was recorded with the respective amount of force required, read from the load cell, until the specimen failed. The method of failure was recorded, and the tested specimen was retained for calcium analysis.

Calcium Carbonate Content

Once the strength testing had been performed, each treated specimen was excavated and treated with acid to determine the calcium carbonate content along the length of the specimens (top, middle, and bottom of the specimen).

In pre-weighed centrifuge tubes, one gram of each dried sample was weighed out in triplicate for each location. In the tubes, this one-gram sample was mixed with five milliliters of 10% nitric acid, which were agitated daily to ensure thorough digestion. After two days, the acid was decanted by removing as much of the acid as possible without removing any of the remaining solids. Once the acid was drained, the caps of the tubes were removed and the tubes were placed into an oven at 55°C to dry. These dried, digested samples were re-weighed and the final weight

was compared to the initial to determine the mass of calcium carbonate per gram of sand which were used to determine a percent calcium content.

Results

The strength results from the UCS testing were assessed for each of the injection strategies. From the graphed results (Figure 2-2a), the top-bottom method of treatment resulted in the highest stress before failure, ranging from 561 to 648 kilopascals. The bottom-top method of treatment resulted in peak stresses of 212 and 433 kilopascals, a 71% difference on average compared with the top-bottom method. The alternating method resulted in peak stresses of 350 and 278 kilopascals, with a 61% difference on average compared to the top-bottom method.

In terms of failure mechanism (Figure 2-2b), specimen T1 featured a completely vertical split-shear failure, compared to the general trends in the B and A specimens which were more isolated to the upper area. T2 did also feature this latter breaking pattern, but within a smaller area and more abruptly, relative to the B specimens which sloughed gently at failure.

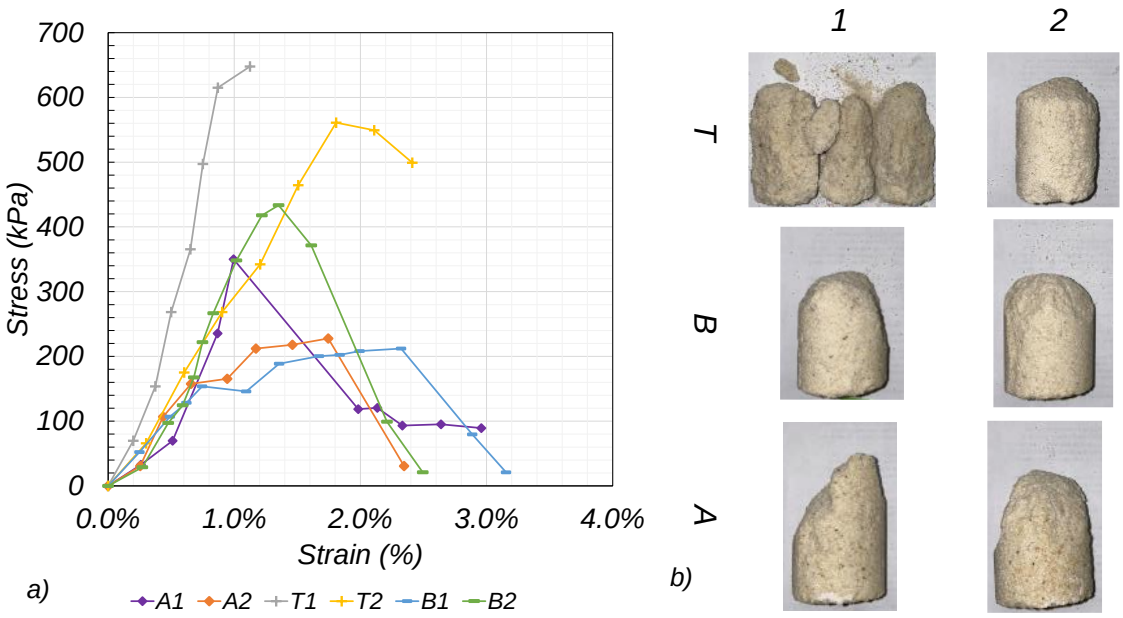

Figure 2-2. – a) Combined UCS testing results and b) failure type by specimen.

From the calcium digest analysis (Figure 2-3), the average calcium carbonate content at each of the tested locations, the top-bottom method provided generally lower values, but with better uniformity. This is visually evident in some of the fracturing patterns observed at failure.

From the digest data, the results for each treatment can be compared by layer. For the topmost layer, the top-down treatment had an average calcium content of 3.6% between the two specimens, compared to 5.6% and 5.3% of the bottom-top and alternating treatments respectively. For the middle layer, this was 5.1% for the top-down method, 7.8% for the bottom-top, and 5.6% for the alternating. Finally, the bottom layer, the content was 4.9% for the top-bottom, 7.4% for the bottom-top, and 8.2% for the alternating. Compared against the compressive strength results, the samples which had *less* cementation near the top (loading surface) relative to the deeper layers performed worse, even if these had more cementation overall. This idea is consistent with typical soil strength profiles, as discussed in the introduction: layering stronger materials over weaker materials is desirable, as the stresses dissipate before reaching the weaker materials.

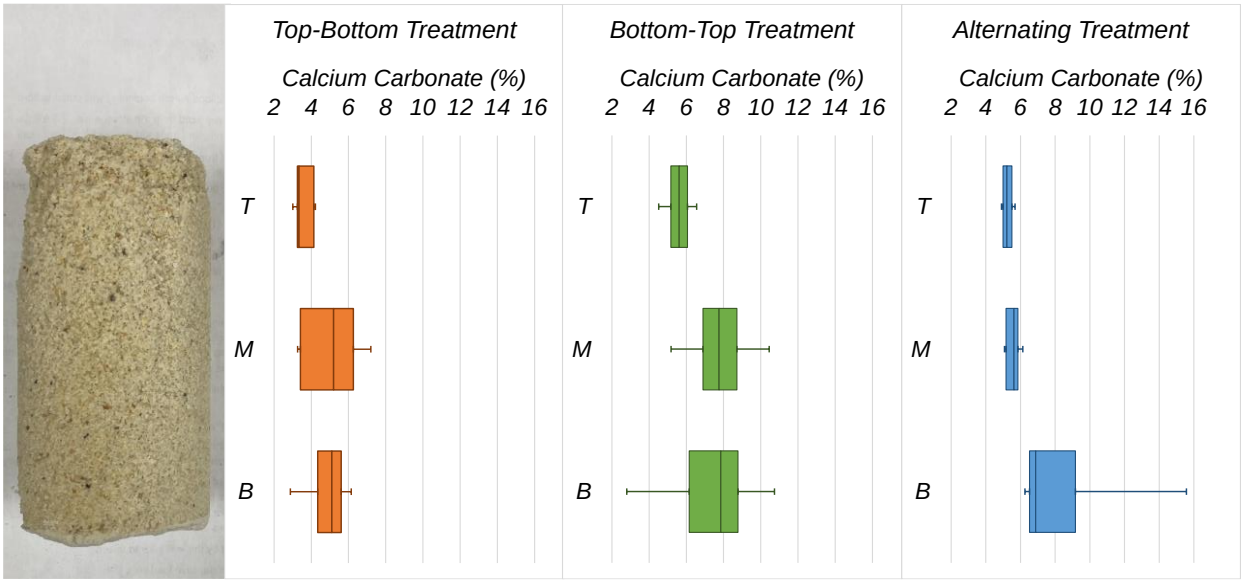

Figure 2-3. – Acid digest data. Data was collected from each of the three layers (top, middle, bottom) for each of the specimens, and used to create respective averages and spreads for each treatment method.

As mentioned, the UCS test's results can be used to estimate resilient modulus. This specific relationship varies by material, but for this application one developed for lime-stabilized soil samples was used to estimate the resilient modulus (Thompson 1966).

M_R (MPa) = 0.124 q_u (kPa) + 68.8 Equation 2-1.

This estimate (Equation 2-1), based on the top-down treatment's peak stresses, results in an estimated resilient modulus of 138 to 149 Megapascals, respectively. Subsequently, using another estimative relationship, the CBR can be determined as well (Equation 2-2), useful in the context of runway construction, where the CBR of material is frequently used (U.S. Dept. of the Army, 2016, p. 4-32). There are numerous proposed relationships between these values, but for an example that proposed by Heukelom and Klomp (1962) will be used.

M_R (MPa) = 10 CBR Equation 2-2.

This results in a predicted CBR of 14 to 15%. Compared to a CBR test conducted on the unimproved sand medium at 35% relative density, with a CBR of 12-15%, this is not a large improvement. However, it should be noted that CBR-resilient modulus relationships can be very speculative and are contestable (Dione et al. 2014), as the parameters in question are very different in loading condition. The resilient modulus is a product of dynamic loading, while CBR is static.

Alternatively, research conducted previously on traditionally cemented soil specimens, using low percent-content Portland cement mixtures, found a degree of correlation between UCS values and California Bearing Ratio (*CBR*) values, illustrated in equations 2-3 and 2-4 respectively (O' Flaherty et al. 1961, Pongsivasathit et al. 2019).

$$\log CBR = 1.115 + 0.660 \log UCS\ (psi) \qquad \text{Equation 2-3.}$$

$$CBR = 0.132\ (UCS\ (kPa)) \qquad \text{Equation 2-4.}$$

Based on these relationships, the estimated CBR for the top-bottom treatment method ranges from 261% (Equation. 2-3) to 74% (Equation. 2-4). These are substantially different compared to the relationship to resilient modulus, Therein, in order to retrieve reliable results, actual CBR testing on MICP-treated specimens is required.

Conclusion

A series of column experiments complemented by unconfined compressive strength testing was conducted to investigate the application of microbially-induced calcite precipitation (MICP) as a viable approach to improving substructures beneath existing asphalt and concrete roadways. Three different injection methods were adopted to develop an efficient MICP treatment strategy including top-bottom, bottom-top, and alternating. From the combined treatment and testing of the material, comparing stress-strain behavior to the calcium carbonate content and the treatment

method, there is a benefit with the top-bottom treatment method, leading to greater uniformity in the resulting distribution of the precipitate. The bottom-top method, either alone or as a component of the alternating method, appears to lead to extended residence in the lower portion of the medium, generating deficient precipitation in the top layer by comparison. MICP can thus offer a potential improvement technique to enhance the strength properties of base and subbase materials beneath pavement, using access to the top of the layer for treatment. Further development of the technique for this application is needed for field implementation, in terms of large-scale treatment.

Acknowledgments

The authors are thankful for the funding, guidance, and feedback provided by personnel of the United States Air Force Research Laboratory (AFRL) at the Wright-Patterson Airforce Base in Dayton, Ohio. Without their continuing contributions, this research would not have been possible.

References

AASHTO. (1993). *AASHTO Guide for Design of Pavement Structures*.

Arab, M.G., Alsodi, R., Almajed, A., Yasuhara, H., Zeiada, W., Shahin, M.A. (2021). State-of-the-Art Review of Enzyme-Induced Calcite Precipitation (EICP) for Ground Improvement: Applications and Prospects. *Geosciences 2021*, Vol. 11, 492.

ASTM. (2010). Standard Test Method for Unconfined Compressive Strength of Cohesive Soil. (D2166). https://www.astm.org/standards/d2166

ASTM. (2014). Standard Test Method for Particle-Size Analysis of Soils. (D422). https://www.astm.org/standards/d422

ASTM. (2016). Standard Test Method for Specific Gravity of Soil Solids by Water Pycnometer. (D854). https://www.astm.org/standards/d854

ASTM. (2016). Standard Test Methods for Minimum Index Density and Unit Weight of Soils and Calculation of Relative Density. (D4254). https://www.astm.org/standards/d4254

ASTM. (2016). Standard Test Methods for Maximum Index Density and Unit Weight of Soils Using a Vibratory Table. (D4253). https://www.astm.org/standards/d4253Beser, G.D. (2018). Ureolysis Induced Mineral Precipitation Material Properties. Master's thesis, Montana State University, Bozeman, MT, USA.

Dione, A., Fall, M., Berthaud, Y., Benboudjema, F., Michou, A. (2014). Implementation of Resilient Modulus – CBR relationship on Mechanistic-Empirical (M.-E) Pavement Design. *Revue du CAMES – Sciences Appliquées et de l'Ingeniuer,* Vol. 1(2), December 2014.

Gunyol, P., Khosravi, M., Phillips, A., Plymesser, K. (2022). Thermal Properties of Bio-Cemented Sand. *Geo-Congress 2022: State of the Art and Practice in Geotechnical Engineering*, p. 356-364.

Heukelom, W., Foster, C.R. (1962). Dynamic Testing of Pavements. *Transactions of the American Society of Civil Engineers,* Vol. 127(1), January 1962.

Ladd, R. S. (1978). Preparing Test Specimens Using Undercompaction. *Geotechnical Testing Journal*, Vol. 1, p. 16-23.

Montoya, B.M., DeJong, J.T., Boulanger, R.W., Wilson, D.W., Gerhard, R., Ganchenko, A., Chou, J.C. (2012). Liquefaction Mitigation Using Microbial Induced Calcite Precipitation. *Geo-Congress 2012: State of the Art and Practice in Geotechnical Engineering*, p. 1918-1927.

O'Flaherty, C.A., David, H.T., Davidson, D.T., (1961). Relationship Between the California Beraing Ratio and the Unconfined Compressive Strength of Sand-Cement Mixtures. *Proceedings of the Iowa Academy of Science,* Vol. 68, Article 52.

Phillips, A.J. (2013). Biofilm-induced Calcium Carbonate Precipitation: Application in the Subsurface. Doctoral dissertation, Montana State University, Bozeman, MT, USA.

Phillips, A.J., Gerlach, R., Lauchnor, E., Mitchell, A.C., Cunningham, A., Spangler, L. (2013a). Engineered applications of ureolytic biomineralization: a review. *Biofouling*, Vol. 29, p. 715-733.

Phillips, A.J., Lauchnor, E., Eldring, J., Esposito R., Mitchell, A.C., Gerlach, R., Cunningham, A., and Spangler, L. (2013b). Potential CO_2 leakage reduction through biofilm-induced calcium carbonate precipitation, *Environmental Science & Technology*, Vol. 47 (1), p. 142-149

Pongsivasathiti, S., Horpibulsuk, S., Piayphipat, S. (2019). Assessment of Mechanical Properties of Cement Stabilized Soils. *Case Studies in Construction Materials*, 11th Edition.

Thompson, M.R. (1966). Shear Strength and Elastic Properties of Lime-Soil Mixtures. Highway Research Board, University of Illinois, Champaign, IL, 1-14.

U.S. Department of the Army. (2016). *Theater of Operations: Roads, Airfields, and Heliports – Airfield and Heliport Design* (TM 3-34.48-2).

Whiffin, V.S. (2004). Microbial $CaCO_3$ Precipitation for the production of Biocement. Doctoral Dissertation, Murdoch University, Perth, WA, AU.

Yasuhara, H., Neupane, D., Hayashi, K., Okamura, M. (2012). Experiments and predictions of physical properties of sand cemented by enzymatically-induced carbonate precipitation. *Soils Found*, Vol. 52, p. 539-549

CHAPTER THREE

PAPER 2 - UREOLYSIS-INDUCED CALCITE PRECIPITATION (UICP): INJECTION STRATEGIES AND THE EFFECT ON STRENGTH AND FAILURE MECHANISM

Contribution of Authors and Co-authors

Manuscript in Chapter Three

Author: Hudson Dorian

Contributions: Held primary research position during experiments, conducting treatment of the soil specimens, strength evaluations, and acid digests. Conducted data analysis. Provided first draft of manuscript and conducted revision.

Co-Author: Mohammad Khosravi

Contributions: Provided research guidance and revision to manuscript.

Co-Author: Adrienne Phillips

Contributions: Coordinated research plans across research team.

Co-Author: Pinar Gunyol

Contributions: Provided research guidance.

Co-Author: Jenna Lauf

Contributions: Provided assistance in treatment of specimens, conducting UCS testing, and conducting data analysis.

Co-Author: Ethan Dudley

Contributions: Conducted batch study and performed data analysis, and conducted treatment of soil specimens using alternative recipes.

Co-Author: Maneesh Gupta

Contribution: Provided research guidance.

Co-Author: Emmanual Parushev

Contribution: Provided research guidance.

Manuscript Information

Hudson Dorian, Mohammad Khosravi, Adrienne Phillips, Pinar Gunyol, Jenna Lauf, Ethan Dudley, Maneesh Gupta, Emmanuel Parushev

Journal of Geotechnical and Geoenvironmental Engineering

Status of Manuscript:
__X__ Prepared for submission to a peer-reviewed journal.
_____ Officially submitted to a peer-reviewed journal.
_____ Accepted by a peer-reviewed journal.
_____ Published in a peer-reviewed journal.

American Society of Civil Engineers

Abstract

In this research effort, a series of Unconfined Compressive Strength (UCS) tests were conducted to evaluate the effect of injection strategy on the failure mechanism and strength properties of sand columns bio-cemented using ureolysis-induced calcite precipitation (UICP). The use of commercial ingredients on the bacterial growth and precipitation was also investigated through a series of batch studies and UCS testing. The results, comparing multiple recipes for the solutions involved, found success in the use of cheaper, commercial ingredients to grow the bacterial cultures needed, producing solutions at costs as low as 20 cents per liter for treatment. Soil columns were treated using different directions of injection, and it was found that administering the solutions from the top down did not inhibit the precipitation of calcite. This result is favorable to the envisioned large-scale, in-situ application of shallow surface treatment. Additional soil columns, treated using the alternative, less costly recipes, were also able to achieve an increase in strength. Overall, these results are positive, providing credibility to the potential for such an application.

Introduction

As the needs of a developing world increase, more is demanded out of the land used to resolve them. Surface stabilization is an especially relevant concern, accounting for erosion, wearability, and liquefaction, often attributable to a lack of internal cohesive strength. These deficiencies result in reduced ‘usability’ of the land, presenting a challenge in effective land development. Highly erodible soils can be subject to transport or loss of soil mass when exposed to external forces like wind or water, potentially undermining structures and leading to differential

settlement. Liquefactible soils are a significant concern in the case of earthquakes, susceptible to sudden failure, requiring specific considerations in the land's use due to the risk posed (e.g. ICC, 2021). As mentioned, a commonality between these soil types is a lack of cohesive strength; could an element of cohesive strength be added to these soils, the concerns posed could be reduced. Herein is the relevance of ureolysis-induced calcite precipitation (UICP). This process uses the enzyme urease, often resourced through the bacterium *Sporosarcina pasteurii*, to take in urea and produce carbonate (Equation. 3-1). This can then precipitate solid calcium carbonate ($CaCO_3$) or 'calcite' when provided a calcium source (Equation. 3-2), usually calcium chloride ($CaCl_2$). When this reaction is conducted in a soil medium, it was found that the calcite crystals would precipitate onto the soil particles, providing as an effective means of soil solidification by bridging particles together (Gollapudi et al., 1995; Kirkland et al., 2021). This process has since become an attractive subject of research as a potential method of soil improvement, in terms of strength and stability.

$$CO(NH_2)_2 + 2H_2O + Urease \rightarrow 2NH_4^+ + CO_3^{2-} \quad \text{Equation 3-1.}$$

$$Ca^{2+} + CO_3^{2-} \rightarrow CaCO_3 \quad \text{Equation 3-2.}$$

When this reaction is conducted in a soil medium, it was found that the calcite crystals would precipitate off the soil particles, providing as an effective means of solidification (Gollapudi et al., 1995; DeJong et al., 2010; Kirkland et al., 2021). This process has since become an attractive subject of research as a potential method of soil improvement, in terms of strength and stability (Phillips et al., 2013; Dick et al., 2006; Jiang et al. 2019; van Paassen et al., 2009).

Previous studies on the use of bio-cementation for surficial soil stabilization have focused on surface-water-induced erosion control (Montaya et al., 2018; Chek et al., 2021; Ghasemi et al., 2019; Hodges and Lingwall, 2020; Jiang et al., 2019; Ghasemi and Montaya, 2022), scour mitigation (Do et al., 2020), wind erosion and dust control (Maleki et al. 2016; Zhan et al., 2016),

and mitigation of wave-induced erosion of coastal sand dunes (Liu et al., 2021; Montoya et al., 2021; Shanahan and Montoya, 2016). The main challenges with the implementation of UICP for surface soil stabilization are uniformity, penetration of the soil, and cost. As such, existing research efforts have included adjustment of the injection scheme to promote uniformity (San Pablo et al. 2020, Martinez et al., 2013; Gunyol et al., 2022), observations of the evident relationship between precipitate quality and soil characteristics (DeJong et al., 2010; Li et al., 2004; Pungrasmi et al., 2019) or mineralogy (Safavizadeh et al., 2019; Liu and Montoya, 2021). Other efforts have endeavored to characterize the impact of treatment on soil behavior, measuring shear stiffness through shear wave velocity measurements (Montoya et al., 2013; DeJong et al., 2017), and the relationship of various treatment conditions to shear strength, such as the treatment solutions (Xiao et al., 2021) and soil characteristics (Simatupang et al., 2018; Nafisi et al., 2020).

Could this treatment be applied on a large scale to exposed, cohesionless soil and increase the internal cohesive strength, the risks associated with internal destabilization could be reduced. As a result, the land could be used more readily. However, there is the concern of this conceptual application's feasibility, as the treatment process used needs to be compatible with large-scale usage. In a state-of-the-art review of UICP applications by Rahman et al. (2020), a comparison between the soil strengths achieved through UICP treatment across multiple research efforts is provided, showing unconfined compressive strength (UCS) ranging from 0.03 and 10 megapascals. In comparing the results for one soil type, 20-30 Ottawa sand for example, results are just as disparate. Comparing two of these research efforts focused on the treatment of Ottawa sand (Choi et al., 2016; Liu et al., 2019), there are apparent differences in the methods of treatment used in each, such as the residence or standing time for each injection or the recipes for the solutions used. The resulting increases to the soil strength also differ; Liu et al. (2019) achieved a

maximum of 2.3 Megapascals (MPa), while Choi et al. (2016) achieved only 1.7 MPa. This suggests that the resulting effect from the UICP process may be reliant on the treatment process.

As related to large-scale application, there is a concern with the direction of treatment. For treating in-situ soil, the most appealing and promising method is to inject solutions from the soil surface, downwards (Jiang et al., 2019, Ghasemi and Montoya, 2022). Smaller scale efforts in the past have treated specimens from the top to the bottom (Choi et al., 2016; Liu et al., 2019), from the bottom to the top (Gunyol et al., 2022), or in an alternating fashion (Mortensen et al., 2011), all met with success in increasing the mechanical properties of the treated soil. Prior to any consideration of large-scale application, it should be known as to whether the most accessible method of treatment (through the soil surface) will provide the most effective improvement to strength. Also, regarding field applications, there is the consideration of the solutions used and the associated cost. In the lab setting typical for these treatments, lab-grade ingredients are used, provoking no issue, but as the required volumes for the injections increase, the costs increase significantly. This aspect of cost reduction has been a subject of previous research efforts, primarily in substituting the source of carbon for the bacteria (Achal et al., 2009; Omoregie et al. 2019) or through other methods of improving the efficiency of the treatment (e.g. Maleki-Kakelar et al., 2021). Could the lab-grade ingredients be substituted for cheaper, commercially-available alternatives, with no negative impact on their performance, this process would be better suited for larger volumes of soil (Yang et al., 2022; Chen et al., 2022). Similarly to the injection direction, any potential effect due to the change of ingredients should be understood before use in treatment of the soil.

To address these current issues, this research effort aimed to investigate 1) the cost reduction that could be achieved through the use of commercial ingredients, and their effect or

lack of on the bacterial growth and precipitation, and 2) the effect of injection direction on the resulting increase to strength and precipitate distribution in the treated soil. To address the first, a cost analysis and batch study are conducted using various alternative recipes. To test the bacterial solutions, samples were inoculated with bacteria, growth monitored over a set period to observe if the alternative recipes performed at least as well as the lab-grade recipes. For the actual administration of the treatment, using the lab-grade recipes, three methods of injection were to be directly compared. To address the second, six soil columns were treated through the UICP process, using the same material compacted to the same relative density, only varying in injection direction: bottom-to-top, top-to-bottom, and alternating, each in replicate. The resulting improvement achieved through each method was evaluated for unconfined compressive strength and calcite content distribution over the length of the respective specimens. An additional set of three columns were subjected to the top-to-bottom treatment method, instead using the alternative recipes, also evaluated for strength and calcium distribution.

Materials and Methods

Microbial Growth

Frozen stocks of *S. pasteurii* were used to produce bacterial 'starter' cultures for testing, thawed and added to 99 mL of a brain-heart infusion and urea solution (BHI), at 3.7% and 2.0% concentrations respectively, in DI water. The flask was covered and placed into a shaking incubator set to maintain 30 degrees Centigrade and 150 revolutions per minute. This sample was allowed to incubate for 16 hours. This starter was then used to inoculate a bacterial solution for the treatment process.

Media

The process of UICP is done using an alternating set of fluids introduced into a medium. Based on the method developed by Whiffin (2004), the two solutions initially used, were CMM- and CMM+. These were referred to as the 'lab-grade' recipes. A set of alternative, 'yeast-extract-based' recipes were proposed as a method of cost reduction. The bacterial growth solutions, BHI + Urea, CMM-, YEH-, YEM-, and YEL- were used to propagate bacterial cultures for treatment, the recipes established by Table 3-1 (product abbreviations established in Table A1). These were evaluated through the use of a comparative batch study. The calcium-providing solutions, recipes established in Table 3-2, share the same base set of ingredients, but include calcium chloride. These were not tested using the batch study.

Table 3-3. - Alternative recipes for bacterial growth solutions. See Table A1 in the appendix for detailed description of ingredient type.

Recipe	Carbon		Urea		Ammonium Chloride	
	Prod.	**Conc (g/L)**	**Prod.**	**Conc (g/L)**	**Prod.**	**Conc (g/L)**
BHI + Urea	*BHI*	37	*FS Urea*	20	*N/A*	
CMM-	*NB*	3	*FS Urea*	20	*FS NH_4Cl*	10
YEH-	*YE*	15.5	*DEF*	20	*FS NH_4Cl*	1
YEM-	*YE*	8	*DEF*	20	*FS NH_4Cl*	1
YEL-	*YE*	4	*DEF*	20	*FS NH_4Cl*	1

Table 3-4. - Alternative recipes for calcium solution. See Table A1 in the appendix for detailed description of individual ingredients.

Recipe	Carbon		Urea		Amm. Chloride		$CaCl_2$	
	Prod.	Conc (g/L)	Prod.	Conc (g/L)	Prod.	Conc (g/L)	Prod.	Conc. (g/L)
CMM+	*NB*	3	*FS Urea*	20	*FS NH_4Cl*	10	*FS $CaCl_2$*	49
YEH+	*YE*	15.5	*DEF*	20	*FS NH_4Cl*	1	*PW*	49
YEM+	*YE*	8	*DEF*	20	*FS NH_4Cl*	1	*PW*	49
YEL+	*YE*	4	*DEF*	20	*FS NH_4Cl*	1	*PW*	49

Batch Studies

The impact of the changes in ingredients on the bacterial growth needed to be considered. Batch studies were conducted to assess the bacterial growth in different combinations of nutrient sources, those tested provided in Table 3-1. Growth of a bacterial culture in the recipes lifted from Whiffin (2004) were compared to that in high, medium, and low-carbon variations of the yeast-extract-based recipe (YEH-, YEM-, and YEL-). The CMM-based and alternative recipes were compared against the performance of a brain-heart infusion with urea (BHI), representing optimal bacterial propagation.

100 mL of each solution was placed inside an Erlenmeyer flask, combined with an initial one-percent dilution of a BHI-based bacterial stater culture, and allowed to incubate for 24 hours. For each recipe, four flasks were prepared; three inoculated, one left as a control. Initially, (zero hours), then 1, 2, 4, 6, 8, 12, and 24 hours after initiating the propagation, these solutions were sampled and tested. The samples were assessed through an optical density (OD) reading and a urea assay. For the 0, 2, 6, 12, and 24-hour samples a pH measurement was also conducted.

Optical Density. The optical density (OD) reading was used to qualitatively measure the bacterial population density. At each testing period, three 200-microliter samples were taken

from each flask and placed into a Greiner 96-well plate. This plate was placed into a Tecan infinite F50 plate readerand read with a light at a fixed wavelength of 600 nanometers. The values from the three samples were averaged. These values were recorded over time as a way of tracking the growth of the bacterial populations for a specific solution.

Jung Assay. The Jung assay was used as a method of tracking the consumption of urea by propagation of the bacteria, the process established by Jung et al. (1975) The test was done according to the same procedure used by Phillips (2013). Samples were diluted at a 1:10 ratio in 10% nitric acid, as to fall within a readable range for the assay and halt the reaction. Results were taken across the 3 samples and averaged, providing a result for that flask.

pH Testing. For the pH reading, a two-milliliter sample was taken from each flask and placed into a 15-milliliter centrifuge tube. After collection, an RS323 pH-probe was used to measure the pH level of the sample, suspended in the fluid until the reading stabilized. The probe used was subjected to three-point calibration in buffer solutions prior to testing. Full ureolysis would be suggested by an increase in the pH of the solution, from neutral to slightly basic (approximately nine pH).

Cost Analysis. To evaluate the comparative cost advantage of the commercially sourced, alternative recipes, the typical market price of the ingredients was investigated, and used to determine the per-liter cost of each recipe. This was done by determining the cost of the unit available for purchase (unit cost), as well as the mass of the product provided in the unit (unit mass). With these values, a unit cost per gram was established for each, which could be applied to the masses used for the concentrations for each recipe.

Soil Column Testing

All soil specimens were prepared in columns with an inner diameter of 50 mm and a height of 100 mm, featuring ports at the bottom and top for passage of fluid. These were previously the subject of a conference paper (Dorian et al., 2023), the design process and analysis of results expanded upon in more detail here. Reactors were constructed from plastic concrete molds with a snapping cap, holes drilled in the top and bottom into which barbed six-millimeter-diameter fittings were fixed. These reactors, and the general setup for treatment, are shown in Figure 3-1. The plastic of the mold was strong enough to contain the specimen during compaction and treatment, and withstand fluid pressure, but was pliable enough to cut through to allow relatively easy sample extraction. Flexible PVC tubing, with an internal diameter of six millimeters, connected the ports to the 60 mL syringes, used to inject fluid to the soil medium at a fixed rate. The port used to introduce fluid was referred to as the 'inlet,' and the port used for drainage the 'outlet.'

Sakrete® medium commercial silica sand was selected, the characteristics of which are provided in Table A2. Properties of the uniform sand included the following: a relative density (D_r) of 35%, maximum void ratio (e_{max}) of 0.97, minimum void ratio (e_{min}) of 0.53, and median grain size, (D_{50}) of 0.67 mm. e_{max} and e_{min} were determined following ASTM standards D4253 (ASTM 2002a) and D4254 (ASTM 2002b), while G_s was determined following standard D854 (ASTM 2014). The soil samples were constructed layer by layer; each layer was compacted to a target relative density of D_r = 35%, up to the top. Soil was compacted into the reactors using a wet-tamping procedure, established by Ladd (1978), and revised by Chan (1985). The amount of soil required for each lift, and the thickness to be achieved through compaction for each, was determined based on the desired density. Compaction was performed in five lifts with moist soil

(a moisture content of 7%) distributed evenly for each layer. To prevent excessive compaction of lower layers, an initial degree of undercompaction was included in the process.

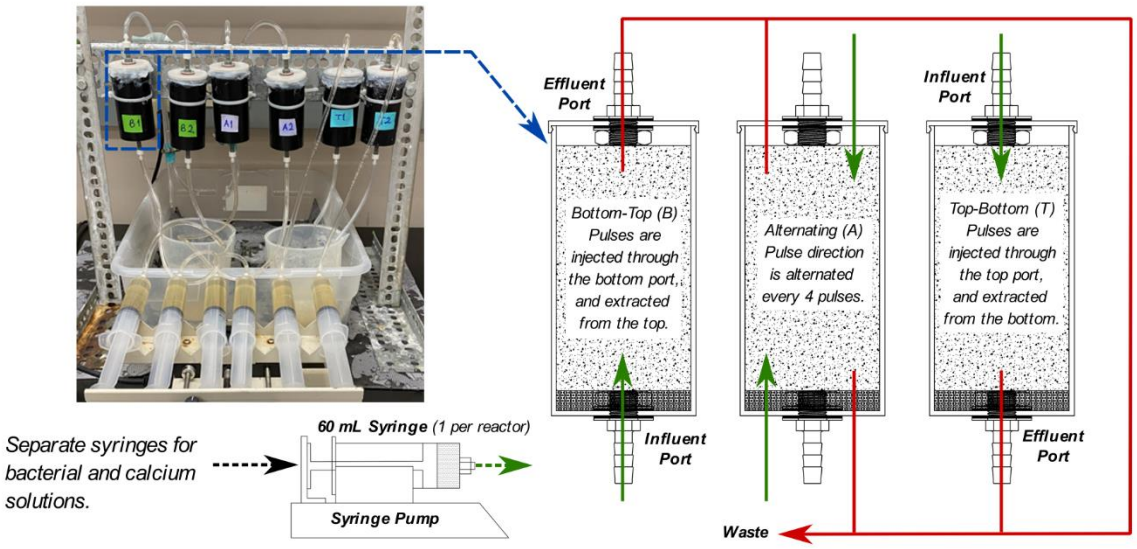

Figure 3-1. - Testing setup for reactors, detailing treatment methods and process, and showing reactor section.

Injection Strategy. The central interest for this experiment was the effect of a specific injection strategy, if any, on the resulting distribution of calcite precipitation and specimen strength. To address this, three strategies were used: Bottom-to-top, (B) where fluids were injected through the bottom and drained from the top; Top-to-bottom, (T) injected through the top and drained from the bottom; and alternating, (A) where direction was changed after every fourth injection. Specifically of interest was the efficacy of a top-down treatment, most suitable for treatment of exposed soil surfaces, as injections could be administered directly to soil surface. The goal was to evaluate relative performance of this method against the bottom-top method, used more frequently, and an alternating treatment method, such as that proposed by Mortensen et al. (2011). Were the top-bottom method found to provide similar results to the bottom-top and

alternating methods, not resulting in a significant loss in cementation strength, the potential for the UICP process would be much greater for large-scale application.

In addition to the six columns discussed, an additional three were treated using one of the injection methods, substituting the original recipes with a yeast-extract-based alternatives. Similar to the previous evaluation, were the substitute recipes to provide a similar degree of precipitation and strength improvement to the soil, there would be greater potential for field applications of the UICP method, reducing the burden of cost without a loss in performance.

Effluent fluid sampling. The injection design allowed for assessment of the reaction progression, primarily though sampling of the effluent. A certain amount of time after the start of each injection, a sample was collected; this waiting period was determined based on the pore volume of the specimen and the injection rate, providing fluid that had been in the approximate center of the soil during its residence. The effluent samples were analyzed for urea concentration via a colorimetric Jung assay (Jung et al., 1975; Phillips, 2013), used to verify that that additional urea in the calcium solution was being effectively consumed, signifying successful ureolysis.

Unconfined Compressive Strength. Strength of the treated soil specimens was evaluated through the unconfined compressive strength (*UCS*) test established by ASTM D2166 (ASTM 2010). The results obtained from UCS testing can be directly applied to engineering design and analysis of shallow soil applications, providing a relative analogue of the stress conditions experienced by shallow soil layers. The specimens were extracted from the reactors after drying and top and bottom surfaces were filed to eliminate high points or unevenness; such irregularities could result in unrepresentatively high stress concentrations over small areas, leading to premature fracturing and failure. Each specimen was placed on a load frame, and the loading piston zeroed

onto its top surface. For the UCS test, both the applied load and deformation of the specimen are monitored, used to determine stress and strain respectively, so the testing process should start when the piston is in contact with the surface. The piston was then driven into the specimen at a controlled rate, causing a one-percent increase in strain every minute until the specimen failed. The failure mode was recorded, and the tested specimen was retained for calcium analysis.

$CaCO_3$ Determination. $CaCO_3$ content was determined using a gravimetric acid washing method, or an 'acid digest.' After treatment and strength testing, specimens were divided into 3 sections along the specimen's length (a top, middle, and bottom section), from which two samples each were taken. Each sample allowed to dry fully, then crushed to eliminate large clumps, and one gram was weighed into a centrifuge tube and combined with five mL of 10 % nitric acid (HNO_3) to dissolve the $CaCO_3$. This fluid was decanted and retained, and the soil was allowed to fully dry. The mass of the $CaCO_3$ present in the soil sample was calculated by measuring the difference between the initial oven-dried mass of the soil sample and that after decanting the acid and drying.

Results

The results of a series of column experiments combined with batch studies are presented to address two common issues associated with the application of MICP for field-scale surface treatment: cost and uniformity. The batch study results include cost analysis, as well as the OD, pH, and Jung assay results for different recipes (BHI, CMM, and the YE-based recipes), monitored over 24 hours. Additionally, the study covers the calcium carbonate precipitation profile and the

evaluation of the strength properties of MICP-treated sand specimens prepared using different injection strategies.

Cost Analysis of Recipes

The completed cost analysis of the different recipes is provided in Tables 3-3 and 3-4, for the bacterial and calcium solutions respectively. The price breakdown for each ingredient is based on the unit cost per gram, established by Table A1 in the supplement. As anticipated, the BHI recipe is the most expensive at $11.89 per liter, primarily due to the unit cost and required concentration of BHI. The typical lab-grade recipes, CMM- and CMM+ are the next-most expensive, with CMM+ ($4.72) costing nearly double that of the CMM ($2.66) due to the high cost per gram of the Fisher Scientific Calcium Chloride. The costs for the commercial-grade recipes are an order of magnitude lower than the lab-grade recipes. Among these, the high-carbon variants are the most expensive, $0.49 for the YEH+ and $0.39 for the YEH-. The low-carbon variants, on the other hand, are appropriately the least expensive, at $0.30 for the YEL+ and only $0.20 for the YEL-. The use of yeast extract instead of the lab-grade analogues proved to be the most significant reduction to the cost, especially when compared to the Becton Dickenson nutrient broth. With this in mind, further investigation for potential usability is justified, as these recipes would reduce the financial burden at larger scales of application.

Table 3-3. - Comparative cost of bacterial growth solution recipes in dollars per liter; YEH, YEM, and YEL are high-carbon, medium-carbon, and low-carbon variations of the same recipe.

Recipe	Carbon			Urea			Ammonium Chloride			Total Cost ($/L)
	Prod.	Conc (g/L)	Cost ($/L)	Prod.	Conc (g/L)	Cost ($/L)	Prod.	Conc (g/L)	Cost ($/L)	
BHI* + *Urea	BHI	37	10.60	FS Urea	20	1.29	N/A			11.89
CMM-	NB	3	1.06	FS Urea	20	1.29	FS NH_4Cl	10	0.31	2.66
YEH-	YE	15.5	0.26	DEF	20	0.10	FS NH_4Cl	1	0.03	0.39
YEM-	YE	8	0.13	DEF	20	0.10	FS NH_4Cl	1	0.03	0.26
YEL-	YE	4	0.07	DEF	20	0.10	FS NH_4Cl	1	0.03	0.20

Table 3-4. - Comparative cost of calcium solution recipes. Recipes are inherently the same as their non-calcium counterparts, but include 49 g/L of Calcium Chloride.

Recipe	Carbon, Urea, and Amm. Chloride Cost ($/L)	Calcium Chloride			Total Cost ($/L)
		Prod.	Conc (g/L)	Cost ($/L)	
CMM+	2.66	FS $CaCl_2$	49	2.16	4.72
YEH+	0.39	PW	49	0.10	0.49
YEM+	0.26	PW	49	0.10	0.36
YEL+	0.20	PW	49	0.10	0.30

Effect of Recipe on Bacterial Propagation

Figures 3-2, 3-3, and 3-4 present optical density, urea consumption, and pH reading over the 24-hour batch study, respectively. Results were collected across all flasks for a given recipe and averaged for the final curve. In Figure 3-2, the OD results plot average absorbance of the samples against time in hours. A higher absorbance indicates greater ‘cloudiness’ of the fluid, attributed to bacterial growth. These results showed that all yeast-extract-based recipes (YEH)

reached a higher optical density than the CMM- could achieve by the 12-hour mark. However, all three alternative recipes showed a slight delay in growth during the early incubation period, where CMM- exhibited more notable growth from one to six hours after inoculation. This delay was particularly pronounced in YEH-, which did not show significant growth until the 12-hour mark, where it suddenly exhibited a substantial increase.

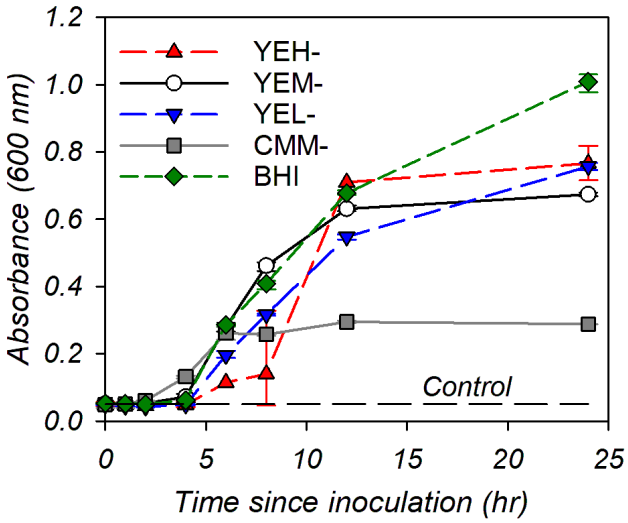

Figure 3-2. - Batch study optical density analysis over 24 hours; averaged across 3 specimens per recipe, with 3 samples per specimen.

The urea consumption results are presented in Figure 3-3, showing that CMM- saw the fastest consumption of urea, but only by a small margin compared to the BHI and YEM-; practically, all three performed the same, having consumed all present urea to non-readable levels by eight hours. YEH- saw a faster initial, but a more prolonged trend in the consumption of urea. This observation aligns with the findings from the OD results for the YEH-. The relationship between the urea concentration and optical density is less visibly correlated for YEL-, however.

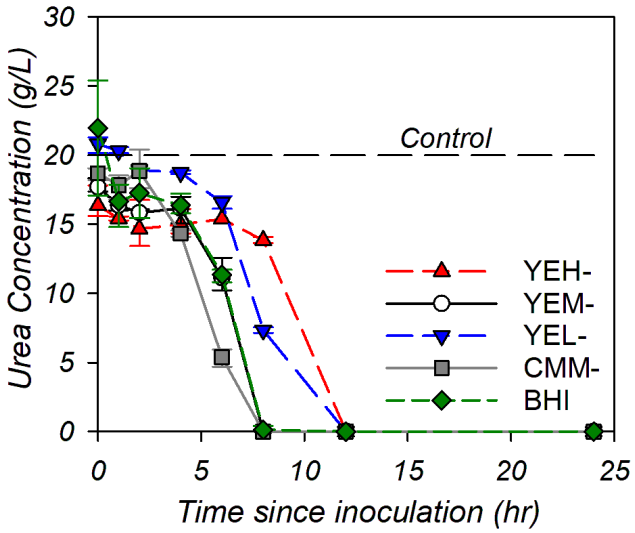

Figure 3-3. – Batch study urea concentration over 24 hours, determined by Jung Assay; averaged across 3 specimens per recipe, 3 samples per specimen.

The pH results are shown in Figure 3-4. The change in pH level throughout incubation saw relatively little difference between the recipes, suggesting a similar observed effect of ureolysis as the fluids become more basic. From the zero-hour datapoints, it appears that YEL- had the highest initial pH, while YEM- had the lowest. Regardless, the progression toward a more basic state appeared to be unimpeded.

In terms of recipe performance for bacterial propagation, the yeast-extract-based recipes performed just as well, if not better in some measures, than the original CMM- recipe. Based on optical density, all yeast-extract-based recipes outperformed the CMM-, indicating a greater resulting bacterial population density. It is possible that with the additional carbon material in these recipes allowed the bacteria to continue to propagate once the urea was depleted, which the lower nutrient content in the CMM- could not. However, this is speculative reasoning.

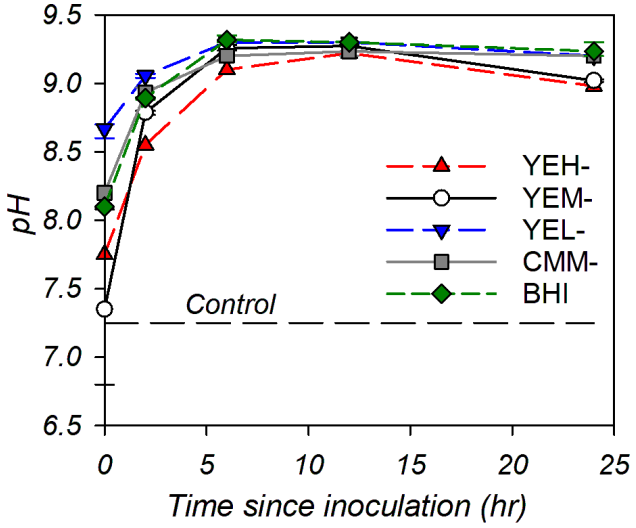

Figure 3-4. - Batch study pH level over 24 hours; measured every other hour and at 24 hours; averaged across 3 specimens per recipe.

Effect of Injection Method on Specimen Strength

The stress-strain response up to the failure of the treated soil specimens through the UCS test are shown in Figure 3-5. Peak strengths were recorded and are presented in Table 3-5. From the results, it can be observed that the top-bottom method consistently provided the highest strength. Specimen one from the top-bottom method, labeled as 'T1,' exhibited the greatest strength and brittle behavior, with T2 following; notably, T2 showed a slightly lower peak strength but displayed a more ductile pattern of behavior. Both the specimens from the top-bottom method appeared to outperform those of the other treatment methods.

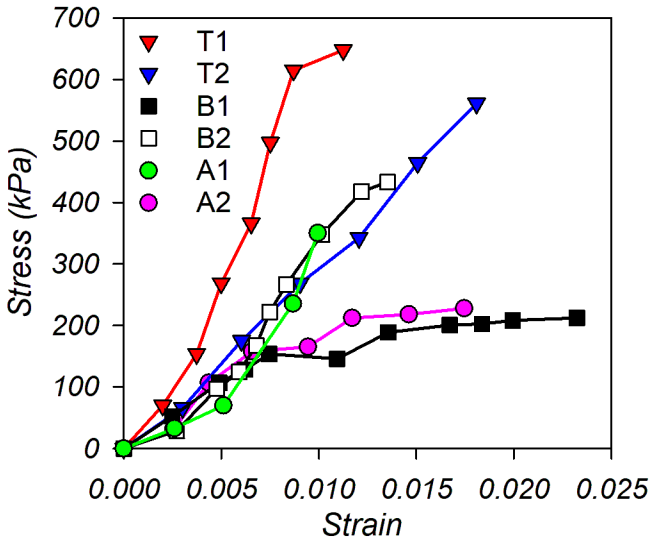

Figure 3-5. - Comparative UCS stress (force over area) versus strain (deformation over original length) between treatment methods using standard recipes (CMM- and CMM+). The amount of strain that a specimen withstood before failure was related to its relative ductility (high strain) or brittleness (low strain); e.g. specimen T1 exhibited relatively brittle behavior, while T2 showed more ductile behavior.

Table 3-5. - Peak UCS strength (kPa) for treated soil columns; letter indicates treatment method, and number is the specimen number for that method.

Peak Deviatoric Stress (kPa)					
B1	**B2**	**A1**	**A2**	**T1**	**T2**
212.1	433.4	350.1	227.7	647.6	560.9

As for a reason why the top-bottom method prevailed in strength, the results of the calcium digest analysis (Figure 3-6) across the specimens suggested that it may be attributable to the relative uniformity of the calcite's distribution along the length of the treated specimen. The digest results for all samples for a specific treatment method were compiled into a box-and-whisker diagram, with each box representing a section of the column, displaying the median value and range. While the top-bottom method did not produce the highest amount of precipitate by percent

mass (only 4.5% on average overall), it did provide the least variability through the length of the column. Comparatively, the bottom-top and alternating methods resulted in more cementation on average (6.9% and 6.3% respectively), but with less even of a distribution through the column's length. This variation in the distribution could be caused by a filtration effect within the soil medium, where 'more' of a reaction takes place at the initial location of injection, less reactants left in the solution moving further along the length of the soil. For the top-bottom method, the force of gravity may simultaneously encourage the penetration of fluid to lower depths. However, an analysis of variance test run on the data showed little evidence (p-value of 0.234) for the effect of the method after accounting for the segment (top, middle, or bottom) on calcium carbonate content. This suggests that the variation in the resulting distributions is not statistically significant enough to claim the effect of each method. More replication of this experiment, accompanied by tracer-fluid analyses would be a better means of evaluating the performance of each of these treatment configurations.

As discussed, the degree of strength improvement to the soil through UICP can vary substantially. Supplementary Table A3 provides a collection of results from various research efforts, showing the maximum UCS achieved through UICP treatment of medium to coarse sands, similar to that used in this experiment, illustrating the range of results possible. Not only did the relationship between treatment and strength vary, but also that between amount of precipitate and strength; for instance, Danjo and Kawasake (2016) achieved a UCS of 10 MPa with an average of 29% calcite by mass, while Terzis and Laloui (2019) achieved 11.3 MPa with only 9% calcite. This may suggest that the strength of treated soil is not only related to the amount of precipitate but also the mechanism of precipitation (IE how the precipitate forms between the soil particles). Such variations are evidently attributable to differences in reactor design, treatment method, and

other parameters as specified by the treatment conditions used to achieve the maximum strength. The specimens generated in this effort, and other experiments as well, are not universal representations of the product of the UICP procedure, and it is unknown if the same trend would be evident had other parameters been changed.

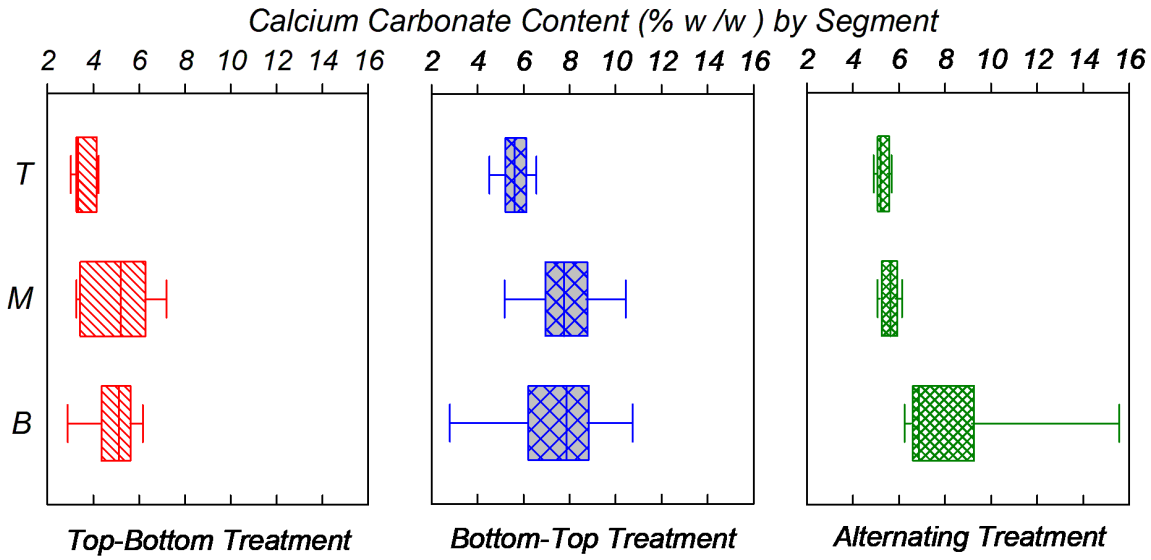

Figure 3-6. - Calcium carbonate ($CaCO_3$) content by column segment, organized by statistical results of 2 samples per method; determined by percent mass through calcium digests of 1-gram samples.

Effect of Recipe on Specimen Strength

In addition to the batch study, the original CMM- recipe was replaced with the base YEH- recipe for treating of three soil columns, the calcium solution, CMM+, replaced with YEL+. The rationale behind this change was that the nutrient content of the calcium solution was less critical than that of the bacterial solution, the calcium solution being more responsible for delivery of urea and calcium and not the further propagation of the bacteria. Soil columns were prepared the same as the previous soil specimens and treated using the top-bottom method. The UCS testing and

calcium carbonate distribution analysis was conducted, and the results are depicted in Figure 3-7, peak strengths summarized in Table 3-6, and Figure 3-8 respectively.

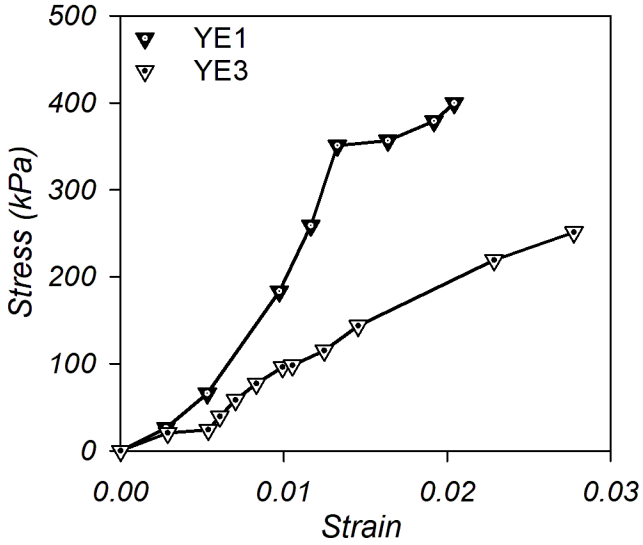

Figure 3-2. - UCS stress versus strain for YEH-/YEL+ treated specimens.

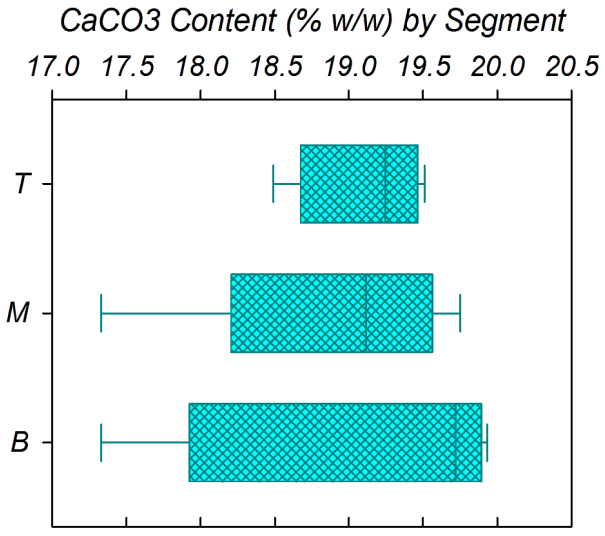

Figure 3-3. - Calcium carbonate content by segment for YEH-/YEL+ treated specimens, determined by percent mass through calcium digests.

Of the three specimens treated with the YEH- and YEL+ recipes, only two were successfully tested, one of the specimens having failed upon removal from the reactor. The results were disparate from the top-bottom-treated specimens using the original CMM recipe, only reaching a maximum of 400 kPa, with more variance in the resulting strength. These specimens still saw an improvement in strength, albeit to a lesser degree compared to the specimens treated using the CMM- and CMM+ recipe set with the same treatment method. It is worth noting that these specimens were treated at a different time, using a different bacterial culture, and done by a different researcher, introducing potential for variability in the specimens.

Table 3-6. - Peak UCS strength (kPa) for treated soil columns using yeast-extract-based solutions (YEH-, YEL+).

Peak Deviatoric Stress (kPa)	
YE 1	**YE 3**
399.8	251.1

Conclusions

A series of column experiments and batch studies were conducted to tackle two common issues associated with the application of MICP for surface application: cost and quality of improvement. Three different strategies, namely Bottom-to-top, (B); Top-to-bottom, (T); and alternating, (A), were employed on soil columns using various recipes. Although it is difficult to definitively determine the superiority of one treatment method over another, it can be asserted that administering the MICP treatment from the top downward proves to be effective in enhancing soil cohesion through the precipitation of calcite. This observation is consistent across the tested treatment strategies.

The results of this study suggested that the substitution of commercially available alternatives to lab ingredients used for the injections in the UICP process do not impede the overall growth of *S. pasteurii* cultures. While the impact of the change in ingredients on degree of soil strength improvement is not fully understood, likely requiring a larger series of tests or more directly comparable testing, it can be concluded that the new ingredients used did result in calcite precipitation, producing an increase in the strength of the soil. Compounding with the significant reduction in cost from their usage, and the success seen in the batch study tests, further research efforts are justified.

These takeaways do provide some additional credit to UICP as a method of soil erosion mitigation, at least in respect to the feasibility of treatment. As the top-bottom method of treatment did not hinder the precipitation process, this general method of treatment could be much more easily applied to existing soil, as opposed to the other methods discussed. Additionally, since the commercially available ingredients did not inhibit or hinder the growth of the bacteria, and did result in successful strengthening of the soil, the process can be done at a fairly low cost, much more conducive to large-scale application.

However, that does not mean the method is ready for large-scale application at this current point. There are other considerations necessary, such as the extraction of fluid, lateral spread of injections and the necessary spatial intervals of treatment, and suitable equipment and procedures for larger scales. As shown in Table A3, additionally, further refinement of the process is still necessary to produce the most effective improvement to strength. At this point, there are other focal points for research that would be best understood before field application, such as the effect of scale on the process and the relationship between the quantity of calcite precipitation and the respective increase in strength. The research conducted, and the results reached, suggest that the

UICP process *could* be used for this purpose, and may serve as a useful steppingstone for future research efforts.

References

Achal, V., Mukherjee, A., Basu, P.C., Reddy, M.S. 2009. "Lactose mother liquor as an alternative nutrient source for microbial concrete production by Sporosarcina pasteurii." Journal for Industrial Microbiology and Biotechnology., Vol. 36, p. 433-438. https://doi.org/10.1007/s10295-008-0514-7.

ASTM. 2002a. *Standard Test Methods for Maximum Index Density and Unit Weight of Soils Using a Vibratory Table.* D4253. https://www.astm.org/d4253-16e01.html.

ASTM. 2002b. *Standard Test Methods for Minimum Index Density and Unit Weight of Soils and Calculation of Relative Density.* D4254. https://www.astm.org/d4254-16.html.

ASTM. 2010. *Standard Test Method for Unconfined Compressive Strength of Cohesive Soil.* D2166. https://www.astm.org/standards/d2166.

ASTM. 2014. *Standard Test Methods for Specific Gravity of Soil Solids by Water Pycnometer.* D854. https://www.astm.org/d0854-14.html.

Chan, C.K. 1985. *Instruction manual, CKC E/P cyclic loading triaxial system users' manual.* San Fransisco, CA: Soil Engineering Equipment Company.

Chek, A., Crowley, R., Ellis, T.N., Durnin, M., Wingender, B. 2021. "Evaluation of Factors Affecting Erodibility Improvement for MICP-Treated Beach Sand." *Journal of Geotechnical and Geoenvironmental Engineering*, Vol. 147 (3). https://doi.org/10.1061/(ASCE)GT.1943-5606.0002481.

Chen, L., Song, Y., Fang, H., Feng, Q., Lai, C., Song, X. 2022. "Systematic optimization of a novel, cost-effective fermentation medium of Sporosarcina pasteurii for microbially induced calcite precipitation (MICP)." *Construction and Building Materials*, Vol. 348, 128632. https://doi.org/10.1016/j.conbuildmat.2022.128632.

Choi, S., Wang, K., Chu, J. 2016. "Properties of biocemented, fiber reinforced sand." *Construction and Building Materials*, Vol. 120, p. 623-629. https://doi.org/10.1016/j.conbuildmat.2016.05.124.

Cord-Ruwich, R., Shahin, M. 2013. "Cementation of sand soil by microbially induced calcite precipitation at various degrees of saturation." *Canadian Geotechnical Journal*, Vol. 50, p. 81-90. https://doi.org/10.1139/cgj-2012-0023.

Danjo, T., Kawasaki, S. 2016. "Microbially Induced Sand Cementation Method Using Pararhodobacter sp. Strain SO1, Inspired by Beachrock Formation Mechanism." *Materials Transactions,* Vol. 57 (3), p. 428-437. https://doi.org/10.2320/matertrans.M-M2015842.

DeJong, J.T., Mortensen, B.M., Martinez, B.C., Nelson, D.C. 2010. "Bio-mediated soil improvement." *Ecological Engineering,* Vol. 36, p. 197–210.DeJong, J.T, Burrall, M., Wilson, D.W., Frost, J.D. 2017. "A bio-inspired perspective for geotechnical engineering innovation." *Geotechnical Frontiers 2017.* American Society of Civil Engineers. p. 862-870. https://doi.org/10.1061/9780784480472.092.

Dick, J., Windt, W.M., Graef, B.D., Saveyn, H., Van der Meeren, P., Belie, N.D., Verstraete, W. 2006. "Bio-deposition of a calcium carbonate layer on degraded limestone by Bacillus species." *Biodegradation,* Vol. 17, p. 357-367. https://doi.org/10.1007/s10532-005-9006-x.

Do, J., B. M. Montoya, and M. A. Gabr. 2020. "Scour mitigation and erodibility improvement using microbially induced carbonate precipitation." *Geotechnical Testing Journal*, Vol. 44 (5): 1467–1483. https://doi.org/10.1520/GTJ20190478.

Ghasemi, P., A. Zamani, and B. Montoya. 2019. "The effect of chemical concentration on the strength and erodibility of MICP treated sands." *Geo-Congress 2020: Soil Improvement,* Geotechnical Special Publication 309, edited by C. L. Meehan, S. Kumar, M. A. Pando, and J. T. Coe, 241–249. Reston, VA: ASCE.

Ghasemi, P., Montaya, B.M. 2022. "Field Implementation of Microbially Induced Calcium Carbonate Precipitation for Surface Erosion Reduction of a Coastal Plain Sandy Slope." *Journal of Geotechnical and Geoenvironmental Engineering*, Vol. 148 (9), 04022071. https://doi.org/10.1061/(ASCE)GT.1943-5606.0002836.

Gollapudi, U.K., Knutson, C.L., Bang, S.S., Islam, M.R. 1995. "A new method for controlling leaching through permeable channels." *Chemosphere,* Vol. 30 (4), p. 695-705. https://doi.org/10.1016/0045-6535(94)00435-W.

Gunyol, P., Khosravi, M., Phillips, A., Plymesser, K. 2022. "Thermal Properties of Bio-Cemented Sand." *Geo-Congress 2022: State of the Art and Practice in Geotechnical Engineering*, p. 356-364. https://doi.org/10.1061/9780784484012.037.

Hoang, T., Alleman, J., Cetin, B., Choi, S. 2020. "Engineering Properties of Biocementation Coarse- and Fine-Grained Sand Catalyzed By Bacterial Cells and Bacterial Enzyme." *Journal of Materials in Civil Engineering,* Vol. 32 (4), 04020030. https://doi.org/10.1061/(ASCE)MT.1943-5533.0003083.

Hodges, T. M., and B. N. Lingwall. 2020. “Case histories of full-scale microbial bio-cement application for surface erosion control.” *Geo-Congress 2020: Biogeotechnics,* Geotechnical Special Publication 320, edited by E. Kavazanjian, J. P. Hambleton, R. Makhnenko, and A. S. Budge, 9–19. Reston, VA: ASCE.

International Code Council. 2021. *International Building Code.* Fall Church, VA, USA: International Code Council.

Jiang, N.-J., C.-S. Tang, L.-Y. Yin, Y.-H. Xie, and B. Shi. 2019. “Applicability of microbial calcification method for sandy-slope surface erosion control.” *Journal of Materials in Civil Engineering,* Vol. 31 (11): 04019250. https://doi.org/10.1061/(ASCE)MT.1943-5533.0002897.

Jung, D., Biggs, H., Erikson, J., Ledyard, P.U. 1975. “New Colorimetric reaction for end-point, continuous-flow, and kinetic measurement of urea.” *Clinical Chemistry,* Vol. 21 (8), p. 1136-1140.

Kirkland, C.M., Hiebert, R., Hyatt, R., McCloskey, J., Kirksey, J., Thane, A., Cunningham, A.B., Gerlach, R., Spangler, L., Phillips, A.J. 2021. “Direct Injection of Biomineralizing Agents to Restore Injectivity and Wellbore Integrity.” *SPE Production & Operations*, Vol. 36. https://doi.org/10.2118/203845-PA.

Ladd, R.S. 1978. “Preparing Test Specimens Using Undercompaction.” *Geotechnical Testing Journal*, Vol. 1 (1), p. 16-23. https://doi.org/10.1520/GTJ10364J.

Lauchnor, E.G., Topp, D.M., Parker, A.E., Gerlach, R. 2015. “Whole cell kinetics of ureolysis by Sporosarcina pasteurii.” *Journal of Applied Microbiology*, Vol. 118, p. 1321-1332. https://doi.org/10.1111/jam.12804.

Li, M., Wen, K., Li, Y., Zhu, L. 2018. “Impact of Oxygen Availability on Microbially Induced Calcite Precipitation (MICP) Treatment. Calcerous Sand.” *Canadian Geotechnical Journal*, Vol. 56, p. 1502-1513. https://doi.org/10.1139/cgj-2018-0007.

Li., X., Scheibe, T.D., Johnson, W.P. 2004. “Apparent decreases in colloid deposition rate coefficients with distance of transport under unfavorable deposition conditions: a general phenomenon.” *Environmental Science Technology*, Vol. 38 (11), p. 5616-5625. https://doi.org/10.1021/es049154v.

Liu, K. W., N. J. Jiang, J. Qin, Y. J. Wang, C. S. Tang, and X. Han. 2021. “An experimental study of mitigating coastal sand dune erosion by microbial- and enzymatic-induced carbonate precipitation.” *Acta Geotechnica,* Vol. 16 (2), p. 467–480. https://doi.org/10.1007/s11440-020-01046-z.

Liu, L., Liu, H., Stuedlein, A.W., Evans, M.T., Xiao, Y. 2019. "Strength, Stiffness, and Microstructure Characteristics of Biocemented Calcerous Sand." *Canadian Geotechnical Journal*, Vol. 56, p. 1502-1513. https://doi.org/10.1139/cgj-2018-0007.

Liu, Q., Montoya, B.M. 2021 "Microbial-induced calcium carbonate precipitation to accelerate sedimentation of fine tailings." *Journal of Geotechnical and Geoenvironmental Engineering*, Vol. 147 (10), 02821001. https://doi.org/10.1061/(ASCE)GT.1943-5606.0002651.

Maleki, M., S. Ebrahimi, F. Asadzadeh, and M. Emami Tabrizi. 2016. "Performance of microbial-induced carbonate precipitation on wind erosion control of sandy soil." *International Journal of Environmental Science Technology*, Vol. 13 (3), p. 937–944. https://doi.org/10.1007/s13762-015-0921-z.

Maleki-Kakelar, M., Aghaeinejad-Meybodi, A., Sanjideh, S., Azarhoosh, A.J. 2022. "Cost-Effective Optimization of Bacterial Urease Activity Using a Hybrid Method Based on Response Surface Methodology and Artificial Neural Networks." *Environmental Processes*, Vol. 9, 7. https://doi.org/10.1007/s40710-022-00564-0.

Martinez, B.C., DeJong, J.T., Ginn, T.R., Montoya, B.M., Barkouki, T.H., Hunt, C., Tanyu, B., Major, D. 2013. "Experimental optimization of microbial-induced carbonate precipitation for soil improvement." *Journal of Geotechnical and Geoenvironmental Engineering*, Vol. 139 (4), p. 587-598. https://doi.org/10.1061/(ASCE)GT.1943-5606.0000787.

Montoya, B.M., DeJong, J.T., Boulanger, R.W. 2013. Dynamic response of liquefiable sand improved by microbial-induced calcite precipitation. *Géotechnique*, Vol. 63 (4), p. 302-312. https://doi.org/10.1680/geot.SIP13.P.019.

Montoya, B. M., J. Do, and M. M. Gabr. (2018). "Erodibility of microbial induced carbonate precipitation-stabilized sand under submerged impinging jet." *IFCEE 2018*, p. 19–28. Reston, VA, ASCE.

Mortensen, B.M., Haber, M.J., DeJong, J.T., Caslake, L.F., Nelson, D.C. 2011. "Effects of environmental factors on microbial induced calcium carbonate precipitation: Environmental factors on MICP." *Journal of Applied Microbiology*, Vol. 111 (2), p. 338-349. https://doi.org/10.1111/j.1365-2672.2011.05065.x.

Nafisi, A., Montoya, B.M., Evans, T.M. 2020. "Shear strength envelopes of biocemented sands with varying particle size and cementation level." *Journal of Geotechnical and Geoenvironmental Engineering*, Vol. 146 (3), 04020002. https://doi.org/10.1061/(ASCE)GT.1943-5606.0002201.

Omoregie, A.I., Ngu, L.H., Ong, D.E.L., Nissom, P.M. 2019. "Low-cost cultivation of Sporosarcina pasteurii strain in food-grade yeast extract medium for microbially induced calcite precipitation (MICP) application." *Biocatalysis and Agricultural Biotechnology*, Vol. 17, p. 247-255. https://doi.org/10.1019.j.bcab.2018.11.030.

Phillips, A.J. 2013. "Biofilm-induced calcium carbonate precipitation: application in the subsurface." Doctoral Thesis, Montana State University, Bozeman, MT, USA.

Pungrasmi, W., Intarasoontron, J., Jongvivatsakul, P., Likitlersuang, S. 2019. "Evaluation of microencapsulation techniques for MICP bacterial spores applied in self-healing concrete." *Scientific Reports*, Vol. 9 (1), 12484. https://doi.org/10.1038/s41598-019-49002-6.

Safavizadeh, S., Montoya, B.M., Gabr, M.A. 2019. "Microbial induced calcium carbonate precipitation in coal ash." *Géotechnique,* Vol. 69 (8), p. 727-740. https://doi.org/10.1680/jgeot.18.P.062.

San Pablo, A.C.M., Lee, M., Graddy, C.M.R., Kolbus, C.M., Khan, M., Zamani, A., Martin, N., Acuff, C., DeJong, J.T., Gomez, M.G., Nelson, D.C. 2020. "Meter-scale biocementation experiments to advance process control and reduce impacts: Examining spatial control, ammonium by-product removal, and chemical reductions." *Journal of Geotechnical and Geoenvironmental Engineering.* Vol. 146 (11), 04020125. https://doi.org/10.1061/(ASCE)GT.1943-5606.0002377.

Shanahan, C., and B. M. Montoya. 2016. "Erosion reduction of coastal sands using microbial induced calcite precipitation." *Geo-Chicago 2016: Sustainability and Resiliency in Geotechnical Engineering,* Geotechnical Special Publication 269, edited by D. Zekkos, A. Farid, A. De, K. R. Reddy, and N. Yesiller, p. 458–466. Reston, VA: ASCE.

Simatupang, M., Okamura, M., Hayashi, K., Yasuhara, H. 2018. "Small-strain shear modulus and liquefaction resistance of sand with carbonate precipitation." *Soil Dynamics and Earthquake Engineering,* Vol. 115, p. 710-718. https://doi.org/10.1016/j.soildyn.2018.09.027.

Whiffin, V.S. 2004. "Microbial $CaCO_3$ Precipitation for the production of Biocement." Doctoral Dissertation. Perth, WA, AU: Murdoch University.

Xiao, Y., Wang, Y., Wang, S., Evans, T.M., Stuedlein, A.W., Chu, J., Zhao, C., Wu, H., Liu, H. 2021. "Homogeneity and mechanical behaviors of sands improved by a temperature-controlled one-phase MICP method." *Acta Geotechnica*, Vol. 16 (5), p. 1417-1427. https://doi.org/10.1007/s11440-020-01122-4.

Terzis, D., Laloui, L. 2019. "Cell-free soil bio-cementation with strength, dilatency and fabric characterization." *Acta Geotechnica*, Vol. 14, p. 639-656. https://doi.org/10.1007/s11440-019-00764-3.

CHAPTER FOUR

PAPER 3 – EFFECT OF UICP TREATMENT ON THE CBR VALUE OF SAND SPECIMENS, AND IMPLICATIONS FOR FIELD-SCALE PAVED STRUCTURE APPLICATIONS

Contribution of Authors and Co-authors

Manuscript in Chapter Four

Author: Hudson Dorian

Contributions: Held primary research position during experiments, conducting treatment of the soil specimens, strength evaluations, and acid digests. Constructed parts for soil reactors. Conducted data analysis. Provided first draft of manuscript and conducted revision.

Co-Author: Mohammad Khosravi

Contributions: Primary design lead in construction of soil reactors, provided revision to manuscript.

Co-Author: Adrienne Phillips

Contributions: Coordinated research plans across research team.

Co-Author: Jenna Lauf

Contributions: Provided assistance in treatment of specimens and in conducting data analysis.

Co-Author: Olayinka Durojaye

Contributions: Assisted in treatment process, data collection, and data analysis.

Co-Author: Alfred Cunningham

Contribution: Provided research guidance.

Co-Author: Maneesh Gupta

Contribution: Provided research guidance.

Co-Author: Emmanual Parushev

Contribution: Provided research guidance.

Manuscript Information

Hudson Dorian, Mohammad Khosravi, Adrienne Phillips, Jenna Lauf, Ethan Dudley, Maneesh Gupta, Emmanuel Parushev

Journal of Geotechnical and Geoenvironmental Engineering

Status of Manuscript:
__X__ Prepared for submission to a peer-reviewed journal.
_____ Officially submitted to a peer-reviewed journal.
_____ Accepted by a peer-reviewed journal.
_____ Published in a peer-reviewed journal.

American Society of Civil Engineers

Abstract

A series of experiments were conducted to assess the feasibility of employing ureolysis-induced calcite precipitation (UICP) to increase the strength of the base or subbase materials of roads and runways. The experiments involved constructing specimens with uniform silica sand profiles at two distinct scales: 15-centimeter-diameter specimens and a 30-centimeter-by-30-centimeter specimen. The smaller-scale specimens were utilized to refine the treatment process and test various recipes, while the larger specimen aimed to simulate in-situ conditions more accurately and provide additional data points for establishing a preliminary correlation between calcium carbonate content and the strength properties of the treated soil. Calcium conversion was measured after each pulse, and the UICP treated specimens were tested for cementation uniformity. The strength properties of soil treated with UICP was assessed using the California Bearing Ratio (CBR) test. The effectiveness of two different treatment methods for soil stabilization was examined, 'top-down' injection and 'probe-injection' methods. Treating directly onto the soil surface resulted in a greater aggregation of the precipitate on the surface, while the probe-based method better treated the deeper portions of the soil, but produced little cementation near the surface. It was also discovered that using cheaper, commercially-sourced ingredients successfully induced precipitation and significantly improved soil strength. Overall, it was found that the UICP process was successful at increasing the CBR value of a soil at a relatively low cost, from approximately 11% prior to treatment up to 188% after treatment.

Introduction

Paved structures such as roads and runways rely heavily on the strength of the underlying soil substructure. However, the native soil, known as the subgrade, often poses challenges for construction due to its low permeability, susceptibility to freeze-thaw cycles, and relatively low compressive strength. To address these issues a stronger, free-draining, natural soil called the sub-base is placed and compacted on top of the subgrade. The base layer, typically a manufactured material such as crushed rock, is then laid over the compacted sub-base, followed by the asphalt concrete layer. Each layer in the pavement structure reduces the load transmitted to the underlying layer, reducing it to levels appropriate for the subgrade soil. Thus, the load dispersal from the surface to the subgrade is crucial in pavement design. This concept is reflected in the structural number (SN) used in flexible pavement design (AASHTO 1993), which determines the appropriate lift thickness based on anticipated traffic loads and soil strength. However, the current design process is challenged when the assumed design loads or traffic volumes are exceeded. Modifying the material strength or lift thickness to meet the new demands is not easily achievable, resulting in a shorter design life and faster degradation of the paved structure. Was there a way to enhance the strength of the underlying substructure with minimal disruption of the pavement, these issues could be resolved, ensuring a longer-lasting, reliable pavement system.

Several methods have been previously employed to improve the strength properties of soils beneath roads and runways, as outlined by the Army Corp of Engineers (1984) and the National Academy of Sciences (2009). These methods include, in conjunction with the compaction of the soil, the utilization of materials such as Portland cement, lime and lime-based mixtures (LCF), bitumen, and fly ash to improve the performance of soil lifts. However, these suggested methods

are typically applied before road construction, mixed with the soil prior to laying. Therefore, they are unable to facilitate a more efficient renovation process. For a potential method of retroactive improvement without extensive renovation, high-mobility polyurethane grout has proven an effective means of strength improvement with the ability to be injected into an in-situ soil (Saleh et al., 2019; Sabri et al., 2018; Sabri et al., 2021). However, this method has admitted caveats, such as susceptibility to bacterial degradation, relatively high material cost, and inhibition of permeability in the treated soil (Saleh et al., 2019). These challenges make its application to road substructures more complex.

This is where the process of ureolysis-induced calcite precipitation (UICP) may be relevant. This process uses the enzyme 'urease' to convert urea to carbonate, which reacts with calcium to produce calcium carbonate (CaCO3) or 'calcite,' a process generally represented by Equations 4-1 and 4-2.

$$CO(NH_2)_2 + 2H_2O + Urease \rightarrow 2NH_4^+ + CO_3^{2-}$$ Equation 4-1.

$$Ca^{2+} + CO_3^{2-} \rightarrow CaCO_3$$ Equation 4-2.

Since its initial application as a form of crack sealant for natural gas wells (Gollapudi et al. 1995, Kirkland et al. 2020), research efforts have expanded to explore potential applications for improving soil strength (DeJong et al., 2006, Gomez et al., 2014), slope stabilization (Salifu et al., 2015), liquefaction mitigation (DeJong et al. 2022), and surface soil stabilization. This process is being realized as a novel method of improving the mechanical properties of soils, considered less invasive and more sustainable compared to traditional methods, consuming fewer non-renewable resources (Rahman et al. 2020, Deng et al. 2021), with the potential to harness native bacteria naturally present in soils or inject cultured strains of bacteria(Gowthaman et al. 2019a and 2019b). Moreover, this could be accomplished without the extensive labor typically required for the

renovation of paved structures, with reduced environmental impact and cost. These considerations, in conjunction with the straightforwardness of treatment, have made UICP appealing as a potential method for the strengthening of substructure materials for road construction (Porter et al. 2016, Smit et al. 2022).

Within the context of surface soil stabilization, relevant studies mainly focused on surface-water-induced erosion control (Montaya et al., 2018; Chek et al., 2021; Ghasemi et al., 2019; Hodges and Lingwall, 2020; Jiang et al., 2019; Ghasemi and Montaya, 2022), scour mitigation (Do et al. 2020), wind erosion and dust control (Maleki et al. 2016; Zhan et al., 2016), and mitigation of wave-induced erosion of coastal sand dunes (Liu et al., 2021; Montoya et al., 2021; Shanahan and Montoya, 2016). The question, then, is whether this method can be applied to the base or subbase of an existing paved structure and effectively increase the strength of these materials to resolve the problem of changing demands. In essence, it is not yet known how the UICP process should be applied to achieve an optimal result: the best improvement to strength (in the context of paved structures) relative to the cost and effort applied. Previous studies have compared different UICP implementation techniques including surface spraying, prefabricated vertical drains (PVDs), and shallow trenches (Ghasemi and Montaya, 2022). The surface spraying method is preferred for the treatment of large surficial areas, while using the PVD method and shallow trenches can achieve deeper depths but in a highly localized manner. However, when regarding the stabilization of roads with asphalt or concrete surfaces, the surface spraying method becomes difficult to implement. Dorian et al. (2023) and Khosravi et al. (“Large-scale Bio-cementation Test to Improve Sub-Structures of Existing Asphalt and Concrete Roadways,” submitted, GeoCongress 2024, ASCE, Reston, VA) sought to address the similar issue of surface stabilization through UICP, finding promise in the use of top-to-bottom treatment to improve soil

strength. Such a treatment design would be best for the envisioned application to road base material. However, this research also suggested a relative importance of precipitate uniformity in the resulting improvements to strength. It was yet uncertain if the increase in the scale of treatment would change its effect on the treated soil (Meile & Tuncay, 2006). Few previous studies have covered a range of scales for treatment (Saneiyan et al., 2021; Nassar et al., 2018), and few larger-scale studies have conducted in-depth analyses of the distribution of calcium carbonate (Gomez et al., 2016), both of which would provide better insight to field application. There was also a desire to develop a relationship between the amount of precipitate to the increase in strength of the soil, as a quantitative effect. This required a large enough body of tests to develop a correlative model, and a method of testing that could be compared directly to the untreated material.

This study presents the results of a series of column experiments used to evaluate the feasibility of using UICP for enhancing base and subbase materials in road and runway construction. Testing was conducted at two scales: 15-centimeter-diameter specimens and a 30-centimeter-by-30-centimeter specimen. Smaller-scale tests were used to examine different injection strategies, and different recipes for treatment. As a criterion for field scale treatment, solutions based on lab-grade ingredients were compared to those using commercial ingredients, procurable in bulk for a much lower cost (Table B1). Specimen strength was compared against other treated specimens, to determine any observable effect of the methods used, and to untreated specimens, to gauge the degree of the increase in compressive strength. The larger-scale test was used to evaluate the treatment process on an open-surface material, using a mock road segment with multiple layers of material. Calcium conversion was measured after each pulse, and cementation uniformity was assessed in the UICP-treated specimens. Soil strength was determined

through California bearing ratio (CBR) strength testing, having been developed for testing of road construction materials.

Materials and Methods

Microbial Growth

The bacteria *Sporosarcina pasteurii* was used as a source of urease, sourced from frozen one-milliliter stocks. Two days prior to use, stocks were thawed, introduced into 99 milliliters of brain-heart-infusion (BHI) growth solution, and allowed to incubate for 16 hours. This mixture was referred to as the 'starter solution,' used to inoculate the 'bacterial solution' for treatment.

Media

The UICP process uses a reaction between urease, urea, and calcium. To accomplish the precipitation within the soil medium, two fluids were separately introduced into the soil medium as 'injections.' One supplies urease, in this case the *S. pasteurii*, known as the 'bacterial solution.' The other supplies urea and calcium, the 'calcium solution.' Both solutions require a specific set of ingredients: urea, ammonium chloride, and a source of 'food' or carbon for the bacteria to grow.

For this set of experiments, two sets of recipes (Table 4-1) were used: CMM- and CMM+, and YEH- and YEL+. The first set, the 'CMM' recipes, established by Whiffin et al. (2004), used lab-grade ingredients. The 'YE' recipes substituted the lab ingredients for commercially-available alternatives. In both sets, the plus sign (+) indicates a source of calcium in the solution, the minus (-) indicating an absence. The different ingredients, with respective sources and per-gram costs, are provided in Table B1. For the concept of field application, likely requiring larger fluid volumes, these cost-effective recipes may be preferred.

Table 4-1. - Solution recipes with associated per-liter costs.

	Carbon			***Urea***			***NH_4Cl***			***$CaCl_2$***			***Total ($/L)***
Recipe	***Prod.***	***g/L***	***$/L***	***Prod.***	***g/L***	***$/L***	***Prod.***	***g/L***	***$/L***	***Prod.***	***g/L***	***$/L***	
CMM-	*NB*	3	1.06	*FS Urea*	20	1.29	*FS NH_4Cl*	10	0.31	N/A			2.66
CMM+	*NB*	3	1.06	*FS Urea*	20	1.29	*FS NH_4Cl*	10	0.31	FS $CaCl_2$	49	2.16	4.82
YEH-	*YE*	15.5	0.26	*DEF*	20	0.10	*FS NH_4Cl*	1	0.03	N/A			0.39
YEL+	*YE*	4	0.07	*DEF*	20	0.10	*FS NH_4Cl*	1	0.03	PW	49	0.10	0.30

Soil Specimens

Soil samples intended for treatment using the UICP process were placed inside specially designed reactors for both treatment and post-treatment testing. Two scales of columns were constructed: 15-centimeter-diameter specimens and a 30-centimeter-by-30-centimeter specimen. Additional details on the construction of the reactors are provided in the supplementary material.

15-centimeter-diameter Specimens. The '15-centimeter-diameter,' cylindrical reactors were used to explore different injection strategies and their effect on uniformity and strength properties of bio-treated soil. These offered advantages in providing reliable, direct, independent, and comparable measurements of strength between specimens and to the original material. Two reactors of this scale were designed with concern for the specific injection method, the remaining aspects of the design dictated by the requirements of the treatment and testing process. The overall design of the 15-cm reactors was constrained by the minimum specimen dimensions required for a California Bearing Ratio (CBR) test, as specified by ASTM standard D1883. The reactors were constructed using transparent, PolyVinyl Chloride (PVC) components, featuring an inner diameter

of 15 centimeters, a height of 14 centimeters, and a wall thickness of 0.95 centimeters, as illustrated in Figure 4-1. The reactor exhibited sufficient rigidity to withstand the applied load during the testing process. It was also designed to withstand internal fluid pressure, thereby controlling fluid flow through designated inlets and outlets, shown in Figure 4-1.

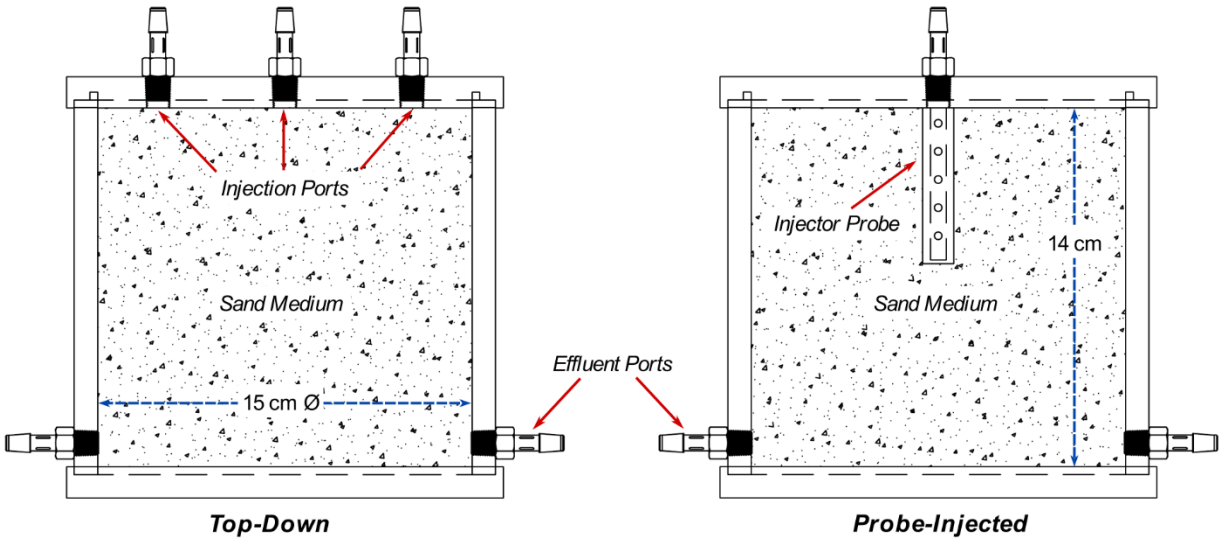

Figure 4-1. – Reactor design for 15-centimeter-scale specimens, showing the two injection methods used: top-down (left), with solutions injected onto the soil surface, and probe-injected (PI), with solutions injected into the soil medium past the surface through a probe.

Two different 15-centimeter reactors were designed, one for a ‘top-down’ injection, and one for a ‘probe’ injection, both shown in Figure 4-1. In the ‘top-down’ (TD) reactor (left), the fluid was to be introduced at the surface of the soil, the inlet ports directing fluid onto the sample’s top surface. In the ‘probe’ injection (PI) method (right), the solutions were injected into the soil medium below the surface, rather than onto it, similar in principle to the methods used by other field-scale studies (e.g., Omoregie et al., 2023). A 6.4-centimeter rigid tube extended into the soil from the top cap, patterned with 3.2-millimeter holes along four sides, through which solutions

were injected. In both designs, four effluent ports were situated at the foot of the reactor for drainage.

30-centimeter-by-30-centimeter Specimen. The ‘30-centimeter-by-30-centimeter’ reactor featured inner dimensions of 30 centimeters long by 30 centimeters wide, with a height of 28 centimeters, as shown in Figure 4-2. There was interest in the results of treatment in a soil system representing an actual road subsurface; the 30-centimeter-by-30-centimeter reactor was thusly designed as an open-topped reactor. Instead of a solid lid, the soil sample was to be topped by a layer of asphalt concrete as will be discussed in more detail. At this scale, a greater number of CBR results could be obtained, as the CBR test requires a specific amount of area for testing (~182 cm^2), without overlapping testing sites. These results can then be associated with an average spatial calcium carbonate content for a specific area, providing grounds for a better understanding of the relationship between the improvement to strength and the amount of precipitate. This approach contributes to improved reproducibility over the smaller specimens and allows for more detailed investigations into the UICP process. As for the injection system, stainless steel probes were to be used, inserted through the asphalt cap placed on top of the soil layer, drainage facilitated by ports at the bottom of the specimen. More detail on these probes is provided in the section dedicated to the treatment process.

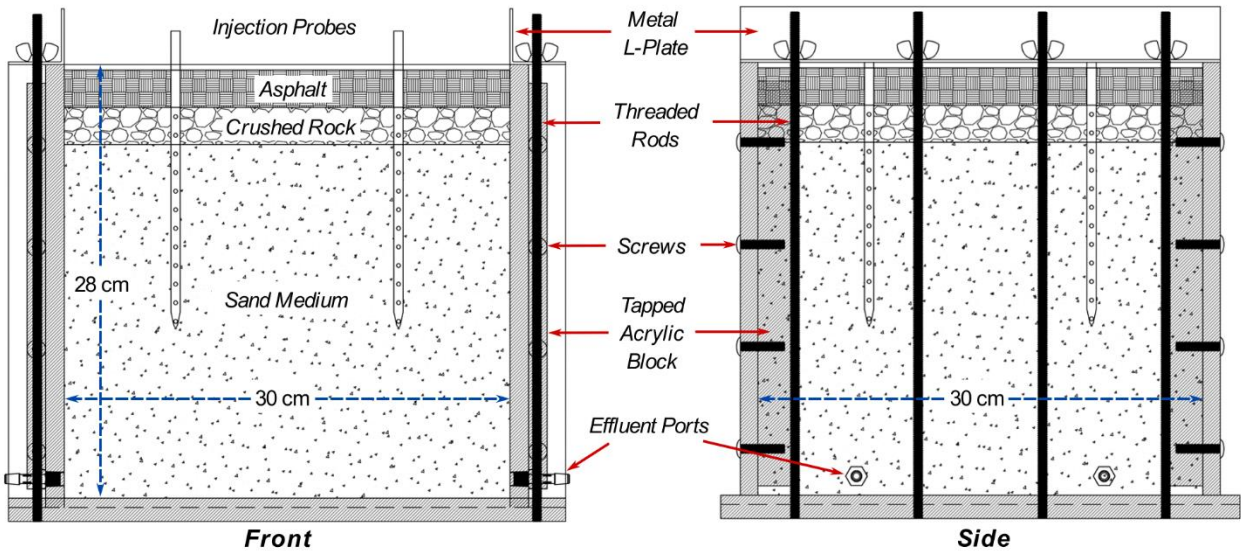

Figure 4-2. – Reactor design for 30-centimeter-by-30-centimeter specimen, assembled from four side walls, secured onto a base using threaded rods and wingnuts. Injection is done through a set of four probes, extending through the asphalt surface and crushed rock layer into the sand medium.

Soil for Treatment and Soil Preparation

Sakrete® medium commercial silica sand was selected as a relatively low-cost option, the characteristics of which are provided in Table B2. Properties of the uniform sand included the following: a maximum void ratio, e_{max}, of 0.97, minimum void ratio, e_{min}, of 0.53, and median grain size, D_{50}, of 0.67 mm. e_{max} and e_{min} were determined following ASTM D4253 (ASTM 2002a) and ASTM D4254 (ASTM 2002b), while G_s was determined following ASTM D792. For the 15-centimeter-diameter columns, soil was compacted into the reactors using a wet-tamping procedure, established by Ladd (1978), and revised by Chan (1985). The soil samples were constructed layer by layer; each layer was of a specified mass, compacted to a specific thickness to reach the target relative density of D_r = 35%. The amount of soil required for each lift was determined based on the desired density. Compaction was performed in five lifts with moist soil (a moisture content of

7%) distributed evenly for each layer. Reactors were sealed after the soil had been compacted. Before treatment, samples were fully saturated using deionized (DI) water.

For the 30-centimeter-by-30-centimeter specimen, instead of using the wet-tamping procedure, a small-scale pluviator was built to place the sand at the desired relative density, influenced by the process used by Black et al. (2016). This device was constructed from a pre-made, sheet-metal hopper, the nozzle extended to 46 centimeters with adjustable metal ducting. A threaded rod was suspended from the opening of the nozzle by a metal cross; this rod extended to the end of the nozzle, and was used to hold perforated plates in place. The placement of these plates, and the size of the perforations, allowed for adjustment of the final relative density of the placed soil. The construction process began by placing mesh filters at the effluent ports to prevent loss of material due to transportation. Sand was then deposited in 10, 2.5-centimeter-thick lifts, positioned at a specific distance from the previous surface (as shown in Figure 4-3 to achieve a required D_r of 35%, the hopper lifted after every lift to maintain the calibrated height. Once the dry pluviation of sand was completed, the soil was saturated with clean water. After saturating the sample, a layer of crushed rock was placed on the surface, as illustrated in Figure 4-2. Finally, the soil sample was topped with a 2.5-centimeter layer of pre-formed asphalt to simulate the paved surface layer of a road.

Figure 4-3. – Demonstration of pluviation process and device used in the soil compaction process for the 30-centimeter-by-30-centimeter specimen.

UICP Treatment

For the 15-centimeter samples a discrete, ‘pulse’-based method of treatment was used. The setup of the treatment process is shown in Figure 4-4. Inlet ports were connected to 6.4-mm flexible tubing, leading from the influent solution’s container, running through a peristaltic pump. Outlet ports were also connected to tubing, running to a separate waste container. Bacterial solutions were allowed at least one hour of residence time in the soil before a calcium injection; calcium injections were allowed four hours of contact time. Based on the relative density and volume of the reactor, it was determined that the volume of the void space inside the soil was approximately one liter. Pulse volumes for the treatment solutions used were set at 1.5 times the pore volume of the sample, each then being 1500 milliliters, to ensure full saturation of the specimen with the necessary reagents.

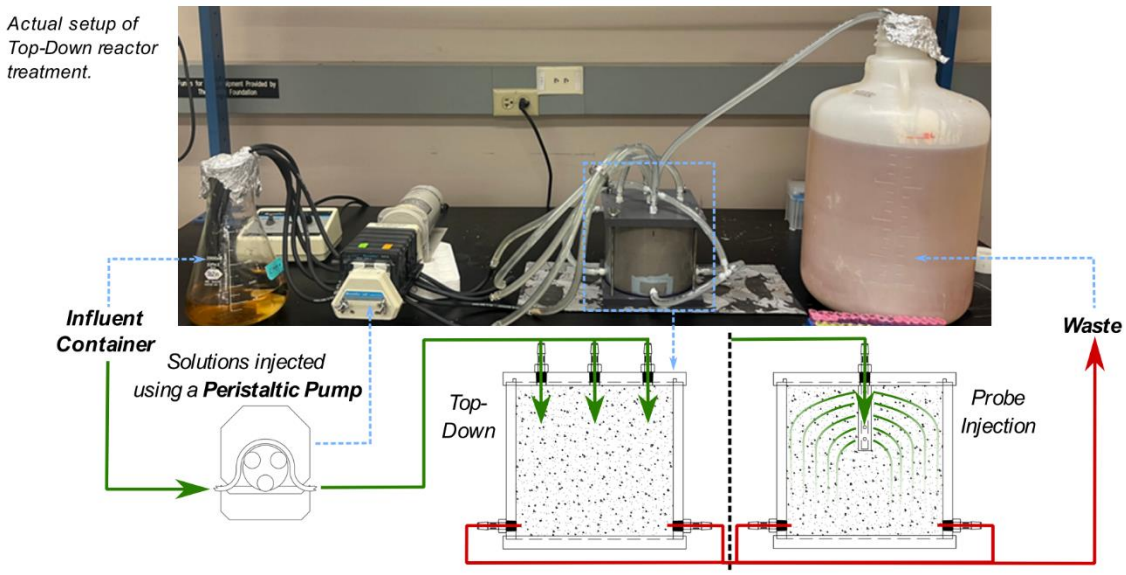

Figure 4-4. - 15-centimeter-scale reactor treatment setup, displaying the alternative injection methods.

After saturation of the soil specimen, the bacterial solution was injected first. The bacterial growth solution (without calcium) was made ahead of the treatment, sterilized for long term storage. A portion of the bacterial starter grown from the frozen stock was combined at a 1:100 ratio with necessary volume of the bacterial growth solution. This inoculated bacterial solution was allowed to incubate at 30 degrees Centigrade for 16 hours, checked using an optical density (OD) test prior to injection. The calcium solution was prepared directly before injection, dry ingredients mixed into DI water in a two-liter flask and agitated with a stir bar until full dissolved, then being ready for injection. Before the calcium pulse, an ammonium chloride solution was used to rinse the inlet tubing to prevent premature reaction, enough in volume only to fill the inlet tubing. Both treatment solutions were injected at six milliliters per minute into the soil. Samples were taken from the effluent line to monitor the progress of the reaction, specifically the consumption of urea.

The resulting specimens were products of differing combinations of reactor design, solution recipes, and number of injections. The specimens produced, along with the treatment conditions, are outlined in Table 4-2. For the first specimen, the sample was treated using the top-down (TD) treatment method with 19 injections in total, referred to as 'TD P19'. For the second specimen, the probe-injected (PI) treatment method was used to deliver 19 pulses in total, referred to as 'PI P19.' The final specimen also used the top-down method, substituting the solutions for the YE-based recipes as shown in Table B2, with only 14 pulses in total, referred to as 'TD P14 YE'.

Table 4-2. – 15-centimeter specimens with associated treatment conditions.

Specimen	**Injection Strategy**	**Pulses**		**Recipe Type**
		Bacteria	***Calcium***	
1	TD	9	10	CMM
2	PI	9	10	CMM
3	TD	5	9	YE

For treatment of the 30-centimeter-by-30-centimeter specimen, the injection strategy was informed by observations during the treatment of smaller column specimens, combining aspects of both the top-down and probe-injected methods to counter each of their perceived caveats. Stainless steel probes extended 10 centimeters into the soil layer, with 3.18-millimeter holes spaced at 1.2-centimeter intervals. A 2.5-centimeter length of holes opened into the more permeable gravel layer, allowing direct treatment of the surface of the sand layer. This method was supposed to result in more uniform cementation, allowing better treatment of the surface and the at-depth portions of the sand layer. These probes were connected to the pumps, as shown in Figure

4-5. Injections were portioned to keep the sand layer fully saturated, with the fluid level present within the crushed rock layer, the acrylic construction of the reactor allowing easy monitoring.

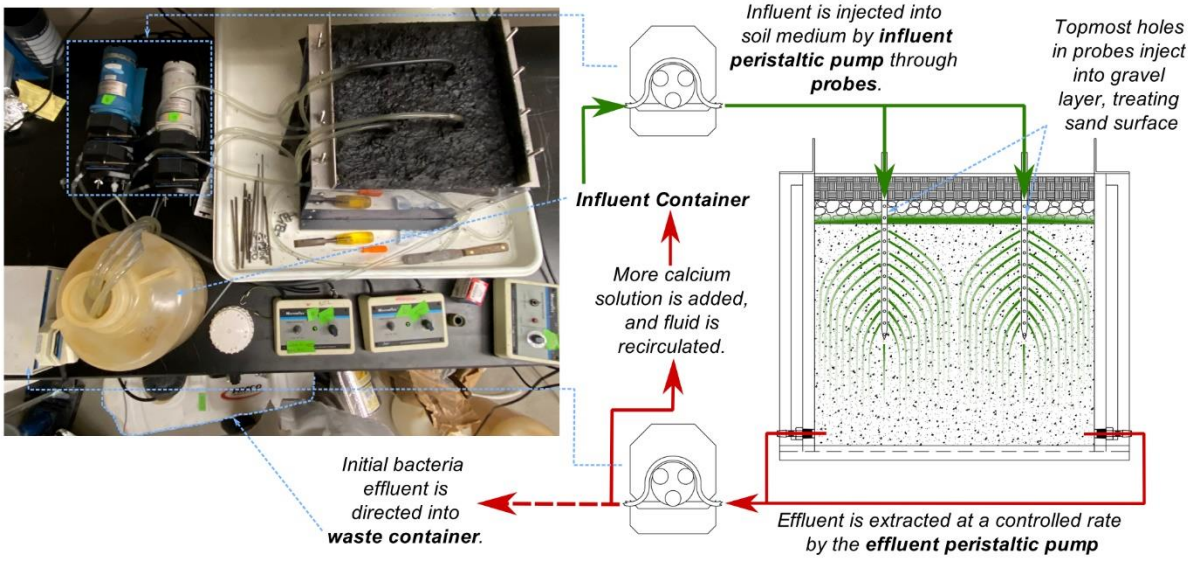

Figure 4-5. – 30-centimeter-by-30-centimeter-scale reactor treatment setup.

As opposed to the discrete-injection method used across the smaller specimens a 'recirculating' treatment method, one that continuously moved the calcium solution through the soil medium was used. After microbes were introduced and allowed to reside in the soil, the bacterial solution was drained into a waste container. Two times the pore volume (11 liters) of the calcium solution was prepared, and injected into the reactor. Once the reactor was filled with the calcium solution, the effluent lines were directed back into the influent container, which was filled with an additional 11 liters of calcium solution. Through rate-controlled peristaltic pumps on the inlet and effluent lines, the calcium solution was recirculated through the reactor for three hours. Samples were taken during this period of recirculation, or each 'cycling' of calcium, with one taken every hour. This process was repeated for four days. For this treatment, only the yeast-

extract-based recipes were used for the solutions, due to the larger volumes needed and as an effort to better emulate on-site practice.

CBR Strength

The effect of the precipitate on the soil specimens was to be evaluated through their strength capacity. The test chosen was the California bearing ratio (CBR) test, having been developed for testing of road construction materials and currently used as a design measure in multiple systems.

For the smaller, 15-centimeter-diameter specimens, each was subjected to a single CBR test, recording stress-strain results to determine an effective value of CBR in accordance with ASTM standard D1883. For this research, the stress needed to drive the piston a specified distance was compared to the standard stress used in Department of Defense document 1212, that of crushed rock in the same testing conditions.

For the larger specimen, providing greater surface area and depth, multiple CBR tests were conducted. The specimen was sectioned off into quarters, with rows ‘1’ and ‘2’ and columns ‘b’ and ‘a,’ each resulting ‘cell’ subjected to testing (Figure 4-6). After testing had been tested across one layer the material for each cell was excavated out and retained for calcium content analysis. The newly revealed, at-depth surface was then tested in the same manner. Depth from one layer to the next was defined as 1.5 times the diameter of the testing piston (five centimeters), resulting in a 7.5-centimeter thickness for each layer. This provided testing surfaces at the surface of the layer, 7.5 centimeters deep from the surface, 15 centimeters deep, and 20 centimeters deep. This last layer was the only exception to the rule, and was conducted to check if cementation was significantly more prevalent near the effluent ports.

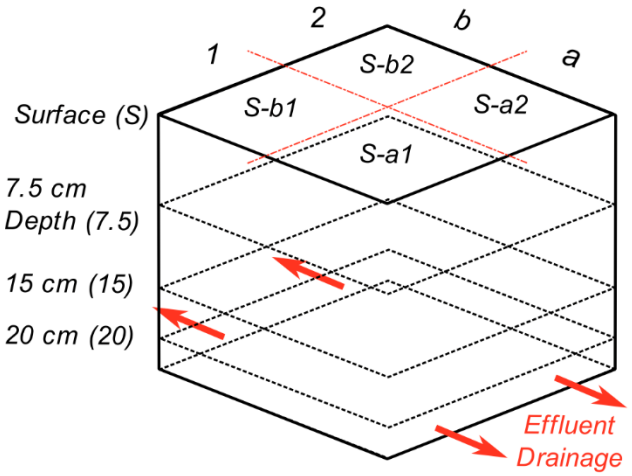

Figure 4-6. - Division of 30-centimeter-by-30-centimeter specimen for CBR testing and calcium digest sampling.

Jung Assay

To monitor and verify the progress of the ureolysis inside the specimen, the samples taken from the effluent line were subjected to a Jung assay, a test used to determine the urea concentration in solution (Jung et al., 1975; Phillips, 2013). Samples were diluted 1:10 in 10% nitric acid (HNO_3), to fall within the readable range of the test and halt any further ureolysis in the effluent sample. The urea content was averaged across the three triplicate samples, the average concentration taken as that of the original effluent sample.

Calcium Digests and Assay

In order to evaluate the degree of calcite precipitated in each specimen and, its distribution through the soil, calcium digests were conducted to determine the percent mass contributed by the calcite. Samples of the treated material were taken from multiple specified locations across each specimen, a portion of which was dried and weighed out into a centrifuge tube. Once weighed,

10% nitric acid was added at a five-to-one ratio (five milliliters to every one gram of dry, sampled material), and allowed to react with any calcite present in the sample, provided regular agitation. Afterwards, acid was decanted from the tube and retained separately, the digested sample being placed into a 50-degree-Centigrade oven to dry again. Once dried, the sample was weighed again. The difference in mass before and after digestion was attributed to the calcite precipitation, relayed as a percent of the original mass.

For the 15-centimeter-diameter specimens, a sampling pattern as established in Figure 4-7 was used. From the testing surface, 13 samples were taken from several key locations, and at each depth below the surface, nine samples were taken. From these, averages were taken and used to establish an average calcite content for specific areas of the surface as shown. Each sample digested was one gram, measured to the 10,000ths place, combined with five milliliters of acid. Due to the small size of the samples, however, and the presence of some fine material in the soil itself, the calcium contents derived from the mass measurements were easily skewed. To account for this, and to verify results, the fluid retained from each digest was subjected to a calcium assay (Kanagasabapathy and Kumari 2000). This test is similar in execution to the Jung assay. The fluid was diluted 1:200 in the same 10% nitric acid, as to fall within the range of standards used by the test, then 10-microliter triplicates from the diluted sample were combined with the reagents in separate wells of a 96-well plate. Optical readings were taken using a plate reader, the results from the standard solutions used to form a standard curve, then applied to the readings of the samples to determine corresponding calcium concentrations. Results were averaged across the triplicates, and reported for that sample.

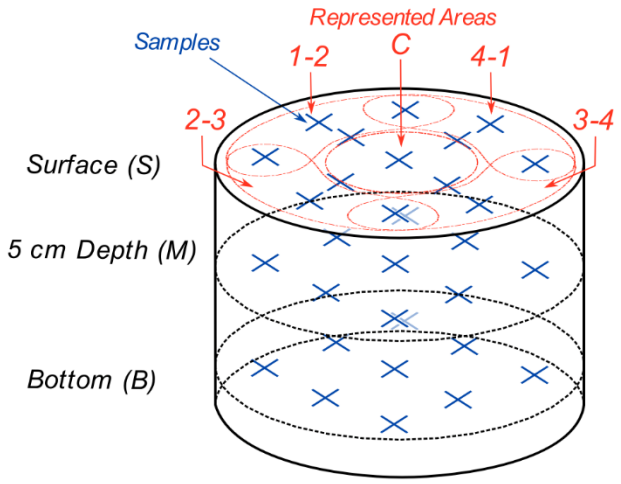

Figure 4-7. - Calcium digest sampling pattern for 15-centimeter specimens.

For the larger specimen, each portion retained of a specific testing surface (corresponding to a cell and a layer) had three 10-gram samples taken for digests, each combined with 45 milliliters of nitric acid. This specimen also provided an opportunity to determine the relationship between the average calcium content and the resulting CBR, since a greater number of CBR tests could be taken, and a respective sample could be associated with each result. The calcium contents were compared against CBR value, and a linear regression analysis was conducted.

Results

As discussed in the introduction, this study's goal was to assess: 1) the effect of injection strategy on resulting calcium carbonate distribution and strength, 2) the effect of the media type used on the treatment characteristics, and 3) the relationship of calcium carbonate distribution and the improvement to strength, addressed in part by both the smaller and larger-scale tests. As such, this section is organized to address these questions in the order presented, beginning with the

findings from the smaller-scale, 15-centimeter column tests. Since this series of smaller-scale tests was used to inform the treatment and testing procedure for the larger-scale, 30-centimeter-by-30-centimeter specimen, it is only appropriate to reflect on the former before discussing the latter.

Injection Strategy and Treatment Characteristics

The smaller specimens, TD P19 (treated by top-down injection with 19 pulses) and PI P19 (treated by probe-injection with 19 pulses) were used to investigate the relative effect of injection strategy on the strength properties of the treated soil. Figure 4-8 presents the CBR values of these two specimens, as well as their stress-strain behavior. To conduct the CBR test on PI P19 specimen, a flat, intact surface was required, therefore, the surface tested for CBR strength was the bottom of the specimen depicted in Figure 1. Between the two, TD P19 had the greater CBR value of 137.5%, compared to that of 82.5% achieved by PI P19. However, the latter featured the highest peak strength during the test, 16.5 MPa, versus the 13.5 MPa peak strength of TD P19. PI P19 did not reach its peak strength until a significant amount of deflection (approximately seven millimeters) had occurred, however, describing a relatively ductile pattern of behavior. Conversely, TD P19 saw a much faster rise in strength between zero and five millimeters of deflection, relatively brittle in comparison.

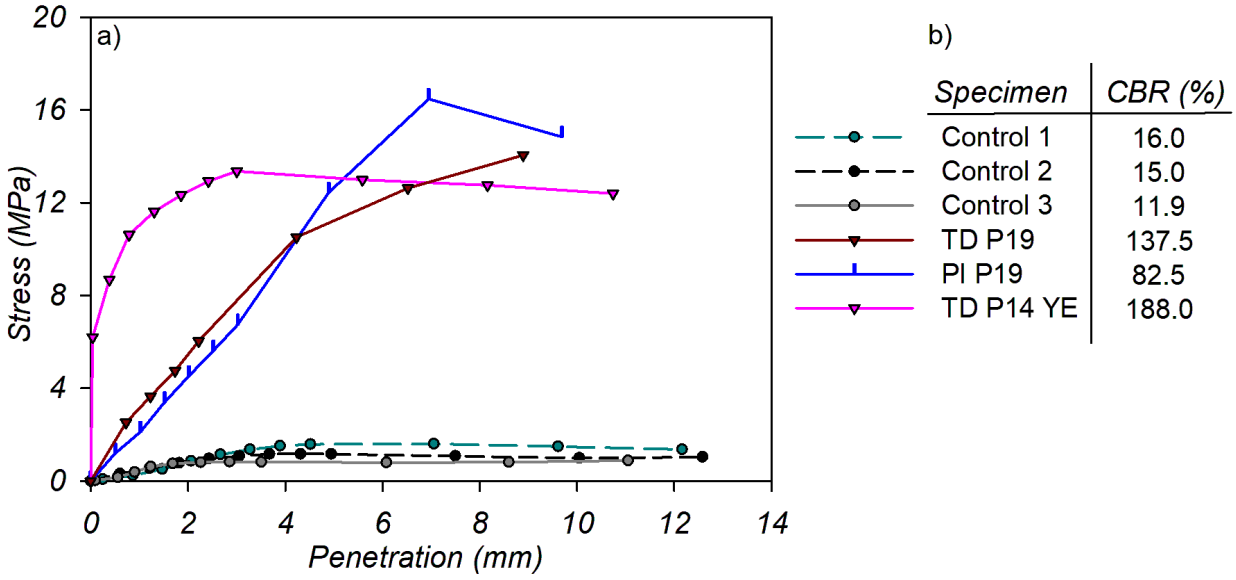

Figure 4-8. - CBR testing results for 15-centimeter-diameter specimens, compared against 3 control specimens, showing a) stress-strain response during testing and b) the resulting CBR value taken at 2.5 mm.

The distribution of calcium carbonate for these two specimens is provided in Figure 9, additional data provided in supplementary Table B3. On average, the probe-injected specimen had a higher amount of precipitation at 3.1% overall (standard deviation of 1.5%), compared to the overall average of 2.3% (standard deviation 0.9%) for the top-down specimen. The top-down specimen showed a higher concentration of calcium carbonate precipitation near the surface (3.1% on average, standard deviation of 0.7%), decreasing over the middle and bottom layers (1.9% and 1.5% on average respectively, with a standard deviation of 0.3% for both). The probe-injected method, however, showed greater quantities of precipitate across the middle and bottom layers, the values fairly similar (3.6% and 4.2% on average respectively, with standard deviations of 0.6% and 0.9%), but very little precipitate near the surface of the specimen (1.0% average, standard deviation 0.4%). In an analysis of variance (ANOVA) test run on the data, there was very strong evidence (p-value of <0.0001) that there was an effect of treatment method on calcium carbonate

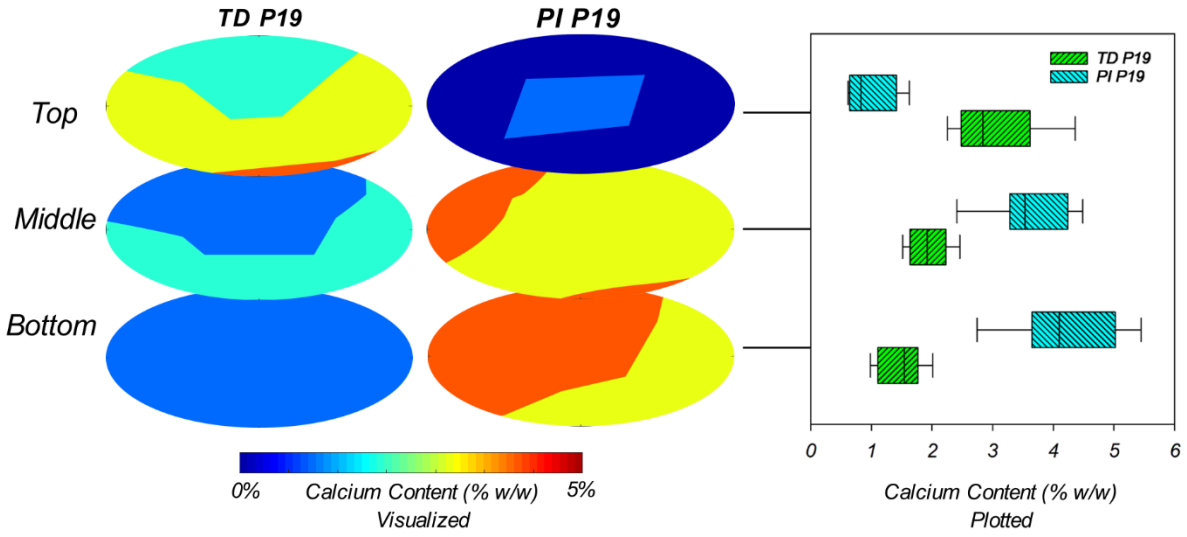

Figure 4-9. - Calcium carbonate distribution over depth for 15-centimeter specimens, evaluated at three discrete layers. These specimens received 19 pulses each, using the same media recipes. The sample PI P19 was inverted for CBR testing, requiring a flat surface, so the 'bottom' during treatment became the CBR testing surface.

content after accounting for depth within the specimen. Therein, the differences in the results are statistically significant enough to claim that there is an effect of the treatment method on the distribution of precipitate. This would suggest that there are to be anticipated caveats for both methods of treatment: for the top-down, there is a kind of filtering effect, the degree of precipitation decreasing with further penetration into the soil; for the probe-injected method, there is a 'blind spot,' where little precipitation occurs. In observing the results of the Jung assay conducted on the effluent samples, provided in Figure B1, it appears that the TD P19 had a more complete conversion of the urea in solution, compared to PI P19, potentially reflecting the relative lack of precipitation near the surface. However, both saw a consistent, significant decrease in the urea concentration when compared to that of the influent solution, indicating successful ureolysis.

Treatment Solution and Treatment Characteristics

Comparing the established results of specimen TD P19 and TD P14 YE, the relative effect of the change in treatment solutions can be evaluated. The CBR strength and stress-strain behavior for TD P14 YE is provided in Figure 4-8, depicting a sharper increase in strength than TD P19 and reaching CBR value of 188%. This was the highest CBR out of all the 15-centimeter specimens, even with only 14 pulses of treatment against the 19 pulses used for the other specimens. This suggests that the alternative, yeast-extract-based recipes may be more effective for facilitating strength improvements over the CMM recipes. However, further investigation would be more valuable to draw a distinct conclusion.

Regarding the calcium distribution, shown in Figure 4-10 for TD P14 YE (also included in Table B3), the amount of precipitation on average is higher than TD P19: at the surface, the average calcium content is 4.9% (standard deviation of 1.8%) at the surface, 2.7% (standard deviation 0.3%) at the middle, and 3.3% (standard deviation 0.2%) at the bottom. The distribution of calcium carbonate also followed a pattern similar to that seen in TD P19, reinforcing the suggestion that the top-down method of treatment at this scale results in more precipitation near the soil surface.

Overall, the average calcium content was 3.8% (standard deviation 1.5%), higher than both of the CMM-treated specimens. This suggest that the YE-based treatment may be more effective at inducing calcium carbonate precipitation. The same ANOVA test found that there was very strong evidence (p-value of <0.0001) that recipe type influenced the amount of precipitate, reinforcing this conclusion. In a previous batch study, comparing the performance of YEH- to CMM-, it was found that the YEH- facilitated a greater bacterial density, incubated under the same conditions as CMM-. Lauchnor et al. (2015) determined that increased bacterial activity is related to an increased rate of ureolysis and higher bacterial populations may provide more nucleating

points for precipitation within the soil. Therein, YEH- may have a distinct benefit at generating precipitation over the lab-grade CMM-. The results of the Jung assay, however, show a similar trend in the consumption of urea between TD P14 YE and TD P19, with only a marginal difference during the later pulses.

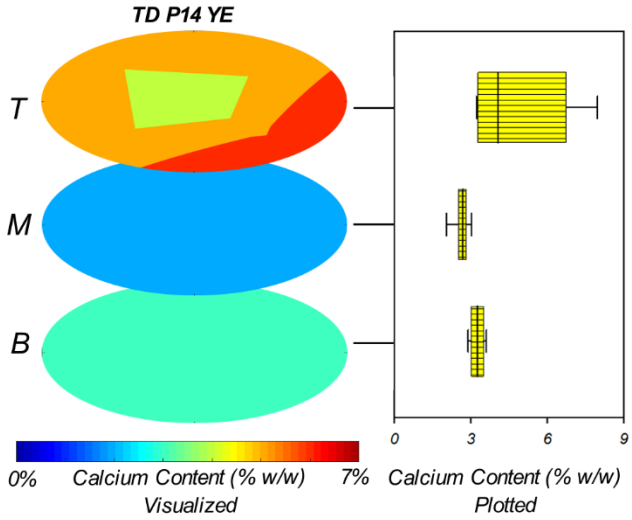

Figure 4-10. – Calcium carbonate distribution over depth for 15-centimeter-diameter specimen, treated with 14 pulses using the top-down method, using the YE-based media.

Lessons from the 15-centimeter Specimens

From the selection of 15-centimeter specimens tested, it can be concluded that the treatment mechanism used may have predictable effects on the resulting character of the treated soil. From the top-down specimens, there is an observable tendency to form more precipitate near the treatment surface, relative to areas deeper in the soil medium. From the probe-injected specimen, the results suggest that this method is more effective at targeting these deeper portions of the soil but is poor at inducing precipitate nearer to the treatment surface. From the results of the CBR testing, it is suggested that more precipitate near the surface provides a greater increase

to the CBR value. However, as the probe-injected specimen returned the highest peak strength, there may be additional benefit to targeting areas deeper in the soil medium. To best utilize these findings, the injection method used for the 30-centimeter-by-30-centimeter was a combination of the two methods used for the smaller scale: probes would allow for treatment of deeper portions of the soil, but the simultaneous injection into an overlying, more permeable layer would allow for direct treatment of the surface. From the results already discussed, it was hypothesized that the combination of the two methods would counteract each other's deficiencies, producing more uniform treatment of the soil.

Results of the 30-centimeter-by-30-centimeter Tests

Figure 4-11 presents the CBR values of the 30-centimeter-by-30-centimeter specimen. The calcium carbonate content distribution over the area and depth of the specimen is illustrated in Figure 4-12, divided into the appropriate cells and layers, standard deviations provided in Table B4. The increases to strength in this specimen were far less pronounced, compared to those of the 15-centimeter specimens, only reaching a maximum CBR of 42.0%. It is suspected that, due to the proximity of the test locations, there may have been a degree of interference between the CBR tests, as evidenced by the development of fissures on the testing surface, as shown in Figure B3. As a result, some of the CBR values found may be unrepresentatively low relative to their calcium carbonate content. For example, the average calcium carbonate contents for cells Sb1 and Sb2 were both found to be 4.1%, but the CBR value of Sb1 was only 13.6%, while that of Sb2 was 42.0%. The only difference between the two was that Sb2 was tested before Sb1, reinforcing the idea that interference may have affected some of the CBR values. However, it is likely that the

change in the treatment conditions also contributed to the differences in the effect of the treatment on the soil strength.

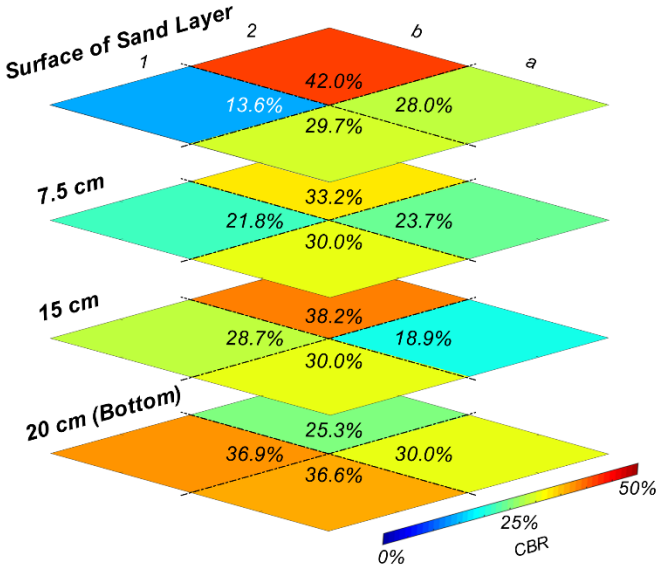

Figure 4-11. – 30-centimeter-by-30-centimeter CBR strength by section over depth.

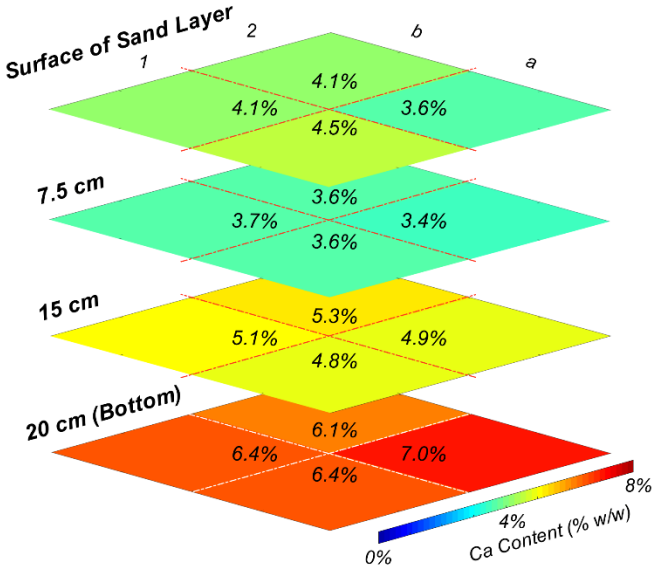

Figure 4-12**.** - 30-centimeter-by-30-centimeter calcium carbonate content by section over depth.

In the CBR results, there is less of an observable trend over the area and depth of the specimen than at the smaller scale, most CBR results remaining near 30%, possibly suggesting an improved uniformity of the treatment. This conclusion is somewhat aided by the calcium carbonate content over the depth, and partially verifies the initial hypothesis formed concerning the combination of the top-down and probe-injected methods. There is some evidence of a gradient of precipitate quantity over depth: the highest amount of precipitate was found near the foot of the specimen, ranging from 6.1% to 7.0% (standard deviations of 0.04% and 0.6% respectively), decreasing at 15 centimeters of depth to a range of 4.8% to 5.3% (standard deviation of 0.2% for both), and further decreasing to between 3.4% and 3.6% (standard deviations 0.07% and 0.2%) at 7.5 centimeters. In another ANOVA test, there was strong evidence (p-value of 0.002) that depth within the specimen was related to the amount of precipitate, after accounting for cell; this suggests that there is a statistically significant difference in the calcium carbonate content depending on depth. However, the surface of the specimen had a calcium carbonate content of 3.6% to 4.5% (standard deviations 0.1% and 0.2%). This suggests that the combination of the two methods was successful at better targeting the entirety of the specimen, compared to their individual performance.

In comparing the results of the Jung assays, those for the larger-scale test presented in Figure B2, there is a notable decrease in the amount of urea relative to the smaller-scale specimens; whereas the smaller specimens reached, at times, 100% conversion, the larger-scale specimen only achieved a maximum of 70% conversion. As the treatment process progressed, this consumption decreased, only around 30% conversion at the final cycle. It may be that, due to the larger volume of calcium solution provided to the specimen, the specimen was able to reach a higher amount of precipitate, but the conversion may not have been as efficient, leading to a large percent of the urea

remaining unconverted. This may have been due to the draining of the bacterial solution prior to the introduction of the calcium, leaving a smaller proportion of bacteria in the soil to perform the conversion. It should be noted that, when the cycle was allowed to continue for longer than three hours, there was a suggestion that the rate of conversion of urea increased, as evidenced by a sample taken at the fourth hour of the third cycle (Figure A2). Thus, it is possible that if the recirculation process were extended, a more efficient conversion of urea may have occurred, but further testing would be necessary to verify this.

Overall, the larger-scale specimen was an insightful experiment in adapting the treatment method to larger volumes of soil. As was true during the smaller-scale experiments, the 30-centimeter-by-30-centimeter treatment process had its own challenges. The large volume of soil made the treatment process difficult to manage with lab equipment; the process required large volumes of bacterial cultures and large amounts of ingredients and generated similarly large volumes of waste. Also like the smaller specimens, clogging of the ports and the near-port areas of soil was a problem, being what eventually halted the treatment process. Likely, some of these difficulties would be similar to those encountered in field application.

Regression of Calcium Carbonate Content and CBR Value

It should be noted that, while specimens of both scales provided a set of CBR values, only those from the 30-centimeter-by-30-centimeter specimen were used to generate a regression. Since numerous variables were changed between the two scales, such as the change from a closed to an open system, the use of pluviation for compaction, and switching to a recirculating treatment method, the evaluation of both together would not provide a reliable model.

Taking the CBR and calcium carbonate data from the larger-scale specimen, the statistical program Rstudio was used to develop a linear regression. Prior to applying the model to the data, a set of residual plots (Figure B4) were generated to verify that none of the assumptions necessary for a linear model were violated. From these plots, no severe violations were visible: the normal Q-Q plot showed a generally normal distribution, the residuals versus fitted points plot showed no patterning of the variance, and no points exhibited overt leverage on the model. With the requirements met, a linear regression was conducted, and a model was generated. The model is summarized in Equation 4-3 and visualized with a 95% confidence interval in Figure 4-13.

$$\mu\{CBR \mid CaCO_3\} = 1.824\ CaCO_3 + 0.204 \qquad \text{Equation 4-3.}$$

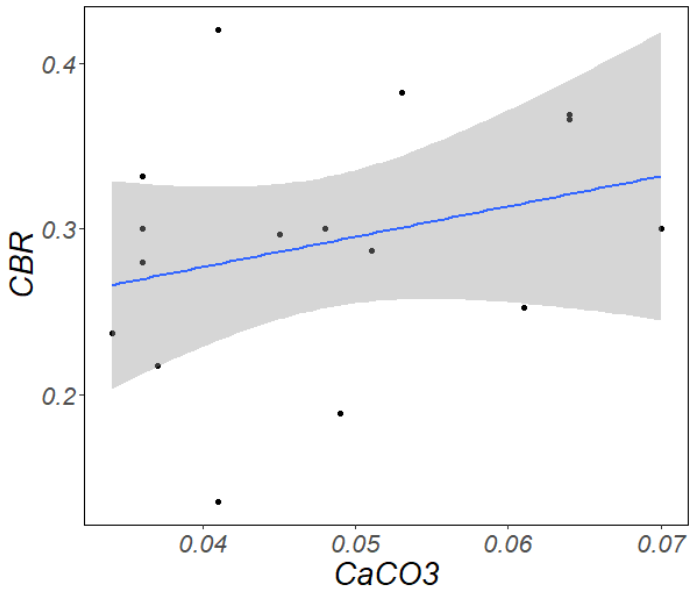

Figure 4-13. - Calcium Content and CBR value linear regression with 95% confidence interval.

From the regression, there is weak evidence that for every one-percent increase in the calcium carbonate content, the average CBR value increases by 1.82%, with an F-value of 1.260 and an associated p-value of 0.281. The 95% confidence interval for this value extends from -

1.662 to 5.309, suggesting that the relative change in the mean CBR value for a one-percent increase in the calcium carbonate content is between a 1.662% decrease to a 5.309% increase. As this interval contains zero, thereby not effectively eliminating the possibility that there is no association between the two (i.e. that there is a zero-percent increase in the CBR), the association is weak.

As discussed, there may have been a component of interference between the tests due to the fissures. Should this be the case, then an assumption for a linear regression (that all datapoints are independent from one-another) is violated, and the resulting model is not reliable. This is compounded by the relatively small number of datapoints, 16 tests in total.

Conclusions

From this research, the results work in favor of the use of UICP as an improvement to paved structures. In the context of road construction, treated soils see an increase in strength, and commercially available ingredients are suitable alternatives, further reducing the cost of implementation. While further replication may be necessary to prove the most effective mechanism of top-down treatment, evidence was found suggesting that the use of some combination of at-depth and surficial treatment provides more uniformity in the resulting distribution of calcite.

While these findings are positive, and mark progress towards the final goal of implementation, there are still barriers. The current model of a road substructure, the one-foot-by-one-foot specimen, treated up to this point is not wholly representative of the actual conditions that will be encountered. The sample treated was finite in volume, and complete saturation and extraction of solutions could be easily maintained, which is not true of actual road substructures.

In field applications, sustained saturation of a free-draining soil would require a different approach, and in such a case full extraction of injected fluids may be more difficult as well. This does not mean that the task is impossible, though, as proven by van Paassen et al.'s successful implementation of large-scale UICP treatment in stabilizing horizontal boreholes (2009, 2011). This effort used a probe-injection-based treatment method, with designated injection and extraction probes inserted into the soil surface. However, the documentation on this research did not specify how much of the injected solutions were successfully extracted. The problem in this is the potential for groundwater contamination, as the process of ureolysis generates significant amounts of ammonium as a byproduct, which can impact local ecosystems. For full-scale application to road construction, there must be an effective way to remove all injected solutions, or a method of eliminating the ammonium produced by the process, to reduce the environmental impact. Deng et al. (2021) also noted that, while the chemical process of UICP itself is neutral in carbon emissions, the manufacturing of the necessary ingredients produces a significant amount of carbon dioxide. As such, the process should be further revised to improve the efficiency of the conversion process or be adapted to using recycled ingredients to fully realize the reduction in environmental impact. There has been success in using recycled urea and ammonia from human urine in growing ureolytic bacteria and precipitating calcite, as shown in Yang et al.'s 2022 paper.

The results found suggest an immense potential for UICP's use in infrastructure: in all of the smaller-scale tests, the CBR value of the soil increased at least 68%, and in all but two of the tests with the larger-scale specimen the CBR value increased marginally. This is especially impressive regarding the specimen TD P14 YE, considering the low cost of the solutions used and the resulting 173% increase in the CBR. It is clear that this envisioned application is possible at field scale, but the exact mechanisms of treatment still need refinement.

References

AASHTO. 1993. *AASHTO Guide for Design of Pavement Structures.*

ASTM. 2021. *Standard Test Method for California Bearing Ratio (CBR) of Laboratory-Compacted Soils.* https://doi.org/10.1520/D1883-21

Black, J.A., Hakhamaneshi, M., Cargill, C.M., Elmrom, T. 2016. "Development and calibration of a sand pluviation device for preparation of a model sand bed for centrifuge tests." *Proceedings of the 3rd European Conference on Physical Modelling in Geotechnics*, p. 73-79.

Chan, C.K. 1985. *Instruction manual, CKC E/P cyclic loading triaxial system users' manual*, Soil Engineering Equipment Company, San Fransisco, CA.

DeJong, J.T., Fritzges, M.B., Nuesslein, K. 2006. "Microbially Induced Cementation to Control Sand Response to Undrained Shear." *Journal of Geotechnical and Geoenvironmental Engineering*, Vol. 132 (11), p. 1381-1391. https://doi.org/10.1061/(ASCE)1090-0241(2006)132:11(1381).

DeJong, J.T., Gomez, M.G., San Pablo, A.C.M., Graddy, C.M.R., Nelson, D.C., Lee, M., Ziotopoulou, K., Kortbawi, M.E., Montoya, B., Kwon, T.H. 2022. "State of the Art: MICP soil improvement and its application to liquefaction hazard mitigation." *Proceedings of the 20th International Conference on Soil Mechanics and Geotechnical Engineering, Sydney 2021*, p. 405-508.

Deng, X., Li, Y., Liu, H., Zhao, Y., Yang, Y., Xu, X., Cheng, X., de Wit, B. 2021. "Examining Energy Consumption and Carbon Emissions of Microbial Induced Carbonate Precipitation Using the Life Cycle Assessment Method." Sustainability, Vol. 13, 4856. https://doi.org/10.3390/su13094856.

Dorian, H., Gunyol, P., Lauf, J., Khosravi, M., Phillips, A., Cunningham, A. 2023. "Evaluating Injection Strategies for Microbially Induced Calcite Precipitation and Implications for Applications to Road Structures." *Geo-Congress 2023: State of the Art and Practice in Geotechnical Engineering*, p. 351-360. https://doi.org/10.1061/9780784484661.037.

Ghasemi, P., Montaya, B.M. (2022). "Field Implementation of Microbially Induced Calcium Carbonate Precipitation for Surface Erosion Reduction of a Coastal Plain Sandy Slope." *Journal Geotech Geoenviromnental Engineering*, Vol. 148 (9), 04022071. https://doi.org/10.1061/(ASCE)GT.1943-5606.0002836.

Gollapudi, U.K., Knutson, C.L., Bang, S.S., Islam, M.R. 1995. "A new method for controlling leaching through permeable channels." *Chemosphere*, Vol. 30 (4), p. 695-705.

Gomez, M., Anderson, C., DeJong, J., Nelson, D., Lau, X. 2014. "Stimulating In Situ Soil Bacteria for Bio-Cementation of Sands." *Geo-Congress 2014: Geo-characterization and Modeling for Sustainability*, p. 1674-1682. https://doi.org/10.1061/9780784413272.164.

Gomez, M.G., DeJong, J.T., Anderson, C.M., Nelson, D.C., Graddy, C.M. 2016. "Large-Scale Bio-Cementation Improvement of Sands." *Geotechnical and Structural Engineering Congress 2016*, p. 941-949. https://doi.org/10.1061/9780784479742.079.

Gowthaman, S., Mitsuyama, S., Makashima, K., Komatsu, M., Kawasaki, S. 2019_1. "Biogeotechnical approach for slope soil stabilization using locally isolated bacteria and inexpensive low-grade chemicals: A feasibility study on Hokkaido expressway soil, Japan." *Soils and Foundations*, Vol. 59, p. 484-499. https://doi.org/10.1016/j.sandf.2018.12.010.

Gowthaman, S., Iki, T., Nakashima, K., Ebina, K., Kawasaki, S. 2019_2. "Feasibility study for slope soil stabilization by microbial induced carbonate precipitation (MICP) using indigenous bacteria isolated from cold subarctic region." *SN Applied Sciences*, Vol. 1, 1480. https://doi.org/10.1007/s42452-019-1508-y.

Gunyol, P., Khosravi, M., Phillips, A., Plymesser, K. 2022. "Thermal Properties of Bio-Cemented Sand." *Geo-Congress 2022: State of the Art and Practice in Geotechnical Engineering*, p. 356-364.

Jung, D., Biggs, H., Erikson, J., Ledyard, P.U. 1975. "New Colorimetric reaction for end-point, continuous-flow, and kinetic measurement of urea." *Clinical Chemistry*, Vol. 21 (8), p. 1136-1140.

Kanagasabapathy, A.S., Kumari, S. 2000. *Guidelines on Standard Operating Procedures for Clinical Chemistry*, SEA-HLM-328.

Kirkland, C.M., Hiebert, R., Hyatt, R., McCloskey, J., Kirksey, J., Thane, A., Cunningham, A.B., Gerlach, R., Spangler, L., Phillips, A.J. 2020. "Direct Injection of Biomineralizing Agents to Restore Injectivity and Wellbore Integrity." *SPE Production & Operations*, Vol. 36. https://doi.org/10.2118/203845-PA.

Ladd, R.S. 1978. "Preparing Test Specimens Using Undercompaction." *Geotechnical Testing Journal*, Vol. 1 (1), p. 16-23. https://doi.org/10.1520/GTJ10364J.

Lauchnor, E.G., Topp, D.M., Parker, A.E., Gerlach, R. 2015. "Whole cell kinetics of ureolysis by Sporosarcina pasteurii." *Journal of Applied Microbiology*, Vol. 118, p. 1321-1332. https://doi.org/10.1111/jam.12804.

Meile, C., Tuncay, K. 2006. "Scale dependence of reaction rates in porous media." *Advances in Water Resources*, Vol. 29, p. 62-71. https://doi.org/10.1016/j.advwatres.2005.05.007.

Nassar, M.K., Gurung, D., Bastani, M., Ginn, T.R., Shafei, B., Gomez, M.G., Graddy, C.M.R., Nelson, D.C., DeJong, J.T. 2018. "Large-Scale Experiments in Microbially Induced Calcite Precipitation (MICP): Reactive Transport Model Development and Prediction." Water Resources Research, Vol. 54, p. 480-500. https://doi.org/10.1002/2017WR021488.

National Academy of Sciences. 2009. *Recommended Practice for Stabilization of Subgrade Soils and Base Materials.* Washington, DC, The National Academies Press. https://doi.org/10.17226/22999.

Omorengie, A.I., Ong, D.E.L., Li, P.Y., Senian, N., Hei, N.L., Esnault-Filet, A., Muda, K., Nissom, P.M. 2023. "Effects of push-pull injection-suction spacing on sand bio-cementation treatment." *Geotechnical Research.* https://doi.org/10.1680/jgere.22.00053.

Porter, H., Dhami, N.K., Mukherjee, A. 2016. "Sustainable Road Bases with Microbial Carbonate Precipitation." *Proceedings of the Fourth International Conference on Sustainable Construction Materials and Technologies.*

Rahman, M.M., Hora, R.N., Ahenkorah, I., Beecham, S., Karim, M.R., Iqbal, A. 2020. "State-of-the-Art Review of Microbial-Induced Calcite Precipitation and Its Sustainability in Engineering Applications." *Sustainability*, Vol. 12, 6281. https://doi.org/10.3390/su12156281.

Sabri, M.M., Shashkin, K.G. 2018. "Improvement of the soil deformation modulus using an expandable polyurethane resin." *Magazine of Civil Engineering*, Vol. 7(83), p. 222-234. https://doi.org/10.18720/MCE.83.20.

Sabri, M.M.S., Vatin, N.I., Alsaffar, K.A.M. 2021. "Soil Injection Technology Using an Expandable Polyurethane Resin: A Review." *Polymers*, Vol. 13, 3666. https://doi.org/10.3390/polym13213666.

Saleh, S., Yunus, N.Z.M., Ahmad, K., Ali, N. 2018. "Improving the strength of weak soil using polyurethane grouts: A review." Construction and Building Materials, Vol. 202, p. 738-752. https://doi.org/10.1016/j.conbuildmat.2019.01.048.

Salifu, E., MacLachlan, E., Iyer, K.R., Knapp, C.W., Tarantino, A. 2015. "Application of microbially induced calcite precipitation in erosion mitigation and stabilization of sandy foreshore slopes: A preliminary investigation." Engineering Geology, Vol. 201, p. 96-105. https://doi.org/10.1016/j.enggeo.2015.12.027.

Saneiyan, S., Ntarlagiannis, D., Colwell, F. 2021. "Complex conductivity signatures of microbial induced calcite precipitation, field and laboratory scales." *Geophysical Journal International*, Vol. 224, p. 1811-1824. https://doi.org/10.1093/gji/ggaa510.

Smit, M.A., Rust, F.C., Akhalwaya, I., Ramdas, V.M. 2022. "Microbial induced calcium carbonate precipitation (MICCP) for road construction." *Proceedings of the 40th Annual Southern African Transport Conference (SATC 2022)*, Vol. 40.

U.S. Department of the Army. 2016. *Theater of Operations: Roads, Airfields, and Heliports – Airfield and Heliport Design*, TM 3-34.48-2.

van Paassen, L.A., Harkes, M.P., van Zwieten, G.A., van der Zon, W.H., van der Star, W.R.L., van Loosdrecht, M.C.M. 2009. "Scale up of BioGrout: a biological ground reinforcement method." *Proceedings of the 17th International Conference on Soil Mechanics and Geotechnical Engineering*, p. 2328-2333. https://doi.org/10.3233/978-1-60750-031-5-2328.

van Paassen, L.A. 2011. "Bio-Mediated Ground Improvement: From Laboratory Experiment to Pilot Applications." *Geo-Frontiers Congress 2011: Advances in Geotechnical Engineering*. https://doi.org/10.1061/41165(397)419.

Whiffin, V.S. 2004. "Microbial $CaCO_3$ Precipitation for the production of Biocement." Doctoral Dissertation, Murdoch University, Perth, WA, AU.

Yang, Y., Chu, J., Cheng, L., Liu, H. 2022. "Utilization of carbide sludge and urine for sustainable biocement production." *Journal of Environmental Chemical Engineering*, Vol. 10, 107443. https://doi.org/10.1016/c.jece.2022.107443.

CHAPTER FIVE

CONCLUSION

The feasibility of UICP's use in road substructure applications has been evaluated through a series of lab-scale experiments. The ideal method of application would be straightforward, treating the surface of a target layer underneath the asphalt, but there was a need to evaluate its necessary components of the treatment process as to whether they would be the most effective option. This included: 1) the administration of treatment solutions, from the top, downwards (as compared to bottom-up and alternating methods of treatment) and the treating of the surface of the soil layer versus an injection into the soil layer's approximate center; 2) the use of solutions composed of commercially available ingredients for treatment; and 3)

From the 50-millimeter-by-100-millimeter specimens, it was determined that treatment administered from the top, downwards, was successful in improving the strength of a soil specimen. Out of the six generated specimens, the two treated using a top-down approach produced the highest UCS strengths (560 to 647 kilopascals). From the 15-centimeter specimens, the treatment was found to produce a significant increase in the CBR value of the soil, from ~11% when untreated, up to 188% when treated. While the top-down, surface treatment seemed to provide a greater increase to the CBR, the probe-injected method seemed to provide better uniformity in the distribution of calcium carbonate from the center of the layer downwards. Commercial-grade alternatives to lab ingredients were found to be successful when used to facilitate the reaction, able to do so at a much lower cost, as little as 20 cents per liter (YEL-) compared to the $2.66 per liter for the lab-grade solution (CMM-). From the 30-centimeter-by-30-centimeter specimen, it was suggested that a combination of surface-level and at-depth

administration of the treatment solutions may provide a more uniform distribution of calcium carbonate. This treatment method also allowed for injection ports to be placed through an overlying layer of asphalt, boding well for field-scale application.

In conjunction, these findings are promising, suggesting that UICP treatment of road base material may be feasible and effective at increasing road capacity. However, some of the results seen during these experiments cannot be generalized to the whole field. For example, even as the top-to-bottom treatment provided the best uniformity of calcium carbonate over the specimen and the highest compressive strength, it cannot be concluded that this will be true in all circumstances. As previously discussed, the resulting effect of UICP treatment on a soil seems to be dependent on a combination of factors in the treatment process itself. It may be that, were the recipe for the solution, the soil type, the bacterial strain, or the patterning of the injections changed, this method would not provide the same result. This may be one of the current difficulties of implementing UICP: it can be accomplished many different ways, using different combinations of ingredients, injection patterns, or sources of bacteria, but each will likely see a varying degree of success. For all of the experiments conducted in this effort, the same soil and bacteria type was used throughout. In order to reach a more general conclusion on the effect of each of the separate factors on the resulting soil strength, the experiments would need be more varied, testing different combinations.

Although, should the scope remain on the application to roads, the results from these experiments are still useful. Of significant benefit were the 30-centimeter-by-30-centimeter tests, proving that treatment of large volumes of coarse-grained soil, in a road-like profile using low-cost ingredients, can produce a notable increase in strength.

Suggested Areas of Research

Beyond the general recommendation to explore a wider range of combinations of treatment conditions, there are several subjects of study that could help further address the feasibility of road application. One of the current concerns of the use of UICP in field applications is that the process produces a significant amount of ammonium (NH_4^+) byproducts, which pose a risk to the local ecological wellbeing through nitrogen imbalance (Britto and Kronzucker, 2002). In-situ, the retention of the effluent from injected solutions is a difficult prospect, especially in highly permeable soils; the loss of solutions into the local water system appears to be unavoidable. However, the use of struvite precipitation has shown promise as a method of negating the ammonium output of UICP (Yu et al., 2022; Yu et al., 2019). Struvite's precipitation involves a reaction between a magnesium ion, phosphate, and ammonium, as illustrated in Equation 5-1.

$$Mg^{2+} + PO_4^{3-} + NH_4^+ + 6H_2O \rightarrow MgNH_4PO_4 \cdot 6H_2O \qquad \text{Equation 5-1.}$$

Yu et al. (2022) has proposed the use of microbially-induced struvite precipitation (MISP), conducted either in tandem with UICP or as an alternative, in order to facilitate soil reinforcement and eliminate the ammonium output. While a potential solution, few studies are available on the use of struvite in this context, especially concerning any relationship between scale and effectiveness at ammonium removal.

There has also been interest in the use of zeolite, an "abundant and low-cost" mineral (Su et al., 2022) to which ammonium adsorbs. Zeolite can be used by itself in solid form, the reaction based around an ionic exchange; provided enough zeolite, the ammonium level in a solution can be reduced significantly with relatively little contact time. The benefit of using zeolites over struvite precipitation is that there is no modification of the treatment solutions needed, the effluent

solution permitted contact time with zeolites. However, research into mechanisms of deployment at the field scale are limited, and zeolite particles are limited in the amount of ammonium that they can remove from solution (Guida et al., 2020).

A current research effort underway at Montana State University seeks to investigate the combined use of zeolites and struvite precipitation to reduce the ammonium produced from the UICP treatment of sand specimens. Should this effort be successful, this may serve as a foundation for larger-scale testing, providing guidance for ecologically-sound, field-scale application of UICP.

CUMULATIVE REFERENCES

AASHTO. 1993. *AASHTO Guide for Design of Pavement Structures*.

Achal, V., Mukherjee, A., Basu, P.C., Reddy, M.S. 2009. "Lactose mother liquor as an alternative nutrient source for microbial concrete production by Sporosarcina pasteurii." *Journal for Industrial Microbiology and Biotechnology*, Vol. 36, p. 433-438. https://doi.org/10.1007/s10295-008-0514-7.

Arab, M.G., Alsodi, R., Almajed, A., Yasuhara, H., Zeiada, W., Shahin, M.A. 2021. "State-of-the-Art Review of Enzyme-Induced Calcite Precipitation (EICP) for Ground Improvement: Applications and Prospects." *Geosciences 2021*, Vol. 11 (12), 492. https://doi.org/10.3390/geosciences11120492.

ASTM. 2002_1. *Standard Test Methods for Maximum Index Density and Unit Weight of Soils Using a Vibratory Table.* D4253. https://www.astm.org/d4253-16e01.html.

ASTM. 2002_2. *Standard Test Methods for Minimum Index Density and Unit Weight of Soils and Calculation of Relative Density.* D4254. https://www.astm.org/d4254-16.html.

ASTM. 2010. *Standard Test Method for Unconfined Compressive Strength of Cohesive Soil.* D2166. https://www.astm.org/standards/d2166.

ASTM. 2014. *Standard Test Methods for Specific Gravity of Soil Solids by Water Pycnometer*. D854. https://www.astm.org/d0854-14.html.

ASTM. 2016_1. *Standard Test Methods for Minimum Index Density and Unit Weight of Soils and Calculation of Relative Density.* D4254. https://www.astm.org/standards/d4254.

ASTM. 2016_2. *Standard Test Methods for Maximum Index Density and Unit Weight of Soils Using a Vibratory Table.* D4253. https://www.astm.org/standards/d4253.

ASTM. 2021. *Standard Test Method for California Bearing Ratio (CBR) of Laboratory-Compacted Soils.* D1883. https://doi.org/10.1520/D1883-21.

Beser, G.D. 2018. "Ureolysis Induced Mineral Precipitation Material Properties." Master's thesis, Montana State University, Bozeman, MT, USA.

Black, J.A., Hakhamaneshi, M., Cargill, C.M., Elmrom, T. 2016. "Development and calibration of a sand pluviation device for preparation of a model sand bed for centrifuge tests." *Proceedings of the 3rd European Conference on Physical Modelling in Geotechnics*, p. 73-79.

Britto, D.T., Kronzucker, H. 2002. "NH4+ toxicity in higher plants: a critical review." *Journal of Plant Physiology*, Vol. 159, p. 567-584. https://doi.org/10.1078/0176-1617-0774.

Buzzi, O., Fityus, S., Sloan, S.W. 2010. "Use of expanding polyurethane resin to remediate expansive soil foundations." *Canadian Geotechnical Journal,* Vol. 47, p. 623-634. https://doi.org/10.1139/T09-132.

Chan, C.K. 1985. *Instruction manual, CKC E/P cyclic loading triaxial system users' manual.* San Fransisco, CA: Soil Engineering Equipment Company.

Chek, A., Crowley, R., Ellis, T.N., Durnin, M., Wingender, B. 2021. "Evaluation of Factors Affecting Erodibility Improvement for MICP-Treated Beach Sand." *Journal of Geotechnical and Geoenvironmental Engineering,* Vol. 147 (3). https://doi.org/10.1061/(ASCE)GT.1943-5606.0002481.

Chen, L., Song, Y., Fang, H., Feng, Q., Lai, C., Song, X. 2022. "Systematic optimization of a novel, cost-effective fermentation medium of Sporosarcina pasteurii for microbially induced calcite precipitation (MICP)." *Construction and Building Materials,* Vol. 348, 128632. https://doi.org/10.1016/j.conbuildmat.2022.128632.

Cheng, L., Cord-Ruwisch, R., Shahin, M.A. 2013. "Cementation of sand soil by microbially induced calcite precipitation at various degrees of saturation." *Canadian Geotechnical Journal,* Vol. 50, p. 81-90. https://doi.org/10.1139/cgj-2012-0023.

Cheng, Y.J., Tang, C.S., Pan, X.H., Liu, B., Xie, Y.H., Cheng, Q., Shi, B. 2021. "Application of microbial induced carbonate precipitation for loess surface erosion control." *Engineering Geology,* Vol. 294, 106387. https://doi.org/10.1016/j.enggeo.2021.106387.

Choi, S., Wang, K., Chu, J. 2016. "Properties of biocemented, fiber reinforced sand." *Construction and Building Materials,* Vol. 120, p. 623-629. https://doi.org/10.1016/j.conbuildmat.2016.05.124.

Cord-Ruwich, R., Shahin, M. 2013. "Cementation of sand soil by microbially induced calcite precipitation at various degrees of saturation." *Canadian Geotechnical Journal,* Vol. 50, p. 81-90. https://doi.org/10.1139/cgj-2012-0023.

Crane, L., Ray, H., Hamdan, N., Boyer, T.H. 2022. "Enzyme-induced carbonate precipitation utilizing fresh urine and calcium-rich zeolites." *Journal of Environmental Chemical Engineering,* Vol. 10 (2), 107238. https://doi.org/10.1016/j.jece.2022.107238.

Danjo, T., Kawasaki, S. 2016. "Microbially Induced Sand Cementation Method Using Pararhodobacter sp. Strain SO1, Inspired by Beachrock Formation Mechanism." *Materials Transactions,* Vol. 57 (3), p. 428-437. https://doi.org/10.2320/matertrans.M-M2015842.

DeJong, J.T., Mortensen, B.M., Martinez, B.C., Nelson, D.C. 2010. "Bio-mediated soil improvement." *Ecological Engineering,* Vol. 36, p. 197–210. https://doi.org/10.1016/j.ecoleng.2008.12.029.

DeJong, J.T, Burrall, M., Wilson, D.W., Frost, J.D. 2017. "A bio-inspired perspective for geotechnical engineering innovation." *Geotechnical Frontiers 2017,* 862-870. https://doi.org/10.1061/9780784480472.092.

DeJong, J.T., Gomez, M.G., San Pablo, A.C.M., Graddy, C.M.R., Nelson, D.C., Lee, M., Ziotopoulou, K., Kortbawi, M.E., Montoya, B., Kwon, T.H. 2022. "State of the Art: MICP soil improvement and its application to liquefaction hazard mitigation." *Proceedings of the 20th International Conference on Soil Mechanics and Geotechnical Engineering, Sydney 2021*, p. 405-508.

Deng, X., Li, Y., Liu, H., Zhao, Y., Yang, Y., Xu, X., Cheng, X., de Wit, B. 2021. "Examining Energy Consumption and Carbon Emissions of Microbial Induced Carbonate Precipitation Using the Life Cycle Assessment Method." *Sustainability*, Vol. 13, 4856. https://doi.org/10.3390/su13094856.

Dick, J., Windt, W.M., Graef, B.D., Saveyn, H., Van der Meeren, P., Belie, N.D., Verstraete, W. 2006. "Bio-deposition of a calcium carbonate layer on degraded limestone by Bacillus species." *Biodegradation*, Vol. 17, p. 357-367. https://doi.org/10.1007/s10532-005-9006-x.

Dione, A., Fall, M., Berthaud, Y., Benboudjema, F., Michou, A. 2014. "Implementation of Resilient Modulus – CBR relationship on Mechanistic-Empirical (M.-E) Pavement Design." *Revue du CAMES – Sciences Appliquées et de l'Ingeniuer,* Vol. 1 (2), December 2014.

Do, J., Montoya, B.M., Gabriel, M. A. 2020. "Scour mitigation and erodibility improvement using microbially induced carbonate precipitation." *Geotechnical Testing Journal*, Vol. 44 (5): 1467–1483. https://doi.org/10.1520/GTJ20190478.

Dorian, H., Gunyol, P., Lauf, J., Khosravi, M., Phillips, A., Cunningham, A. 2023. "Evaluating Injection Strategies for Microbially Induced Calcite Precipitation and Implications for Applications to Road Structures." *Geo-Congress 2023: State of the Art and Practice in Geotechnical Engineering*, p. 351-360. https://doi.org/10.1061/9780784484661.037.

Fouladi, A.S., Arulrajah, A., Chu, J., Horpibulsuk, S. 2023. "Application of Microbially Induced Calcite Precipitation (MICP) technology in construction materials: A comprehensive review of waste stream contributions." *Construction and Building Materials*, Vol. 388, 131546. https://doi.org/10.1016/j.conbuildmat.2023.131546.

Ghasemi, P., A. Zamani, and B. Montoya. 2019. "The effect of chemical concentration on the strength and erodibility of MICP treated sands." *Geo-Congress 2020: Soil Improvement*, Geotechnical Special Publication 309, edited by C. L. Meehan, S. Kumar, M. A. Pando, and J. T. Coe, 241–249. Reston, VA: ASCE.

Ghasemi, P., Montaya, B.M. 2022. "Field Implementation of Microbially Induced Calcium Carbonate Precipitation for Surface Erosion Reduction of a Coastal Plain Sandy Slope." *Journal of Geotechnical and Geoenvironmental Engineering*, Vol. 148 (9), 04022071. https://doi.org/10.1061/(ASCE)GT.1943-5606.0002836.

Gollapudi, U.K., Knutson, C.L., Bang, S.S., Islam, M.R. 1995. "A new method for controlling leaching through permeable channels." *Chemosphere*, Vol. 30 (4), p. 695-705. https://doi.org/10.1016/0045-6535(94)00435-W.

Gomez, M., Anderson, C., DeJong, J., Nelson, D., Lau, X. 2014. "Stimulating In Situ Soil Bacteria for Bio-Cementation of Sands." *Geo-Congress 2014: Geo-characterization and Modeling for Sustainability*, p. 1674-1682. https://doi.org/10.1061/9780784413272.164.

Gomez, M.G., DeJong, J.T., Anderson, C.M., Nelson, D.C., Graddy, C.M. 2016. "Large-Scale Bio-Cementation Improvement of Sands." *Geotechnical and Structural Engineering Congress 2016*, p. 941-949. https://doi.org/10.1061/9780784479742.079.

Gowthaman, S., Mitsuyama, S., Makashima, K., Komatsu, M., Kawasaki, S. 2019_1. "Biogeotechnical approach for slope soil stabilization using locally isolated bacteria and inexpensive low-grade chemicals: A feasibility study on Hokkaido expressway soil, Japan." *Soils and Foundations*, Vol. 59, p. 484-499. https://doi.org/10.1016/j.sandf.2018.12.010.

Gowthaman, S., Iki, T., Nakashima, K., Ebina, K., Kawasaki, S. 2019_2. "Feasibility study for slope soil stabilization by microbial induced carbonate precipitation (MICP) using indigenous bacteria isolated from cold subarctic region." *SN Applied Sciences*, Vol. 1, 1480. https://doi.org/10.1007/s42452-019-1508-y.

Guida, S., Potter, C., Jefferson, B., Soares, A. 2020. "Preparation and evaluation of zeolites for ammonium removal from municipal wastewater through ion exchange process." *Scientific Reports*, Vol. 10, 12426. https://doi.org/10.1038/s41598-020-69348-6.

Gunyol, P., Khosravi, M., Phillips, A., Plymesser, K. 2022. "Thermal Properties of Bio-Cemented Sand." *Geo-Congress 2022: State of the Art and Practice in Geotechnical Engineering*, p. 356-364. https://doi.org/10.1061/9780784484012.037.

Heukelom, W., Foster, C.R. 1962. "Dynamic Testing of Pavements." *Transactions of the American Society of Civil Engineers*, Vol. 127 (1), January 1962.

Hoang, T., Alleman, J., Cetin, B., Choi, S. 2020. "Engineering Properties of Biocementation Coarse- and Fine-Grained Sand Catalyzed By Bacterial Cells and Bacterial Enzyme." *Journal of Materials in Civil Engineering*, Vol. 32 (4), 04020030. https://doi.org/10.1061/(ASCE)MT.1943-5533.0003083.

Hodges, T. M., and B. N. Lingwall. 2020. “Case histories of full-scale microbial bio-cement application for surface erosion control.” *Geo-Congress 2020: Biogeotechnics,* Geotechnical Special Publication 320, edited by E. Kavazanjian, J. P. Hambleton, R. Makhnenko, and A. S. Budge, 9–19. Reston, VA: ASCE.

International Code Council. 2021. *International Building Code.* Fall Church, VA, USA: International Code Council.

Jain, D., Das, S.K. 2023. “Influence of Size and Concentration of Carbonate Biomineral on Biocementation and Bioclogging for Mitigating Soil Degradation.” *Biogeotechnics,* 100021. https://doi.org/10.1016/j.bgtech.2023.100021.

Jiang, N.-J., C.-S. Tang, L.-Y. Yin, Y.-H. Xie, and B. Shi. 2019. “Applicability of microbial calcification method for sandy-slope surface erosion control.” *Journal of Materials in Civil Engineering,* Vol. 31 (11): 04019250. https://doi.org/10.1061/(ASCE)MT.1943-5533.0002897.

Jung, D., Biggs, H., Erikson, J., Ledyard, P.U. 1975. “New Colorimetric reaction for end-point, continuous-flow, and kinetic measurement of urea.” *Clinical Chemistry*, Vol. 21 (8), p. 1136-1140.

Kanagasabapathy, A.S., Kumari, S. 2000. *Guidelines on Standard Operating Procedures for Clinical Chemistry,* SEA-HLM-328.

Kirkland, C.M., Hiebert, R., Hyatt, R., McCloskey, J., Kirksey, J., Thane, A., Cunningham, A.B., Gerlach, R., Spangler, L., Phillips, A.J. 2021. “Direct Injection of Biomineralizing Agents to Restore Injectivity and Wellbore Integrity.” *SPE Production & Operations*, Vol. 36. https://doi.org/10.2118/203845-PA.

Ladd, R.S. 1978. “Preparing Test Specimens Using Undercompaction.” *Geotechnical Testing Journal*, Vol. 1 (1), p. 16-23. https://doi.org/10.1520/GTJ10364J.

Lauchnor, E.G., Topp, D.M., Parker, A.E., Gerlach, R. 2015. “Whole cell kinetics of ureolysis by Sporosarcina pasteurii.” *Journal of Applied Microbiology*, Vol. 118, p. 1321-1332. https://doi.org/10.1111/jam.12804.

Li, M., Wen, K., Li, Y., Zhu, L. 2018. “Impact of Oxygen Availability on Microbially Induced Calcite Precipitation (MICP) Treatment. Calcerous Sand.” *Canadian Geotechnical Journal*, Vol. 56, p. 1502-1513. https://doi.org/10.1139/cgj-2018-0007.

Li., X., Scheibe, T.D., Johnson, W.P. 2004. “Apparent decreases in colloid deposition rate coefficients with distance of transport under unfavorable deposition conditions: a general phenomenon.” *Environmental Science Technology*, Vol. 38 (11), p. 5616-5625. https://doi.org/10.1021/es049154v.

Liu, K. W., N. J. Jiang, J. Qin, Y. J. Wang, C. S. Tang, and X. Han. 2021. "An experimental study of mitigating coastal sand dune erosion by microbial- and enzymatic-induced carbonate precipitation." *Acta Geotechnica*, Vol. 16 (2), p. 467–480. https://doi.org/10.1007/s11440-020-01046-z.

Liu, L., Liu, H., Stuedlein, A.W., Evans, M.T., Xiao, Y. 2019. "Strength, Stiffness, and Microstructure Characteristics of Biocemented Calcerous Sand." *Canadian Geotechnical Journal*, Vol. 56, p. 1502-1513. https://doi.org/10.1139/cgj-2018-0007.

Liu, Q., Montoya, B.M. 2021 "Microbial-induced calcium carbonate precipitation to accelerate sedimentation of fine tailings." *Journal of Geotechnical and Geoenvironmental Engineering*, Vol. 147 (10), 02821001. https://doi.org/10.1061/(ASCE)GT.1943-5606.0002651.

Maleki, M., S. Ebrahimi, F. Asadzadeh, and M. Emami Tabrizi. 2016. "Performance of microbial-induced carbonate precipitation on wind erosion control of sandy soil." *International Journal of Environmental Science Technology*, Vol. 13 (3), p. 937–944. https://doi.org/10.1007/s13762-015-0921-z.

Maleki-Kakelar, M., Aghaeinejad-Meybodi, A., Sanjideh, S., Azarhoosh, A.J. 2022. "Cost-Effective Optimization of Bacterial Urease Activity Using a Hybrid Method Based on Response Surface Methodology and Artificial Neural Networks." *Environmental Processes*, Vol. 9, 7. https://doi.org/10.1007/s40710-022-00564-0.

Martinez, B.C., DeJong, J.T., Ginn, T.R., Montoya, B.M., Barkouki, T.H., Hunt, C., Tanyu, B., Major, D. 2013. "Experimental optimization of microbial-induced carbonate precipitation for soil improvement." *Journal of Geotechnical and Geoenvironmental Engineering*, Vol. 139 (4), p. 587-598. https://doi.org/10.1061/(ASCE)GT.1943-5606.0000787.

Meile, C., Tuncay, K. 2006. "Scale dependence of reaction rates in porous media." *Advances in Water Resources*, Vol. 29, p. 62-71. https://doi.org/10.1016/j.advwatres.2005.05.007.

Montoya, B.M., DeJong, J.T., Boulanger, R.W. 2013. Dynamic response of liquefiable sand improved by microbial-induced calcite precipitation. *Géotechnique*, Vol. 63 (4), p. 302-312. https://doi.org/10.1680/geot.SIP13.P.019.

Montoya, B.M., DeJong, J.T., Boulanger, R.W., Wilson, D.W., Gerhard, R., Ganchenko, A., Chou, J.C. (2012). Liquefaction Mitigation Using Microbial Induced Calcite Precipitation. *Geo-Congress 2012: State of the Art and Practice in Geotechnical Engineering*, p. 1918-1927.

Montoya, B. M., J. Do, and M. M. Gabr. (2018). "Erodibility of microbial induced carbonate precipitation-stabilized sand under submerged impinging jet." *IFCEE 2018*, p. 19–28. Reston, VA, ASCE. https://doi.org/10.1061/9780784481592.003.

Mortensen, B.M., Haber, M.J., DeJong, J.T., Caslake, L.F., Nelson, D.C. 2011. "Effects of environmental factors on microbial induced calcium carbonate precipitation: Environmental factors on MICP." *Journal of Applied Microbiology*, Vol. 111 (2), p. 338-349. https://doi.org/10.1111/j.1365-2672.2011.05065.x.

Naeimi, M., Chu, J., Khosroshahi, M., Zenouzi, L.K. 2023. "Soil stabilization for dunes fixation using microbially induced calcium carbonate precipitation." *Geoderma,* Vol. 429, 116183. https://doi.org/10.1016/j.geoderma.2022.116183.

Nafisi, A., Montoya, B.M., Evans, T.M. 2020. "Shear strength envelopes of biocemented sands with varying particle size and cementation level." *Journal of Geotechnical and Geoenvironmental Engineering*, Vol. 146 (3), 04020002. https://doi.org/10.1061/(ASCE)GT.1943-5606.0002201.

Nassar, M.K., Gurung, D., Bastani, M., Ginn, T.R., Shafei, B., Gomez, M.G., Graddy, C.M.R., Nelson, D.C., DeJong, J.T. 2018. "Large-Scale Experiments in Microbially Induced Calcite Precipitation (MICP): Reactive Transport Model Development and Prediction." Water Resources Research, Vol. 54, p. 480-500. https://doi.org/10.1002/2017WR021488.

National Academy of Sciences. 2009. *Recommended Practice for Stabilization of Subgrade Soils and Base Materials.* Washington, DC, The National Academies Press. https://doi.org/10.17226/22999.

Omoregie, A.I., Ngu, L.H., Ong, D.E.L., Nissom, P.M. 2019. "Low-cost cultivation of Sporosarcina pasteurii strain in food-grade yeast extract medium for microbially induced calcite precipitation (MICP) application." *Biocatalysis and Agricultural Biotechnology*, Vol. 17, p. 247-255. https://doi.org/10.1019.j.bcab.2018.11.030.

Phillips, A.J. 2013. "Biofilm-induced Calcium Carbonate Precipitation: Application in the Subsurface." Doctoral dissertation, Montana State University, Bozeman, MT, USA.

Phillips, A.J., Gerlach, R., Lauchnor, E., Mitchell, A.C., Cunningham, A., Spangler, L. 2013_1. "Engineered applications of ureolytic biomineralization: a review." *Biofouling*, Vol. 29, p. 715-733. https://doi.org/10.1080/08927014.2013.796550.

Phillips, A.J., Lauchnor, E., Eldring, J., Esposito R., Mitchell, A.C., Gerlach, R., Cunningham, A., and Spangler, L. 2013_2. "Potential CO_2 leakage reduction through biofilm-induced calcium carbonate precipitation." *Environmental Science & Technology*, Vol. 47 (1), p. 142-149. https://doi.org/10.1021/ess301294q.

Pongsivasathiti, S., Horpibulsuk, S., Piayphipat, S. 2019. "Assessment of Mechanical Properties of Cement Stabilized Soils." *Case Studies in Construction Materials*, 11th Edition. https://doi.org/10.1016/j.cscm.2019.e00301.

Porter, H., Dhami, N.K., Mukherjee, A. 2016. "Sustainable Road Bases with Microbial Carbonate Precipitation." *Proceedings of the Fourth International Conference on Sustainable Construction Materials and Technologies.* https://doi.org/10.18552/2016/SCMT4S169.

Pungrasmi, W., Intarasoontron, J., Jongvivatsakul, P., Likitlersuang, S. 2019. "Evaluation of microencapsulation techniques for MICP bacterial spores applied in self-healing concrete." *Scientific Reports*, Vol. 9 (1), 12484. https://doi.org/10.1038/s41598-019-49002-6.

Rahman, M.M., Hora, R.N., Ahenkorah, I., Beecham, S., Karim, M.R., Iqbal, A. 2020. "State-of-the-Art Review of Microbial-Induced Calcite Precipitation and Its Sustainability in Engineering Applications." *Sustainability*, Vol. 12, 6281. https://doi.org/10.3390/su12156281.

Rahmaninezhad, S.A., Farnam, Y.A., Schauer, C.L., Najafi, A.R., Sales, C.M. 2022. "Influence of culturing media components on the growth and microbial induced calcium carbonate precipitation (MICP) activity of Lysinibacillus sphaericus." bioRxiv. https://doi.org/10.1101/2022.05.23.493178.

Safavizadeh, S., Montoya, B.M., Gabr, M.A. 2019. "Microbial induced calcium carbonate precipitation in coal ash." *Géotechnique*, Vol. 69 (8), p. 727-740. https://doi.org/10.1680/jgeot.18.P.062.

Sabri, M.M., Shashkin, K.G. 2018. "Improvement of the soil deformation modulus using an expandable polyurethane resin." *Magazine of Civil Engineering*, Vol. 7 (83), p. 222-234. https://doi.org/10.18720/MCE.83.20.

Sabri, M.M.S., Vatin, N.I., Alsaffar, K.A.M. 2021. "Soil Injection Technology Using an Expandable Polyurethane Resin: A Review." *Polymers*, Vol. 13, 3666. https://doi.org/10.3390/polym13213666.

Saleh, S., Yunus, N.Z.M., Ahmad, K., Ali, N. 2018. "Improving the strength of weak soil using polyurethane grouts: A review." *Construction and Building Materials*, Vol. 202, p. 738-752. https://doi.org/10.1016/j.conbuildmat.2019.01.048.

Salifu, E., MacLachlan, E., Iyer, K.R., Knapp, C.W., Tarantino, A. 2015. "Application of microbially induced calcite precipitation in erosion mitigation and stabilization of sandy foreshore slopes: A preliminary investigation." *Engineering Geology*, Vol. 201, p. 96-105. https://doi.org/10.1016/j.enggeo.2015.12.027.

San Pablo, A.C.M., Lee, M., Graddy, C.M.R., Kolbus, C.M., Khan, M., Zamani, A., Martin, N., Acuff, C., DeJong, J.T., Gomez, M.G., Nelson, D.C. 2020. "Meter-scale biocementation experiments to advance process control and reduce impacts: Examining spatial control, ammonium by-product removal, and chemical reductions." *Journal of Geotechnical and Geoenvironmental Engineering.* Vol. 146 (11), 04020125. https://doi.org/10.1061/(ASCE)GT.1943-5606.0002377.

Saneiyan, S., Ntarlagiannis, D., Colwell, F. 2021. "Complex conductivity signatures of microbial induced calcite precipitation, field and laboratory scales." *Geophysical Journal International*, Vol. 224, p. 1811-1824. https://doi.org/10.1093/gji/ggaa510.

Shanahan, C., and B. M. Montoya. 2016. "Erosion reduction of coastal sands using microbial induced calcite precipitation." *Geo-Chicago 2016: Sustainability and Resiliency in Geotechnical Engineering*, Geotechnical Special Publication 269, edited by D. Zekkos, A. Farid, A. De, K. R. Reddy, and N. Yesiller, p. 458–466. Reston, VA: ASCE. https://doi.org/10.1061/9780784480120.006.

Shirakawa, M.A., Cincotto, M.A., Atencio, D., Gaylarde, C.C., John, V.M. 2011. "Effect of culture medium on biocalcification by Pseudomonas putida, Lysinibacillus sphaericus and Bacillus subtilis." *Brazilian Journal of Microbiology*, Vol. 42, p. 499-507. https://doi.org/10.1590/S1517-838220110002000014.

Simatupang, M., Okamura, M., Hayashi, K., Yasuhara, H. 2018. "Small-strain shear modulus and liquefaction resistance of sand with carbonate precipitation." *Soil Dynamics and Earthquake Engineering*, Vol. 115, p. 710-718. https://doi.org/10.1016/j.soildyn.2018.09.027.

Smit, M.A., Rust, F.C., Akhalwaya, I., Ramdas, V.M. 2022. "Microbial induced calcium carbonate precipitation (MICCP) for road construction." *Proceedings of the 40th Annual Southern African Transport Conference (SATC 2022)*, Vol. 40.

Su, F., Yang, Y., Qi, Y., Zhang, H. 2021. "Combining microbially induced calcite precipitation (MICP) with zeolite: A new technique to reduce ammonia emission and enhance soil treatment ability of MICP technology." *Journal of Environmental Chemical Engineering*, Vol. 10, 107770. https://doi.org/j.jece.2022.107770.

Sun, X., Miao, L., Wang, H., Wu, L., Fan, G., Xia, J. 2022. "Sand Foreshore Slope Stability and Erosion Mitigation Based on Microbiota and Enzyme Mix-Induced Carbonate Precipitation." *Journal of Geotechnical and Geoenvironmental Engineering*, Vol. 148 (8), 04022058. https://doi.org/10.1061/(ASCE)GT.1943-5606.0002839.

Terzis, D., Laloui, L. 2019. "Cell-free soil bio-cementation with strength, dilatency and fabric characterization." *Acta Geotechnica*, Vol. 14, p. 639-656. https://doi.org/10.1007/s11440-019-00764-3.

Thompson, M.R. 1966. "Shear Strength and Elastic Properties of Lime-Soil Mixtures." Highway Research Board, University of Illinois, Champaign, IL, 1-14.

U.S. Census Bureau. 2020. 2020 Annual Surveys of State and Local Government Finances. https://www.census.gov/data/datasets/2020/econ/local/public-use-datasets.html

U.S. Department of the Army. 2016. *Theater of Operations: Roads, Airfields, and Heliports – Airfield and Heliport Design*, TM 3-34.48-2.

van Paassen, L.A., Harkes, M.P., van Zwieten, G.A., van der Zon, W.H., van der Star, W.R.L., van Loosdrecht, M.C.M. 2009. "Scale up of BioGrout: a biological ground reinforcement method." *Proceedings of the 17th International Conference on Soil Mechanics and Geotechnical Engineering*, p. 2328-2333. https://doi.org/10.3233/978-1-60750-031-5-2328.

van Paassen, L.A. 2011. "Bio-Mediated Ground Improvement: From Laboratory Experiment to Pilot Applications." *Geo-Frontiers Congress 2011: Advances in Geotechnical Engineering*. https://doi.org/10.1061/41165(397)419.

Whiffin, V.S. 2004. "Microbial $CaCO_3$ Precipitation for the production of Biocement." Doctoral Dissertation. Perth, WA, AU: Murdoch University.

Xiao, Y., Wang, Y., Wang, S., Evans, T.M., Stuedlein, A.W., Chu, J., Zhao, C., Wu, H., Liu, H. 2021. "Homogeneity and mechanical behaviors of sands improved by a temperature-controlled one-phase MICP method." *Acta Geotechnica*, Vol. 16 (5), p. 1417-1427. https://doi.org/10.1007/s11440-020-01122-4.

Yang, Y., Chu, J., Cheng, L., Liu, H. 2022. "Utilization of carbide sludge and urine for sustainable biocement production." *Journal of Environmental Chemical Engineering*, Vol. 10, 107443. https://doi.org/10.1016/c.jece.2022.107443.

Yasuhara, H., Neupane, D., Hayashi, K., Okamura, M. 2012. "Experiments and predictions of physical properties of sand cemented by enzymatically-induced carbonate precipitation." *Soils and Foundations*, Vol. 52 (3), p. 539-549. https://doi.org/10.1016/j.sandf.2012.05.011.

Yu, X., Zhan, Q., Qian, C., Ma, J., Liang, Y. 2019. "The optimal formation of bio-carbonate and bio-magnesium phosphate cement to reduce ammonia emission." Journal of Cleaner Production, Vol. 240, 118156. https://doi.org/10.1016/j.jclepro.2019.118156.

Yu, X., Yang, H., Wang, H. 2022. "A cleaner biocementation method of soil via microbially induced struvite precipitation: A experimental and numerical analysis." Journal of Environmental Management, Vol. 316, 115280. https://doi.org/j.jenvman.2022.115280.

APPENDICES

APPENDIX A

SUPPLEMENTARY MATERIAL FOR PAPER 2

Table A1. - Comparative per-gram costs of ingredient sources; 'unit' refers to the purchase unit, price is MSRP estimate based on 2021 pricing.

Purpose	***Product (Abbreviation)***	***Brand***	***Unit Cost ($)***	***Unit Mass (g)***	***$/g***
Carbon & Nutrients	*Nutrient Broth (NB)*	*Becton Dickenson*	176.71	500	0.353
	Brain-Heart Infusion (BHI)	*Becton Dickenson*	572.84	2000	0.286
	Yeast Extract (YE)	*Agros Organic*	16.5	1000	0.017
Urea	*Urea Granules (FS Urea)*	*Fisher Scientific*	32.35	500	0.065
	Diesel Exhaust Fluid (DEF)	*BlueDEF*	330	66528	0.005
Amm. Chloride	*Ammonium Chloride (FS NH_4Cl)*	*Fisher Scientific*	305.75	10000	0.031
Cal. Chloride	*Calcium Chloride Dihydrate (FS $CaCl_2$)*	*Fisher Scientific*	133.17	3000	0.044
	Peladow (PW)	*Occidental Chem. Corp.*	45.99	22680	0.002
	Liquidow (LW)	*Occidental Chem. Corp.*	1490	283500	0.005

Table A2. – Soil characteristics for the Sakrete® silica sand used in this experiment.

Parameter	**Sakrete® Silica Sand**
Specific Gravity – G_S	2.66
Median Particle Size – D_{50}	0.67 mm
Uniformity Coefficient – C_U	1.69
Curvature Coefficient – C_C	0.91
Minimum Void Ratio – e_{min}	0.53
Maximum Void Ratio – e_{max}	0.97

Table A3. - Comparison between peak UCS achieved through UICP across multiple studies.

D50 (mm)	*Cu*	*Cc*	*Dr (%)*	*Size (H × D in mm)*	*Peak UCS (MPa)*	*% CaCO3*	*Treatment Conditions*	*Source*
0.72	1.21	1.02	64.6	100 × 50	2.3	16	Top-down injection, recirculated, 16 pulses.	Hoang et al. 2020
0.7	1.67	0.91	--	100 × 50	~10	29	Gravity-saturated, 0.3M CaCO3 and Urea in solution, cured for 28 days.	Danjo and Kawasaki 2016
0.69	1.37	1.01	--	160 × 55	2.3	5.7	Gravity-saturated, 20% saturation.	Cord-Ruwisch and Shahin 2013
0.42	--	--	--	80 × 39	1.8	9.9	Submersion, forcibly aerated during treatment	Li et al. 2018
0.36	2.36	1.11	40	80 × 40	2.3	--	Injected, calcium solution recirculated; ratio of 5:1 calcium solution volume to sample volume	Liu et al. 2019
0.39	1.6	0.91	*"Maximum"*	100 × 50	11.3	~9	Alternating injection, 16 pulses, samples cored from larger treated specimen, treated using lyophilized bacteria cells.	Terzis and Laloui 2019
0.67	1.69	0.91	35	100 × 50	0.6	4.5	Top-down injection, 14 pulses.	Current Research

APPENDIX B

SUPPLEMENTARY MATERIAL FOR PAPER 3

Reactor Construction

The 15-centimeter-diameter soil column was sealed at both ends using flat plates. The plates measured 17.8 by 17.8 centimeters and were 1.27 centimeters thick. A 3.2-millimeter groove was machined into each plate to fit onto the ends of the cylinder. The top plate featured an additional smaller groove within the larger one for an ‘o’ ring. Each plate had holes at the corners to accommodate threaded rods, which were used to close and seal the reactor. The holes in the top plate were clean-bored, while the holes in the bottom plate were threaded. The bottom plate was glued to the cylinder using PVC cement, and the top plate was secured to the top by wingnuts on threaded rods, screwed into the bottom plate.

The larger, 30-centimeter-by-30-centimeter reactor was constructed using acrylic and PVC components, the acrylic allowing for improved viewing of the soil during treatment over the clear PVC. Like the smaller specimens, this reactor was designed to withstand the anticipated load for testing. Although the reactor would not be pressurized, it needed to be leak resistant when the sample was saturated. The resulting design is shown in Figure 4-2. This reactor consisted of five main pieces: two longer walls (38 centimeters long) for the front and rear, with eight cleanly-bored holes for screws and a groove for a gasket to be placed; two shorter side walls (30 centimeters long) affixed with an additional acrylic block with tapped holes complementing those on the longer walls, also having threaded holes near the foot of the reactor for outlet lines to be connected; and a base plate, featuring two-centimeter-deep grooves for the side walls to situate in and a smaller 30-millimeter groove for an ‘o’ ring, as well as eight, upward-facing threaded holes. The longer walls were affixed to the side walls using screws, the gasket being compressed between the meeting point of these two walls. This top assembly was then fitted into the groove of the base

plate, on top of the 'o' ring. Threaded rods were driven into the holes along the base, and metal plates placed on top of the top assembly, making contact with the extending portions of the longer walls and the entire top of the side walls. These plates had holes placed similarly to those on the base plate, and would be used to secure the top assembly to the base by means of wingnuts. When the wingnuts were tightened, the 'o' ring was compressed between the top assembly and the base plate, creating a seal along the foot of the reactor. Additionally, waterproof tape was placed along the inner seams of the reactor to further ensure no leaks would occur.

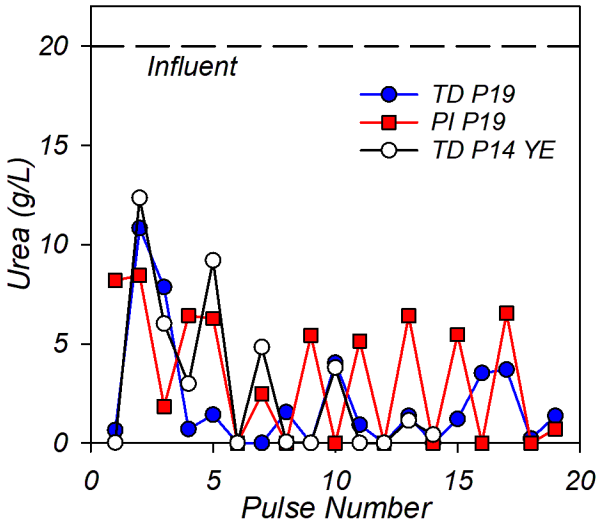

Figure B1. – Jung-assay-determined urea concentration monitored over the treatment process for 15-centimeter specimens. Each reading corresponds to the effluent from the previous injection.

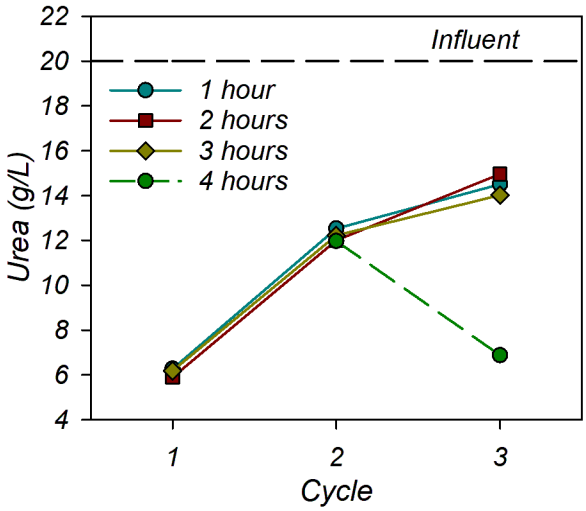

Figure B2. - Jung-assay-determined urea concentration over the treatment process for the 30-centimeter-by-30-centimeter specimen. Readings correspond to samples of effluent during recirculation periods, one taken every hour.

Figure B3. – Example of fissures that developed during the CBR testing of the 30-centimeter-by-30-centimeter specimen, potentially contributing to the lower CBR values returned in some areas.

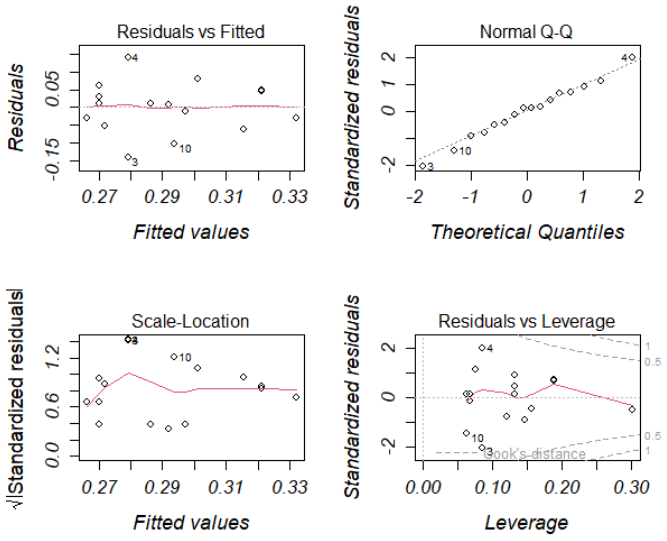

Figure B4. - Residual plots for calcium content and CBR value linear regression

Table B1. - Ingredient per-unit costs.

Purpose	***Product (Abbreviation)***	***Brand***	***Unit Cost ($)***	***Unit Mass (g)***	***$/g***
Carbon/ Nutrients	*Nutrient Broth (NB)*	*Becton Dickenson*	176.71	500	0.353
	Brain-Heart Infusion (BHI)	*Becton Dickenson*	572.84	2000	0.286
	Yeast Extract (YE)	*Agros Organic*	16.5	1000	0.017
Urea	*Urea Granules (FS Urea)*	*Fisher Scientific*	32.35	500	0.065
	Diesel Exhaust Fluid (DEF)	*BlueDEF*	330	66528	0.005
Amm. Chloride	*Ammonium Chloride (FS NH_4Cl)*	*Fisher Scientific*	305.75	10000	0.031
Cal. Chloride	*Calcium Chloride Dihydrate (FS $CaCl_2$)*	*Fisher Scientific*	133.17	3000	0.044
	Peladow (PW)	*Occidental Chem. Corp.*	45.99	22680	0.002
	Liquidow (LW)	*Occidental Chem. Corp.*	1490	283500	0.005

Table B2. - Soil parameters for sand used in treatment process.

Parameter	**Sakrete® Silica Sand**
Specific Gravity – G_S	2.66
Median Particle Size – D_{50}	0.67 mm
Uniformity Coefficient – C_U	1.69
Curvature Coefficient – C_C	0.91
Minimum Void Ratio – e_{min}	0.53
Maximum Void Ratio – e_{max}	0.97

Table B3. - Calcium content of 15-centimeter-diameter specimens. Results are divided between the surface layer (S), 5 centimeters deep from the surface (M), and the bottom of the specimen (B).

		Calcium Content		
Layer	***Section***	**TD P19**	**TD P14 YE**	**PI P19**
	1-2	2.9%	5.1%	0.8%
	2-3	3.5%	5.3%	1.0%
S	*3-4*	3.7%	6.1%	0.7%
	4-1	3.0%	5.4%	0.9%
	C	2.7%	4.0%	1.5%
S AVG		*3.1%*	*4.9%*	*1.0%*
S St Dev		*0.7%*	*1.8%*	*0.4%*
	1-2	1.7%	2.4%	4.1%
	2-3	2.2%	2.6%	3.8%
M	*3-4*	2.2%	2.9%	3.8%
	4-1	1.9%	2.7%	3.3%
	C	1.5%	2.7%	3.2%
M AVG		*1.9%*	*2.7%*	*3.6%*
M St Dev		*0.3%*	*0.3%*	*0.6%*
	1-2	1.5%	3.3%	4.8%
	2-3	1.7%	3.5%	4.3%
B	*3-4*	1.6%	3.2%	3.5%
	4-1	1.6%	3.3%	4.0%
	C	1.0%	3.3%	4.7%
B AVG		*1.5%*	*3.3%*	*4.2%*
B St Dev		*0.3%*	*0.2%*	*0.9%*
Overall AVG		*2.2%*	*3.8%*	*3.1%*
Overall St Dev		*0.9%*	*1.5%*	*1.5%*

Table B4. – Standard deviations of calcium content of 30-centimeter-by-30-centimeter specimen. Results are divided between the surface layer (S), 7.5 centimeters below the surface (7.5), 15 centimeters below the surface (15), and at the bottom (B)

	Calcium Content Standard Deviation (%)			
Layer	**a1**	**a2**	**b1**	**b2**
S	0.2	0.1	0.1	0.1
7.5	0.2	0.3	0.1	0.02
15	0.2	0.07	0.5	0.2
B	0.04	0.6	0.04	0.2